KTH Machine Design

Characterisation of airborne particles from rail traffic

SAEED ABBASI

Licentiate thesis
Department of Machine Design
Royal Institute of Technology
SE-100 44 Stockholm

TRITA – MMK 2011:11
ISSN 1400-1179
ISRN/KTH/MMK/R-11/11-SE
ISBN 978-91-7501-056-4

TRITA - MMK 2011:11
ISSN 1400 -1179
ISRN/KTH/MMK/R-11/11-SE
ISBN 978-91-7501-056-4

Characterisation of airborne particles from rail traffic

Saeed Abbasi

Licentiate thesis

Academic thesis, which with the approval of Kungliga Tekniska Högskolan, will be presented for public review in fulfilment of the requirements for a Licentiate of Engineering in Machine Design. The public review is held at Kungliga Tekniska Högskolan, Brinellvägen 83, B242, On August 30, 2011 at 10:00.

Department of Machine Design
Royal Institute of Technology
S-100 44 Stockholm
SWEDEN

TRITA - MMK 2011:11
ISSN 1400 -1179
ISRN/KTH/MMK/R-11/11-SE
ISBN 978-91-7501-056-4

Document type
Thesis

Date
2011-08-30

Author
Saeed Abbasi

(sabbasi@kth.se)

Supervisor(s)
Ulf Olofsson. Ulf Sellgren

Sponsor(s)
KTH Railway group; Including Bombardier, Interfleet, Association of Swedish Train Operators , Swedish National Rail Administation, Stockholm Lokaltrafik

Title
Characterisation of airborne particles from rail traffic

Abstract

Since the investigation of wear particles in rail transport started in late-1910s, the high mass concentration of these particles has raised worries among researchers concerned with air quality. However, effective action has yet to be taken because of lack of relevant knowledge. This thesis provides applicable information for the airborne wear particles in rail transport. Some aspects of their characteristics such as diameter size, mass concentration, number concentration, and morphology of particles were investigated in field tests and laboratory tests.

The effects on particle characterisations from different operational conditions in the field tests, and applying different braking materials, conducting tests in different applied loads or sliding velocities in the laboratory tests were studied. The main advantage of conducting laboratory tests was to focus on studying particles from one source. The possibility of repetition, using high sensitive instruments and conducting tests at low costs are the other advantages of laboratory studies.

Paper **A** describes how a pin-on-disc machine was used to reproduce similar real operational conditions during mechanical braking in a train. The results were validated by comparing the field tests results with the laboratory studies. The particles morphology and size distribution were also studied.

Paper **B** presents a summary of field tests results. The effects of curve negotiating and applying braking in different real conditions were investigated with an on-board measurement.

The element composition of the particles and their potential sources were also investigated outside of the particles morphologies.

Paper **C** presents comprehensive results from laboratory studies on airborne particles from different braking materials. The differences in the particle characteristics in similar test conditions were attributable to different material compositions and dominant wear mechanisms. A new index was introduced in this paper and is suggested to be used as a qualitative factor with regard to the airborne wear particle emission rate.

Paper **D** is a review of the recent studies of exhaust emission and non-exhaust emission from rail vehicles. A summary of results, measurements, adverse health effects, and proposed or applied solutions are reviewed in this paper.

Keywords
Airborne, railway, brake pad, brake block

Language
English

Acknowledgements

This thesis covers the major part of the work I have conducted from May 2009 to May 2011 in the machine design department of the Royal Institute of Technology (KTH).

I would like to thank my supervisors Docent Ulf Sellgren and Professor Ulf Olofsson. Many thanks also to my papers‘ co-authors Professor Lars Olander, Dr. Anders Jansson, Mrs. Christina Larsson, and Dr. Jens Wahlström.

Thanks to all of my colleagues at KTH. Special thanks to Mr. Peter Carlsson, Ms. Minoo Arzpeima and Professor Wubeshet Sahle, who assisted me during my experimental works.

The author gratefully acknowledges the financial support for this work supported by KTH Railway Group.

Finally, I want to show my most heartfelt gratitude to my immediate family, who not only led me for my entire life but also support, encourage and facilitate my progress. Their efforts are beyond any words to be expressed!

Stockholm, May 2011

Saeed Abbasi

List of appended publications

This thesis consists of a summary and the following appended papers:

Paper A

S. Abbasi, J. Wahlström, L. Olander, C. Larsson, U. Olofsson, U. Sellgren, A study of airborne wear particles generated from organic railway brake pads and brake discs, Accepted for publication in ***Wear, special issue Nordtrib 2010.***

The author performed the major part of the writing and experimental works and contributed to the planning and evaluation.

Paper B

S. Abbasi, L. Olander, C. Larsson, A. Jansson, U. Olofsson, U. Sellgren, A field test study of airborne wear particles from a running regional train, Accepted for publication in ***IMechE, Part F: Journal of Rail and Rapid Transit, 2011.***

The author performed the major part of the writing and contributed to the planning, experimental works and evaluation.

Paper C

S. Abbasi, A. Jansson, L. Olander, U. Olofsson, U. Sellgren, A pin-on-disc study of the rate of airborne wear particles emission from railway braking materials‘, Submitted to ***Wear, 2011.***

The author performed the major part of the writing and experimental works and contributed to the planning and evaluation.

Paper D

S. Abbasi, U. Sellgren, U. Olofsson, Particle emissions from rail vehicles (A review paper) Submitted to ***Atmospheric Environment, 2011.***

The author performed the major part of the writing and contributed to the planning and evaluation.

Abbreviation

AD: Aerodynamic diameter

AAR: The Association of American Railroads

ACGIH: American Conference of Governmental Industrial Hygienists

ASTM: The American Society for Testing and Materials

ASHREA: American Society of Heating, Refrigerating and Air-Conditioning Engineers

ATSDR: Agency for Toxic Substances and Disease Registry

BoBo: In this axle arrangement, all two-axle bogies are driving

Bo2: In this axle arrangement, one two-axle bogie is driving while the other is trailing

CEN: The European Committee for Standardization

CFCB: Compact freight cars brake

CNS: Central nervous system

DFG: Deutsche forschungsgemeinschaft

DMA: First driving motor car in an electric multiple unit

DMB: Last/second driving motor car in an electric multiple unit

DNA: Deoxyribonucleic acid

DPM: Diesel particulate matter

D_{50}: A particle diameter value in case cumulative distribution percentage reaches 50%.

EC: European commission

EDS: Energy dispersive X-ray

EDX: Energy-dispersive X-ray spectroscopy

EPA: Environmental Protection Agency

EU: European Union

EUROMOT: The European association of Internal Combustion Engines Manufacturers

FESEM: Field emission scanning electron microscope

GI: Gastrointestinal

HGVs: Heavy goods vehicles

IARC: International agency for research cancer

ICP-MS: Inductive coupled plasma mass spectrometry

IRW: Independently rotating wheels

ISO: International Organization for Standardization

LRT: Light rail transit

LGVs: Light goods vehicles

MECA: Manufacturers emissions control association

MMT: Methylcyclopentadienyl manganese tricarbonyl

MMD: Mass median diameter

MSHA: Mine Safety and Health Administration

NIOSH: The National Institute for Occupational Safety and Health

NRMM: Non-road mobile machinery

NYC: New York City

OPC: Ordinary Portland cement

PAHs: Polycyclic aromatic hydrocarbons

PM: Particulate matter

PNS: Peripheral nervous system

ppm: Parts per million

RZS: Compact brake caliper unit for wheel-mounted brake disc (from Knorr-Bremse)

SEM: Scanning electron microscope

SMPS: Scanning mobility particle sizer

TSI: The technical specification of interoperability

UFP: Ultrafine particles

UIC: International union of Railways

UNIFE: The Association of the European Rail Industry

WHO: World health organization

TABLE OF CONTENTS

1. INTRODUCTION

This chapter presents the background information to airborne particles, the terminology used, the objective and research questions, as well as briefly describing the research methodology used and outlining the structure of this thesis.

1.1 Background to airborne particles

The suspension of solid particles or liquid droplets in a gas or another liquid is referred to as particulate matter (PM). It conveys the suspension in both liquid and gas. In contrast, aerosol refers to the particles or droplets only in a gas (Hinds, W., 1999). In ISO 4225:1994, dust has been defined as ―Small solid particles, conventionally taken as those particles below 75 μm in diameter, which settle out under their own weight but which may remain suspended for some time". Particulate matter, aerosol, dust, and airborne particles are the common terms that we normally deal with in topics related to air quality.

The relation between PM and atmospheric phenomena have been proven and well-documented, for example by Cheremisinoff (2002) and Ruzer (2005). Health problems in human and animals, inverse effects on visibility, and global climate changes are the common adverse effects of particulate matter.

These relations are not new topics for humans, although they were not priorities in the past. For instance, an Assyrian king, Tukulti-Ninurta II (890-884 BC), reported a strange smell in the air during a visit to Hit, a town located west of Babylon and the centre of asphalt mining (Hopke, 2009).
One of the oldest descriptions of these relations can be found in the Hippocratic Corpus, which details that Greek and Romans were familiar with these problems in crowded cities and mines (Hippocrates, 460–377 B.C) (Sundell, 2004). In 61 AD, the Roman philosopher Seneca also reported air pollution in Rome and its adverse effects on him. However, the first serious report on air pollution and its adverse health effects was published by John Evelyn in 1661. Evelyn reported that burning wood would be less harmful than burning sea-coal to the human lungs. He also suggested to relocate London's polluting industries such as lime-burning and brewing (Krech et al., 2003).

Ramazzini conducted investigations about people's diseases and their occupations. He wrote *De Morbis Artificum* Diatriba', Diseases of Workers) in 1713. Ramazzini identified airborne particles as the second factor of worker diseases after ergonomics (Schenk, 2011). In the Victorian era, six different factories were identified as ―dangerous trade" and using ventilation systems became obligatory to diminish harmful air pollutant (Lee, 1973). However, only in the recent century has the mechanisms of particles effects and characteristics been identified and more active efforts are achieved (Nielsen and Ovrebø, 2008).

We refer to the suspension of solid particles or liquid droplets in the air as airborne particles. Throughout this thesis, the term ―particles" refers to the airborne particles unless otherwise specified.

PM is a mass-based criterion, and many different sub classifications have been defined for PM based on the so-called aerodynamic diameter (AD). AD expresses the same gravitational

settling velocity for a particle in standard air as if it were perfectly sphere with the unit density.

Some examples of PM subcategories are:

- $PM_{2.5}$ refers to particles with an AD up to 2.5 µm.
- PM_{10} refers to particles with an AD up to 10 µm.
- Ultrafine fraction ($PM_{0.1}$) refers to particle/s with an AD up to 0.1 µm.
- Fine fraction ($PM_{(2.5-0.1)}$) refers to particle/s with an AD between 0.1-2.5 µm.
- Coarse fraction ($PM_{(10-2.5)}$) refers to particle/s with an AD between 2.5-10 µm.

Figure 1 shows a rough comparison of the size of $PM_{2.5}$, PM_{10} particles, fine beach sand, and a human hair.

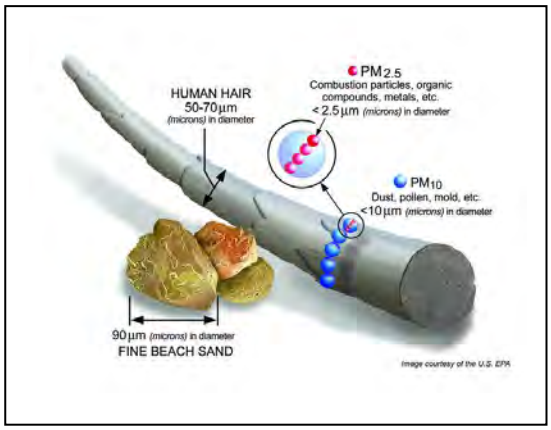

Figure 1. A comparison between the size of fine sand beach diameter, human hair diameter and PM_{10} , $PM_{2.5}$. (EPA PM Research, 2011).

1.2 Objective and research questions

The main research question for the project, of which the work presented in this thesis is the first part, within the context of rail transport is:

- How can the emission of airborne particles from a running train be efficiently controlled?

In the presented work, this main question has been broken up into the following sub-questions:

- What is the state-of-the-art knowledge of airborne particles generation mechanisms, characteristics and sources?
- What is the element composition of airborne particles generated by a running train?
- How can the composition of the airborne particles be classified with respect to their health effects?
- What are the effects of different operational conditions on airborne particle characteristics?
- Is it feasible to study the generation of airborne particles with reduced testing in a controlled laboratory environment?
- How large of a portion of the total amount of non-exhaust particles originates from wear processes?
- What is the best criterion to quantify airborne particle emission factors?

1.3 The research method

This thesis is part of the KTH Railway Group project entitled –Airborne particles in rail transport". The aim of the project is to provide practical solutions that make it possible to control the generation of particles that are emitted from rail transport into the ambient air. In this regard, two stages are considered. The aim of the first stage is to increase the general knowledge of particle characteristics, evaluation of and distinction between different particle sources, and investigate technical specifications and operational conditions of the sources. Further, one of the objectives is to develop methods to generate particles in controlled laboratory conditions that are similar to those created in field operations. This thesis is a part of stage one of that project. The objective of the second stage will be to develop, verify and validate computerised models that can be used to predict and control the generation of airborne particles from the main wear processes. The validation should be based on a combination of experimental methods and laboratory tests.

Figure 2 shows a schematic view of the proposed method for this project.

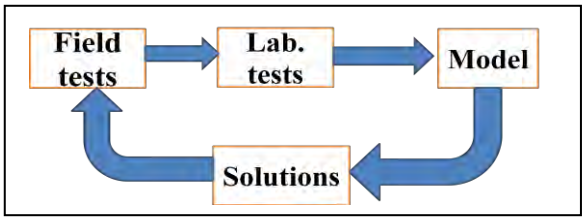

Figure 1. A schematic view of the methodology used in the current project.

1.4 Thesis outline

Chapter 1 gives a short introduction of the purpose for the thesis and the research questions. Chapter 2 reviews basic concepts of environmental engineering, railway engineering and tribology. In Chapter 3, the research methodology, that is the used methods and tools, are more thoroughly described. First, the particle instruments are described followed by the instrumented test train, and the laboratory test set-up with a modified pin-on-disc machine. Chapter 4 summarises the results from the appended papers, and in Chapter 5 these results are discussed. The answers to the stated research questions are answered in Chapter 6 and future work is proposed.

2. FRAME OF REFERENCE

This chapter provides some fundamental information about the adverse health effects of particles, particle legislations, and rail vehicle dynamic and its main systems with non-exhaust emission as the context.

2.1 Airborne particles: adverse health effects and legislation

2.1.1 Health effects

Humans are subjected to risks from particles through different routes. The routes of exposure can be classified as:
-Contact with the skin (dermal)
-Breathing (inhalation)
-Drinking or eating (ingestion or oral)
-Injection (nanoparticles for medical treatment)

Allergy/irritation of eyes and irritation or discoloring of the skin are common dermal symptoms caused by particles. Particles can come in contact with the skin and be absorbed as pre-formed solutions, or become soluble by sweat, blood or fatty acids on the skin. After solution, the penetrations process starts (Hostynek, 2004). The skin absorption and its reactivity have been well-documented in (Guy, R.H., 1999). However, there are several factors that affect skin absorption. Hostynek introduced several exogenous factors (such as size, dose, PH, protein reactivity, solubility) and endogenous factors (such as skin age, anatomical site and skin tissue section) in this regard (Hostynek, 2004).

It must be noted that the deposited particles in the skin can also be due to ingestion. Hand to mouth is one on the most common routes to ingest particles. According to Hawley (2005), an individual might ingest up to 25% of the dirt present on the fingers by hand-to-mouth contact (25% of the amount on the hands for children, 14% for adults). Recently, Xue et al. (2007) reported that hand-to-mouth behaviour among children is highly dependent on age group and location.

According to their work, the highest hand-to-mouth frequency belonged to two-year-olds during indoor activities (Xue et al., 2007).

Inhaling particles has a more intense and rapid effect, as particles can enter into the blood via the respiratory system. The surface area in the respiratory system is hundreds of times larger than the total area of the human skin. Also, the size and shape of different parts of the respiratory system are quite suitable to deposit particles. Figure 3 shows different parts of the upper respiratory and lower respiratory tracts. A real image from the bronchiole-alveolar duct is presented in the upper-right image.

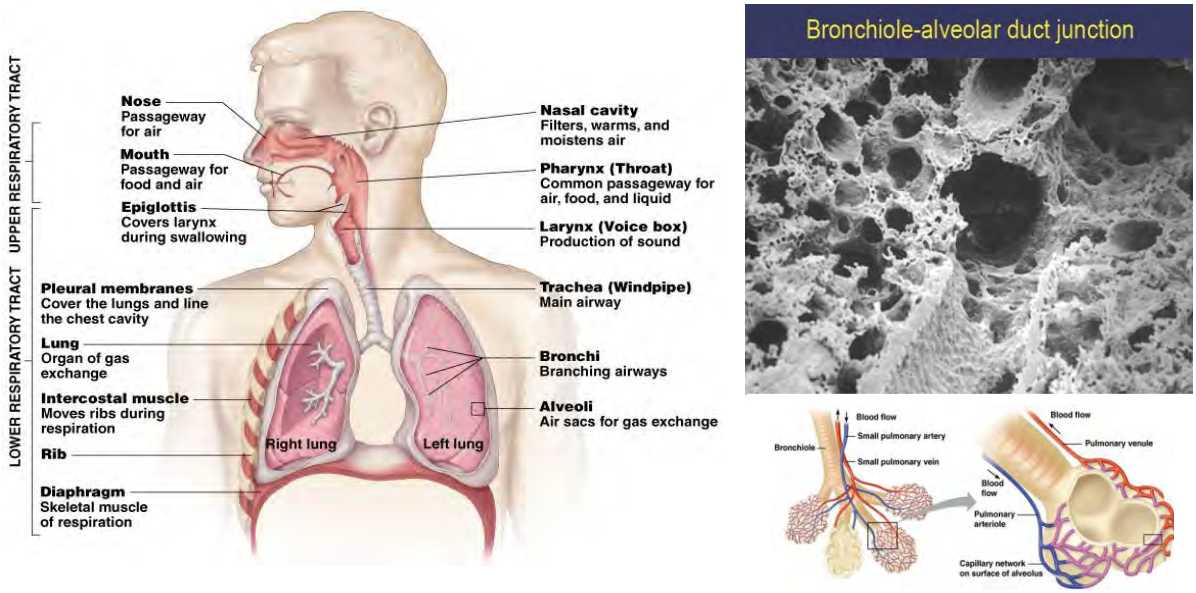

Figures 3. These figures show different parts of upper and lower respiratory tracts. (By permission from Prof. K. Pinkerton.)

In the early 1990s, the ISO, ACGIH and CEN reached a general agreement to define the inhalable fraction, the thoracic fraction and the respirable fraction of particles. The inhalable fraction of airborne particles in ambient air, which can penetrate the respiratory system via the mouth or nose, was called the inhalable fraction. The inhalable fraction was defined based on D_{50} equal to 100 µm in aerodynamic diameter. The thoracic fraction refers to the fraction of inhalable particles that pass the larynx and penetrate into the conducting airways. This fraction was defined based on D_{50} equal to 10 µm in aerodynamic diameter. A portion of inhalable particles could reach the deepest part of the lungs and alveoli. This was referred to as the respirable fraction and was defined as D_{50} equal to 4 µm in aerodynamic diameter.

Particles penetrate and can deposit in different parts of the respiratory system depending on their size. Tager (2005) has summarised the particle size criteria for penetration and deposition in the respiratory system. His results are shown in Table 1.

Table 1. The respiratory tract penetration of particles in various sizes (Adopted from Tager,2005)

Paricle size range(µm)	***Level of penetration***
≥11	*Donot penetrate*
7-11	*Nasal passages*
4.7-7	*Pharynx*
3.3-4.7	*Trachea and primary bronchi (1^{st})*
2.1-3.3	*Secondary bronchi (2^{nd}- 7^{th})*
1.1-2.1	*Terminal bronchi (8^{th})*
0.65-1.1	*Bronchioles (9^{th} -23^{rd})*
<0.65	*Alveolar ducts (24^{th}-27^{th}) and alveoli*

According to Tager‘s work, particles with a size less than 11 µm penetrate the respiratory system and the finest ones with a size less than 0.65 µm can reach the alveolar duct and alveoli. He also mentioned that the particles deposition rate in tracheobronchial and alveolar regions is highly dependent on sex, age and respiratory diseases. It has been proven that for an equal particle size interval, the greater deposition occurs in female groups, young adults in the age span of 14-18 years, and individuals with pre-existing respiratory diseases.

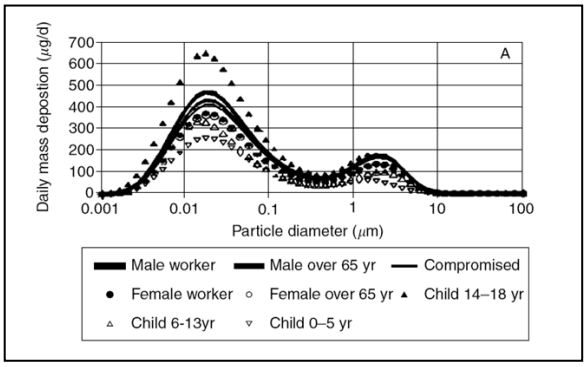

Figure 5. Daily mass particle deposition rate for 24-h exposure at 50 µg/m3 in tracheobronchial and alveolar regions. (Adopted from Tager, 2005.)

Figure 5 illustrates the variability in mass deposition (µg/d) as a function of age and sex according to these results.

It must be noted that the particle hygroscopic growth factor is another important issue in studying particle deposition rate in the respiratory system. In Li and Hopke (1993), this effect was studied in detail.

Recently, Madl and Pinkerton reported more than 30 different characteristics in particles and exposure factors that must be evaluated when studying the adverse health effects of particles in respiratory systems (Madl and Pinkerton, 2009). It has also been proven that diabetics are more susceptible to adverse health effects when inhaling particles (Golhd, D. R., 2008).

Figure 6 shows a view of how nanoparticles enter the blood through different routes. If we skip drug delivery by injection, other parts can be used and generalised for the particles‘ effects on humans. It also shows how particles can reach different body organs. The inputs and outputs of organs have been shown schematically. In fact, the particles‘ toxic effect starts when the accumulation amounts of elements exceed the certain amount, which can be tolerated by the natural metabolism in the human body.

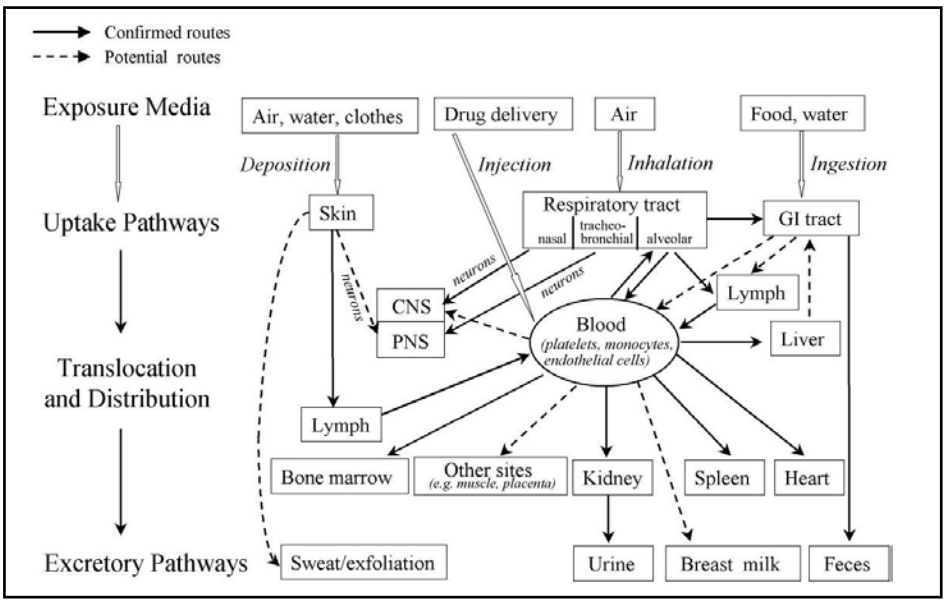

Figure 6. A schematic view of particles' exposure routes and their potential effects in different organs. (Adopted from Oberdörster et al. 2005.)

According to studies by ATSDR, such accumulations of lead, copper, zinc, nickel, aluminum, chromium, mercury, manganese, iron, and cadmium can damage human organs, including the kidney, liver, bones, lungs or GI tract. It must be noted the adverse health effects and damages caused by particles are not limited to accumulation problems in different organs. It has been proven that particles can cause some other long-term damages or short-term damages with regard to their characteristics and human exposure. Vomit, metal fever, effects on the nervous system, siderosis, oxidative stress, and cancer are reported because of exposure to these particles (ATSDR website, 2011). It must be noted that some health problems appear after a markedly long period from the first exposure. For instance, mesothelioma, a type of lung cancer caused by exposure to asbestos, has a latency period of more than 40 years, and after this period it can be diagnosed (Blanchi and Blanchi, 2007).

2.1.2 Legislations

Almost all of the present legislations have defined their criteria based on particles‘ mass concentration for certain materials when inhaling air, particularly for outdoor air quality. Concerning particle composition, water solubility or insolubility, inhalable fraction or respirable fraction, and the total time of measurement or exposure are other factors that they have considered been in the workplace. The effects of human gender, age, pre-existing disease (e.g., diabetes, asthma) and particles with a size less than three respirable fractions have not been defined in the legislations until now. The carcinogenicity of materials is important for particles as well. According to IARC, soot, quartz, asbestos, lead, arsenic, nickel, and chromium (VI) compounds are carcinogens. Making some limitations to apply these compounds or stop their use are other issues that are followed by national and international organisations.

In both the US and EU, legislation has determined limitations for the amount of PM_{10} ,$PM_{2.5}$, and certain metal compounds for outdoor air quality. These criteria are considered alongside the amount of nitrogen dioxide, sulphur dioxide, ozone, and carbon monoxide. Table 2 shows a comparison between some of the selected criteria from EU legislation and the US standard. (EPA NAAQS, 2011; EU Directive 2008/50/EC, 2008)

Table 2. A comparison between US and EU legislation for outdoor air quality in some of parameters.

		$PM_{2.5}$ (µg/ m³)	PM_{10} (µg/ m³)	Lead (µg/ m³)	Nickel (ng/ m³)	Arsenic (ng/ m³)	Cadmium (ng/ m³)	PAHs (ng/ m³)
US EPA NAAQS	Daily (24 h)	35	150	–	–	–	–	–
	Annual	15		0.15 [a]	–	–	–	–
EU directive 2008/50/EC	Daily (24 h)	–	50 [b]	–	–	–	–	–
	Annual	25	40	0.5	20[c]	6[c]	5[c]	1[c]

a) The rolling three-month average.
b) The limit 50 µg/ m³ must not be exceeded 35 times in a calendar year.
c) Target value enters into force 31.12.2012.

Occupational exposure limits (OELs) are defined to specify guidelines which assist protecting human‘s health during exposure to natural or man-made substances. Currently, several national and international organisations are actively investigating OELs. Some of those organisations claim to consider only health factors without concerning the feasibility or economical limitations. ACGIH is one of these pioneers. Recently, Schenk et al. (2008) compared exposure limit values between ACGIH and 17 well-known organisations from Europe, North America, Japan, and Australia. They reported that the highest substance coverage was offered by ACGIH. Furthermore, the offered OELs by ACGIH were usually the lowest or closer to the lowest OELs. The threshold limit values (TLVs) is one of the

indices used by ACGIH, and refers to conditions under which nearly all workers may be exposed day after day without adverse health effects.

Table 3. A summary of selected Occupational exposure limits (OELs) from ACGIH

Substance	Chemical abstract number, (CAS)	The threshold limit values (mg/ m³), Time-weighted averages (TWA) for an 8 h day during a 40 h week
Iron	7439-89-6	5
Nickel	7440-02-0	0.2 insoluble compound 10 metal/elemental
Chromium	7440-47-3 7440-47-3 13765-19-0 7789-06-2 7758-97-6	0.5 Chromium (III) 0.05 Soluble compounds of Chromium (VI) 0.01 Insoluble compounds of Chromium (VI) unless listed below 0.001 Calcium chromate 0.0005 Strontium chromate 0.012 Lead chromate
Molybdenum	7439-98-7	10 metal/ insoluble/ inhalable fraction 3 metal/ insoluble/ respirable fraction 0.5 metal/ soluble/ respirable fraction
Manganese	7439-96-5	0.2 Inhalable fraction 0.02 Respirable fraction
Silicon	7440-21-3	5 Inhalable fraction 0.1 Respirable fraction
Cobalt	7440-48-4	0.02
Cadmium	7440-43-9	0.01 Inhalable fraction 0.002 Respirable fraction
Aluminum	7429-90-5	10 Inhalable fraction 1 Respirable fraction
Titanium	7440-32-6	10
Zinc	7440-66-6	2
Tin	7440-31-5	2
Zirconium	10101-52-7	5
Calcium	7789-78-8	10 Inhalable fraction 3 Respirable fraction
Vanadium pentoxide	1314-62-1	0.05
Barium	7440-39-3 7727-43-7	0.5 10 for Barium sulfate
Copper	7440-50-8	1 Dust 0.2 Fume (0.1 in STEL) 0.05 Respirable fraction
Lead	7439-92-1	0.05
Antimony	1345-04-6	0.5
Aresenic	7440-38-2	0.01
Carbon	7440-44-0	10 Inhalable fraction 3 Respirable fraction
DPM (soot)	58-32-2	0.02 EC fraction[1], 0.16 TC fraction[2], 0.35 EC fraction[2]

1. ACGIH withdrawed the TLV of DPM from their lists in 2003
2. These TLVs are suggested by MSHA in 2005

Table 3 shows the TLVs of substances that are related to the topic of this thesis.

These OELs are set for time-weighted averages (TWA) and are usually set for an 8-hour day during a 40-hour week. The short-term exposure limits (STEL) are used in some rare cases

and refer to 15-minute exposure. OELs are dependent on chemical composition of substances and a few particle characteristic factors such as solubility, respirable fraction and inhalable fraction.

It must be noted that when a mixture of different substances are considered, the cumulative effects must also be considered. The summation ratios of recorded concentration

the OELs must be less than unity. It can be shows as:

$$\frac{C_1}{OELs_1} + \frac{C_2}{OELs_2} + \ldots + \frac{C_n}{OELs_n} < 1 \quad (1)$$

2.2. An overview of rail vehicles

2.2.1 Rail vehicle definition

A rail vehicle can be defined as a movable rail guided/interacted device that is used to transport objects or provide essential services to facilitate transporting objects. Rail vehicles can be classified based on their main functionalities.

a) Transportation in long distance: Rail vehicles such as passenger cars, freight cars, locomotives, multiple units, LRTs, and rail buses.

b) Transportation in short distance: Rail vehicles such as rollercoasters and carriages in cable railways or funiculars. These kinds of rail vehicles are usually used for distances less than five km.

c) Supporting machineries for transportation: Rail vehicles such as track maintenance machines (tamping machines, ballast stabilizing machines, etc.), rail snowplows and railway cranes.

Almost all of these functionalities can be achieved either when both rails interact with rail vehicle components such as conventional railways, or when only one rail exists and interacts with rail vehicle components such as monorails.

The main focus in this thesis is group (a), with exception of rail vehicles of single-based rail and rail vehicles with rubber tires. Nevertheless, some results and discussions can be extended to the other rail vehicles that were out of scope of this thesis.

2.2.2 Main systems in rail vehicles

The main systems in a rail vehicle are carbody, running gear and brake systems.

2.2.2.1 Carbody

The main role of a carbody is to carry loads that are either passengers or goods. Carbodies must fulfill demands such as safety, comfort, aesthetic design, aerodynamic design, maintenance aspects, and economical limitations (Andersson et al., 2007) According to EU legislation for end-of-life vehicles (EU Directive 2000/53/EC , 2000), up to 95% of a vehicle‘s total mass must be recovered. Therefore, the recoverability of a carbody must also be considered, as the main fraction of a rail vehicle‘s mass comes from the carbody. Recycling, reusing and energy recovery of materials are factors in the recoverability rate that must be taken into account and added to the previous demands in the design of a carbody.

The carbody has six different movements and all of them are important in the study of rail vehicle dynamics. They are three translation motions and three rotational motions. The translation in the direction of travel is called longitudinal movement. The translation in the transverse direction parallel to the track plane is called lateral movement. The translation perpendicular to the track plane is called vertical movement. The rotation on longitudinal axis is called roll. The rotation on the transverse direction parallel to the track plane is called pitch. The rotation on an axis perpendicular to the track plane is called yaw. Figure 7 shows a schematic view of these six relative motions.

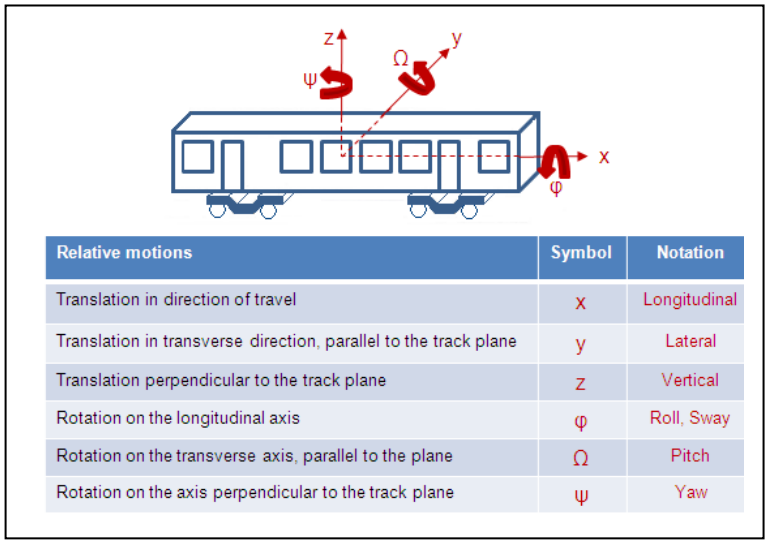

Relative motions	Symbol	Notation
Translation in direction of travel	x	Longitudinal
Translation in transverse direction, parallel to the track plane	y	Lateral
Translation perpendicular to the track plane	z	Vertical
Rotation on the longitudinal axis	φ	Roll, Sway
Rotation on the transverse axis, parallel to the plane	Ω	Pitch
Rotation on the axis perpendicular to the track plane	ψ	Yaw

Figure 7 A Schematic view of six possible relative motions in a carbody or a rail vehicle.

2.2.2.2 Running gear

The interaction between rails and a rail vehicle‘s carbody occurs in the running gear. The running gear must support the carbody, and accelerate or decelerate vehicle. Wheelsets and brake systems play crucial roles in the dynamic functionalities of the running gear.

Wheelsets are the fundamental components in all rail vehicles (Figure 8a). Wheelsets are classified as Solid wheelsets and IRW. A solid wheelset consists of an axle and a wheel on each side of axle. In IRW, however, each wheel can rotate independent of the other wheel. Railway wheel material are generally classified as medium carbon steel with a carbon (0.3%-0.6%) and manganese amount (0.6%-1.65%). Recently, a review of railway wheel material compositions and mechanical properties was completed by Clarke (2008).

Wheel profile is divided into three parts: wheel tread, wheel flange and wheel chamfer (Figure 8b, c). The lowest contact stress, lateral force and wear occur when the wheel tread is in contact with the rail profile (Tournay, 2001).

A special conical profile is designated for railway wheels (Figure 8a). This conicity facilitates the curve negotiating performance during curve negotiation. This conicity also allows for a sinusoidal motion for a wheel when it runs in a straight track. Higher conicity induces higher instability in the vehicle motion, as an increase in the conicity is associated with an increase in the frequency and acceleration in the vehicle oscillating motion. Recently, the limit value for conicity was reported in the EU directive 2008/232/CE according to the maximum operational speed of the vehicle (2008). The sinusoidal motion also causes the movement of the contact patch between wheel tread and wheel flange (Figure 8b, c). Figure 8c shows one point contact and Figure 8c shows two points of contact between the wheel and rail. In the latter, the difference between the two points‘ radius causes two different rolling radiuses, and consequently larger slippages can occur which lead to higher wear in the wheel. This effect is studied by Markine et al. (2007) in detail.

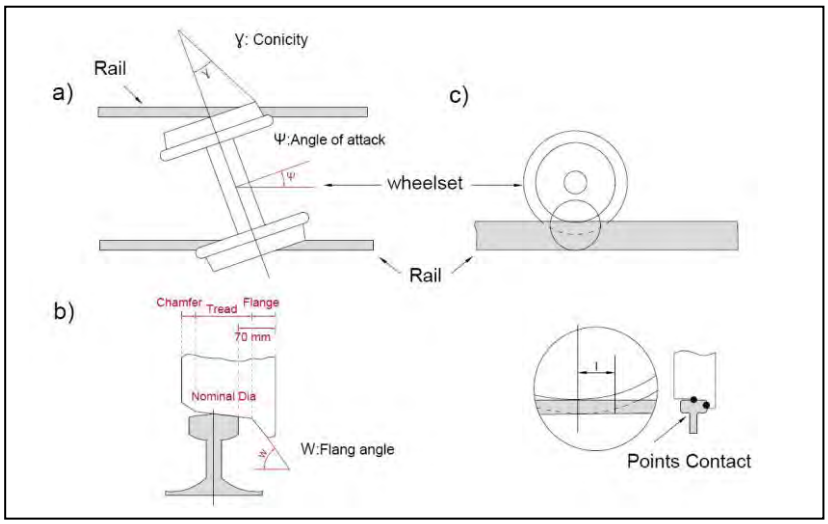

Figure 8. The schematic views of key parameters in a railway wheel profile. A wheelset view along with referring to the conicity and angle of attack (a). An one point contact view of a wheel and rail along with addressing wheel tread, wheel flange, flange angle, and nominal wheel diameter (b). An illustration of two points contact (c).

According to Nadal's equation (1986), the magnitude of the flange angle plays a crucial role in flange climbing and consequently the derailment of a rail vehicle. The angle of attack presents the yaw motion in a wheelset as it has been depicted in Figure 8. The effect of the angle of attack in wheel wear rates was confirmed by different researchers. In models presented by Heumann (1954), Marcotte (1978), Ghenonem (1978), Kalousek (1982), and Vogel (1981), the wheel wear was linearly or quadratically dependent on the angle of attack (Barghini, F. et al., 2009).

The single axle running gear is used in a "rigid-frame" vehicle. In other words, only two wheelsets exist in a rigid-frame rail vehicle. These vehicles were normally light, simple and inexpensive, but their payload capacity and curving performance were limited. Furthermore, their maximum operational speed was less than 120 km/hr because of their used suspension system, which resulted in limitations and an uncomfortable ride characteristic. In order to solve this problem, bogies were introduced. Rail vehicles with bogies are called a bogie vehicle. Distinctively, the behaviour of the wheel and its yawing motion affects the bogie performance. Figure 9 shows a typical bogie.

Several configurations can be defined to achieve different performances and functionalities. The main factors in these configurations can be summarised as:

a) The type of wheel connections to the bogie frame.

b) The dependency or independency of two wheels on one axle axis.

c) The existence and type of applied steering systems

The review of different running gears wasconducted by Wickens (2009); Goodall et al. (2006); Jönsson (2002); Hecht (2001); Hawthorne (1996); and Scales (1996).

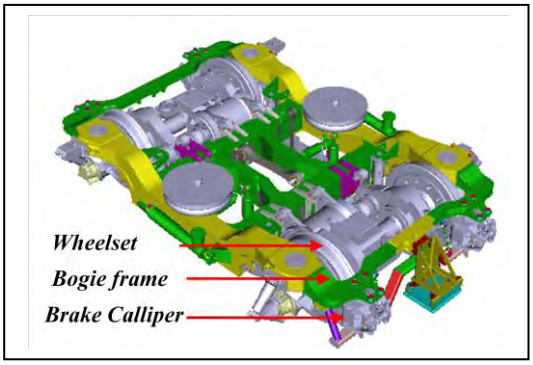

Figure 9. A typical bombardier bogie.

2.2.2.3 Brake systems

Converting kinetic energy to heat is an old system that is still in use in railway brake systems. Applying wooden blocks to the wheel treads were the oldest design of friction brake systems

to stop the initial steam locomotives. It was the driver‘s task to actuate a lever or operate a screw to make a contact between the wooden block and running wheel to apply the brake. This kind of manual system did not match the increasing demand of a suitable brake system, and a system with higher reliability and safety was needed. In the mid-1870s, new systems were introduced replacing the old ones. Compressed air brakes in the US and vacuum brakes in the UK were introduced simultaneously (Elliot, 2006).

Figure 10 shows the block diagrams of these two systems.

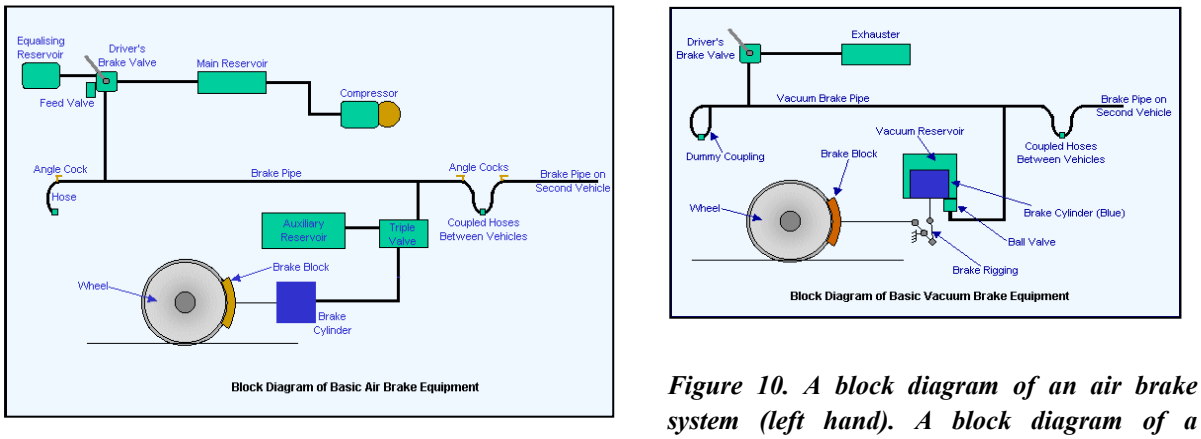

Figure 10. A block diagram of an air brake system (left hand). A block diagram of a vacuum brake system (right hand). (Adopted from a railway technical website, 2011.)

The operating principles of these two systems were fairly similar. Charging the pipe with the compressed air or with a vacuum resulted in releasing the brake. Releasing the brake was the normal situation, so making any pressure changes in the pipe resulted in applying the brake. Today, the vacuum brake system is obsolete, now outnumbered by the compressed air brake system.

Both the air brake and vacuum brake systems are friction brakes, although the latter is not popular. The principle functions of all friction brake types are quite similar even though there are many different types of friction brakes. The interaction between different mechanical parts results in controllable contacts between friction materials and rotating objects. This kind of frictional contact converts the kinetic energy into heat. The friction brake system can be classified as a tread brake, disk brake systems and hydraulic retarders.

The tread brakes are broadly used in freight cars or other rail vehicles where high speed is not the main concern. The tread brake rigging systems (conventional) are the most famous types of tread brake types.

Figure 11 shows schematic views of these systems.

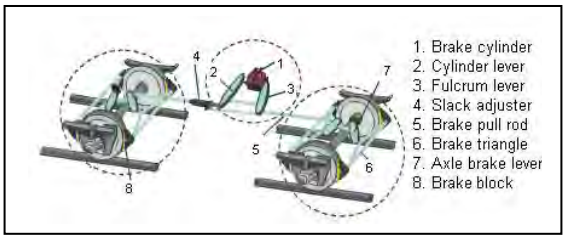

Figure 11. A simple view of the tread brake rigging system with main components. (Conventional tread brake) (Inspired by Gfatter et al., 2007.)

Figure 11 explains that when the brake cylinder is actuated, it pushes/pulls different levers until finally the brake blocks are compressed to the wheel.

Figure 12 shows a rough comparison between a conventional brake rigging system and CFCB, which are two common types of brake rigging systems. Elstorpff and Mathieu (2008) reported higher efficiency, lower noise and vibration, lower weight in the bogie total weight, and less air consumption for the CFCB in comparison to a conventional brake rigging system. They reported a lower wear rate of brake blocks in a conventional brake rigging system after running 60,000 km. They explained this phenomenon by degrading efficiency in the conventional brake rigging system.

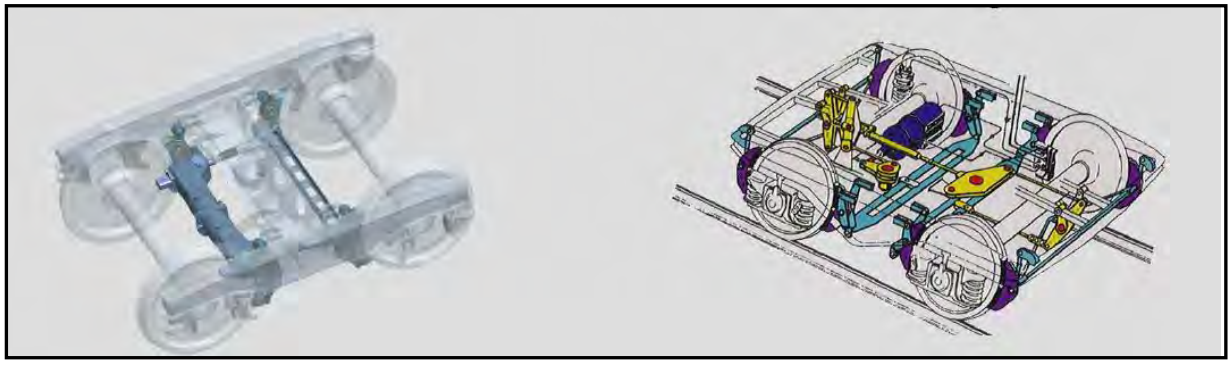

Figure 12. Two different types of brake rigging systems in a Y25 bogie. The CFCB (left) the conventional brake rigging system (right). (Adopted from Elstorpff and Mathieu, 2008.)

In the tread brake unit and CFCB, most of the mechanical parts have been combined and the same functionality is provided. The second category is disc brake systems, which are used in multiple units and passenger cars. Figure 13 shows examples of these systems. The brake discs in these systems are mounted in two different ways. If they are mounted on the wheel they are called wheel mounted (Figure 13 on the left). If they are mounted on the axle, they are called axle mounted (Figure 13 on the right).

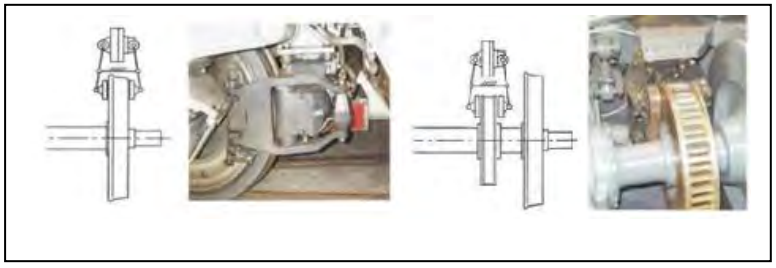

Figure 13. This figure shows a typical wheel mounted disc brake (left) and a typical axle mounted disc brake (right). (Inspired by Gfatter et al., 2007.)

Railway brake discs are usually made of cast iron (with spherical shape graphite), cast steel and ceramic matrix composite (CMC).

In tread brake systems, the brake blocks (Brake shoes) are used and in the brake disc systems the brake pads are used. The mounting arrangement of these friction materials also affects the subcategories of these brake systems. One-sided braking shoe and double-sided braking shoe are the subcategories of tread braking. The number of brake blocks in each side of a wheel and their relative rotational movement is another factor that can be used in the mounting classification. In this regard, Bg (divided), Bgu (Divided with subdivided sole) and Bdg (Double divided) are the common terms that extensively used to explain mounting of brake blocks (Gfatter et al., 2007).

Type of friction material is the key point to classify the brake blocks and brake shoes. According to (Yamaguchi, 1990) steel, brass, bronze, wood, textile were the old frictional materials that were used as frictional materials in the brake systems. Nowadays, the cast iron brake blocks, sintered brake blocks, organic brake blocks (asbestos free), sintered brake pads, and organic brake pads (asbestos free) are the common frictional materials that are used as braking materials.

Figure 14 shows typical brake pads and brake blocks. The organic brake pads are a combination of a binder, filler and other materials to stabilise mechanical properties and improve the coefficient of friction characteristics. Therefore, they are called composite brake pads in some literature.

The UIC and AAR have provided detailed standards and legislations to define frictional materials properties.

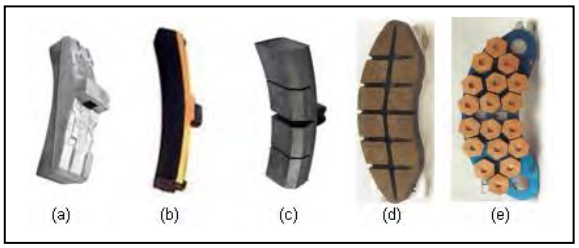

Figure 14. Different braking materials in rail traffic: (a) cast iron brake block; (b) K-type organic brake block; (c) LL-type brake bloc; (d) organic brake pad; (e) sintered brake pad.

These properties and their response to the actual tests in a standard dynamometer are crucial to facilitate reliable and safe rail transport. UIC leaflets 541-3, 541-4, and UIC 832 (UIC website, 2011), and AAR standards M 926, M996 and M997 (AAR website, 2011) are typical examples of these legislations. There are three kinds of organic brake blocks with regard to their friction coefficients. The brake blocks with a high friction coefficient, low friction coefficient, and direct replacement with cast iron brake blocks are called UIC ‗K' type or AAR ‗H' type, UIC ‗L' type or AAR ‗L' type, and UIC ‗LL' type, respectively.

The hydrulic retarder is another type of railway brake system. It works based on viscous drag force and converts kinetic energy to heat. These types of brake systems are used in diesel hydraulic (DH) locomotives or diesel hydraulic multiple units (DHMU) trains.

In Gfatter et al. (2007), other brake systems are introduced for rail traffic. One of the main ones are electrodynamic brakes. Electric motive power units usually use a rheostatic brake or a combination of regenerative (RG) and reheostatic brakes. In the rheostatic brake, the current from the traction motors is dissipated in banks of resistors. During RG braking, the kinetic energy transfers to other forms of energy, particularly the electric forms. One of the popular alternatives in railway RG brake systems is returning the current to the overhead line or third rail. The RG brake was employed only for DC systems for many years, but it can be employed for AC systems in the current decay by using microprocessors. Saving energy is another main concern when using RG brake systems, and up to 15% energy savings are reported when using RG brakes in c2c's fleet of Bombardier Class 357 EMUs (Ford, 2007). However, less wear particles and less noise are the other motivations to implement RG brakes.

In the 1900s, the electrical control was added to the brake systems to facilitate more precise control and convenient operation. It was successfully used in the New York subway in 1909 and the London underground in 1916, and has developed since then. This new system was called electropneumatic brakes (EP) and provided enormously new features in brake systems (railway technical website). Furthermore, it eliminated the propagation time of air pressure waves in air brake systems. Nowadays, EP is widely used in locomotives, passenger cars, multiple units, and some special freight cars.

The electrodynamic brake system plays a crucial role in high-speed rail transport. Recently, Liudvinavičius and Lingaitis (2007) suggested new solutions to improve the rheostatic brake. They suggested a new system in order to achieve better control in braking.

The eddy current brake (ECB) and electromagnetic brake (EMB) are two other systems that can be used independent to adhesion between the wheel and rail. The track brakes are another name for these two systems (Gfatter et al., 2007).

The principle of these two systems is quite similar, as both work based on the effects of a magnetic field. These kinds of magnetic fields can be generated by a permanent magnet or electric systems. However, in ECB there is no contact with the rail and no wear occurs. EMBs are widely used in tramways, mine railways, and railbuses of a maximum speed of 100 km per hour. As there is no wear in eddy current brakes, it doesn‘t generate any noise, dust or smell that is the intrinsic outcomes of other brake systems. However, its relatively high costs and weights are the main drawbacks of this system. Knorr-Bremse research shows ECB costs two to four times higher than the EMB (Schofield, 2002). In 2008, the ECB was written about in EU directives and recommended by the TSIOF European high-speed rail system (EU Directive 2008/232/CE). Recently, using the combination of the ECB and EMB in high-speed trains has been evaluated by Podol‘skii and Kitanov (2008).

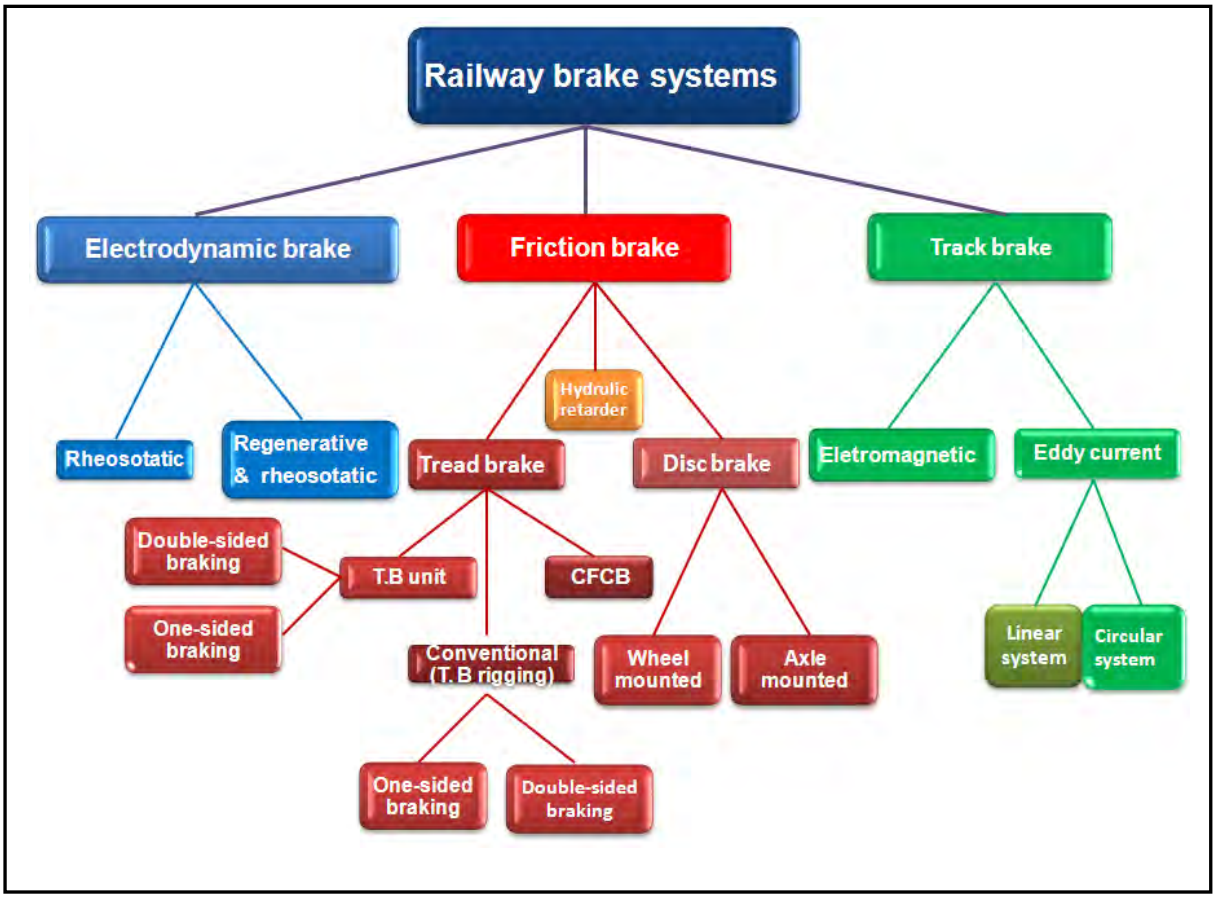

Figure 15. A summary of different railway brake systems in rail vehicles.

Figure 15 presents a summary of different types of brake systems in rail transport along with their subcategories.

In this thesis, our main focus is on friction brakes with the exception of hydraulic retarders. Here in after the friction brake system is addressed to the mechanical brake and electrodynamic brake is referred to the electrical brake.

2.3 Particle sources in rail transport

Commercialised rail transport appeared in the UK between 1804-1812. The steam locomotives were applied on cast iron rails those days to achieve this task. The London underground, the oldest subway in the world, was opened in 1863, which was 10 years before Carl Benz invented the first four-stroke cycle gasoline engine and commercialised car in road transport (Williams et al., 2000). Today, both of these transport modes have been recognised as particle emission sources. However, the numbers of researches and legislations to limit particle emission in rail transport are markedly low. It is noteworthy to mention that the particle high mass concentration in subways was raised a century ago, but few effective action plans have been achieved since that time.

Tabe 4 shows the summary of particle sources in rail transport. As it has been shown, rail vehicles, different stationary processes, air circulation, and passenger and rail staff can be taken into account as the sources of particles. Actually, most of the research is focused on particles from rail vehicles. The main focus of this thesis is non-exhaust (engine) emission from rail vehicles.

Table 4. A summary of different particles sources in rail transport.

Sources	**Sub classification**	**Examples**
Rail Vehicles	Exhaust(engine) emission	Diesel exhaust
	Non - exhaust(engine) emission	Wheel-rail contact Braking process Interaction of third rail and contact shoe Interaction of contact strip and overhead line Spraying sand to increase wheel-rail adhesion Erosion by air turbulence which is caused by a running rail vehicle (Piston effect)
Stationary process (Maintenance & construction)	Direct	Tunneling Rail cutting Rail welding Tamping process
	Indirect	Volatilization of oil and other lubricants Volatilization of cleaning material
Air circulation	Natural airflow	Moving and transferring particle emission from road transport Natural erosion of masonry structure
	Forced ventilation	Moving and transferring particle emission from road transport
Passengers and Rail staff	Human activities	Smoking in the platforms Smoking in the rail vehicle
	Others	Particle shed by passengers‘ clothes Degrading perishable materials and garbage

2.4 Wear and airborne particles

In tribology, wear has been defined as ―Damage of a solid surface, generally progressive loss of material, due to relative motion between that surface and a contacting substance or substances" (ASTM, 2003). Tribologists are active to predict, and manage and control these kinds of issues in different applications. Generally, it is a big challenge to manage or control any physical or chemical process, but in this particular issue even predicting the amount of wear volume is also a big challenge.

In 1953, Archard introduced his model to predict the volume of removed material. He acknowledged the earlier work of Holm in 1946 and suggested that the volume of removed material per unit sliding distance is in relation to the applied normal load and hardness of material in contact:

$$Q=KW/H \qquad (2)$$

Where

Q: volume of removed material per unit sliding distance

K: wear coefficient

W: applied normal load in contact

H: hardness of the material

"K" is a dimensionless factor in the above equation and dependent on wear conditions.

The wear condition can be classified as: unlubricated sliding, lubricated sliding and wear by hard particles.

The K value can change from 10^{-6} up to 10^{-2} in unlubricated conditions, so-called dry contact. When K is lower than 10^{-4}, it is called mild wear. When it is higher than 10^{-4}, it is called severe wear.

Figure 16 shows different ranges of K in different wear conditions.

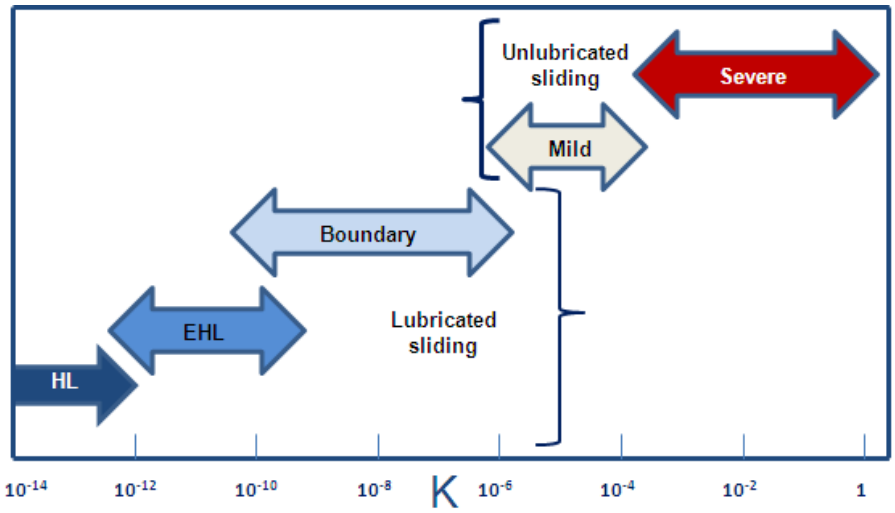

Figure 16. A rough comparison between the wear coefficient (K) in different contact conditions. (Adopted from Stachowiak, 2005)

According to Ludema, until 1994 more than 180 equations were suggested by researchers to predict wear in dry contact (Ludema, K.C.; Meng, H.C., 1995). These efforts have been in progress till this moment, but no precise and applicable equation has been provided to cover all conditions in dry contact.

In Table 5, some of the equations, which can be used to predict wear in the dry contact conditions, are presented.

Table 5. Some examples of wear models to predict wear volume.

References	Model	Parameters definitions
Archard model, 1953	$V \propto W\frac{d}{H}$ (3)	W: Applied normal load d: Sliding distance H: Hardness of softer material μ: Friction coefficient R_a: Surface roughness v: Sliding velocity e: Elongation to break S: Ultimate tensile stress a,b,c: material-dependent set parameters t: Time γ: Surface energy β: Flange angle to horizontal T_y:Longitudinal Creep force T_x:Lateral creep force γ_y:Longitudinal creepage γ_x:Lateral creepage μ_f:Adhesion at flange contact Y: Horizontal guide force μ_a: Resultant adhesion coefficient on flanging wheel ψ: Angle of attack δ: Superelevation angle
Ratner and Lancaster, 1969	$V \propto \frac{\mu W v}{HeS}$ (4)	
Rhee's model, 1973	$V \propto W^a v^b t^c$ (5)	
Kar and Bahadur, 1978	$V \propto \frac{1.5P^{1.47}d^{1.25}\gamma^{1.775}}{E^{3.225}}$ (6)	
Wang et al., 1995	$V \propto \frac{W^{1.5}\,Ra^{1.5}}{eS^{1.5}}$ (7)	
Elkins and Eickhoff, 1979	$V \propto (T_y\gamma_y + T_x\gamma_x)$ (8)	
Vogel and Kurek, 1981	$V \propto \frac{f}{sin\beta}(Y+\mu_a W\cos\delta)\psi$ (9)	

In fact, there are physical and chemical changes in the contact surfaces during wear process. These changes are dependent on material properties, and relative speed and position of contact surfaces to each other. These conditions make it hard and quite complicated to provide a general model to cover all conditions. It is noteworthy to mention that Archard's wear equation has many limitations that cover all conditions in dry contact. Yet, it deals with some limited factors that can be measured more easily in practice. These advantages motivated researchers to use Archard's wear model over the previous seven decades.

Wear can be classified as abrasive wear, adhesive wear, fatigue wear, oxidative wear, erosive wear, and corrosive wear. We skip the last one, as the main focus of this thesis deals with unlubricated conditions. The mechanisms of different wear process, which lead to material loss, has been reviewed in Stachowiak and Batchelor (2007).

We summarised them as follows:

In abrasive wear, four mechanisms are more well-known. As Figure 17 depicts, microcutting, microfracture, fatigue by repeated ploughing, and grain poll-out are four mechanisms that can be described as abrasive wear.

The microcutting occurs when hard asperities cut the softer surface and lead to generate wear debris (Figure 17a).

The microfracture in brittle material causes wear debris. In these materials the convergence cracks cause wear debris (Figure 17b).

The fatigue wear debris are generated by the repeated deformation when a blunt grit abrades a ductile material (Figure 17c)

The grain detachment or grain pull-out occurs usually in ceramics. It happens quite fast when the inter-grain bonding is weak and the grain size is large (Figure 17d).

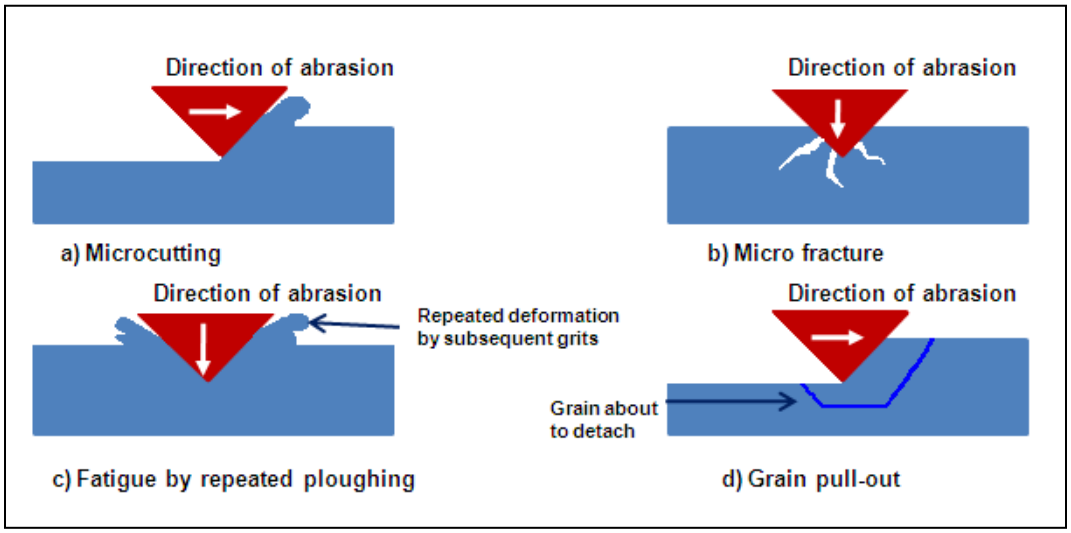

Figure 17. A schematic view of different possible mechanisms lead to abrasive wear. (Inspired by Stachowiak and Batchelor, 2007.)

The impact of particles of solid or liquid against the surface of an object causes erosive wear. The particle material, the angle of impingement, the impact velocity, and the particle size are factors that affect mechanisms involved in erosive wear.

Figure 18 shows different possible mechanisms that can occur during erosion.

When the impact angle is low, the abrasion mechanisms can be occurred (Figure 18a). By increasing the impact angle, the particle speed and substrate material interfere the process and specify the mechanisms. The fatigue mechanism occurs when the speed is still low (Figure 18b). At medium speed, plastic deformation for ductile materials or brittle fracture for brittle materials (Figure 18c) can occur. Melting would be a possible mechanism at a high speed (Figure 18d). The cones of debris can also interfere the process individually and initiate any of the above mechanisms (Figure 18e). Finally, the crystal lattice can degrade by atom (Figure 18f).

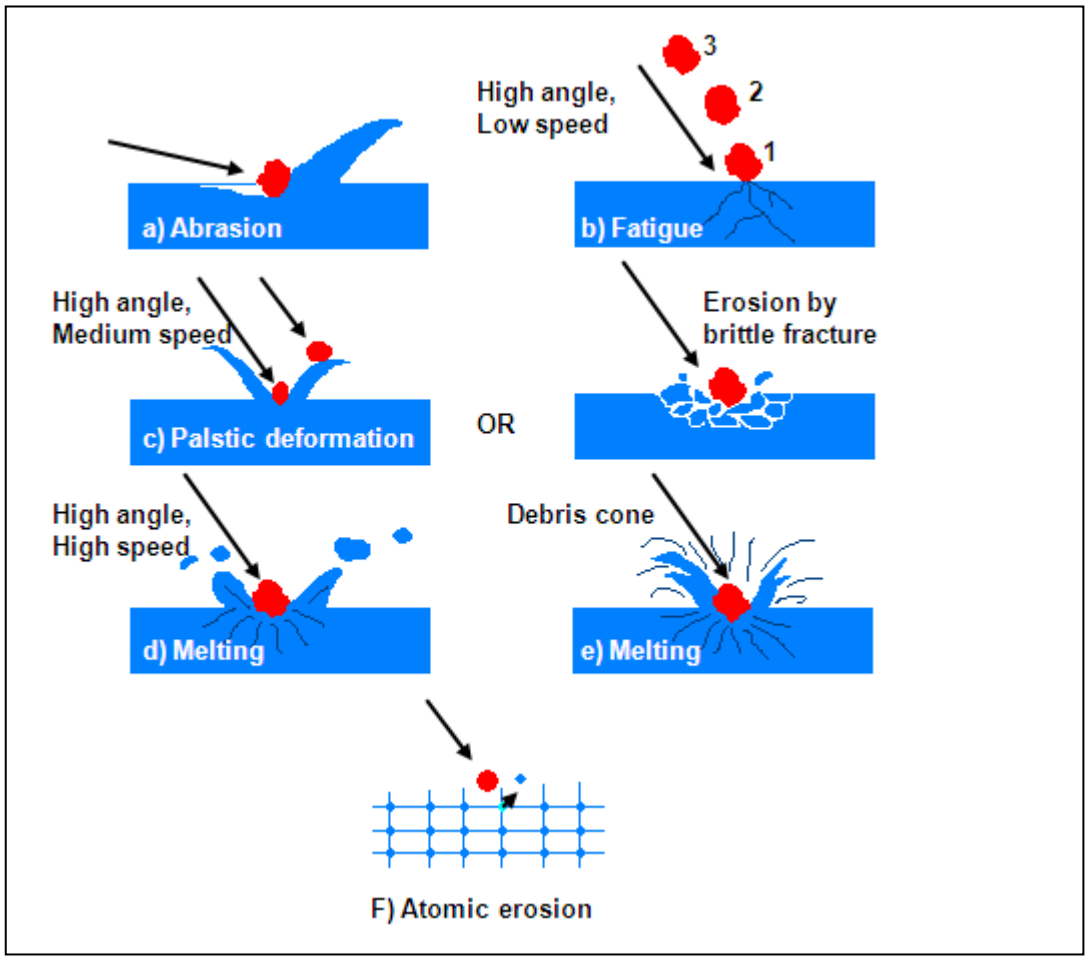

Figure 18 A schematic view of different possible routes that lead to erosive wear (Inspired by Stachowiak and Batchelor, 2007).

The simultaneous effects of the sliding motion and adhesion between asperities of contact surfaces cause a plastic deformation in asperities. This deformation can lead to the adhesion of material from one surface to another and result in adhesive wear.

Figure 19 shows a schematic view of adhesive wear. It has been proven that the low slope angle asperities are reluctant to lose material to the high slope asperities because the latter are keen to lose material. It must be noted that this kind of material loss can lead to a generation of wear debris or produce a film in a contact surface.

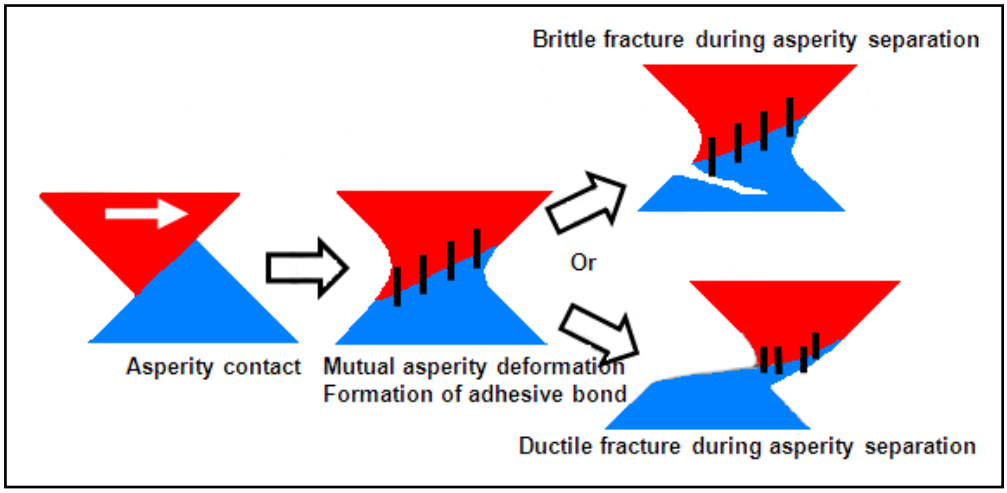

Figure 19. A schematic view of different possible mechanisms that lead to adhesive wear. (Inspired by Stachowiak and Batchelor, 2007.)

In the presence of air or oxygen, oxidative wear occurs in dry contact conditions. At low temperature or ambient temperature, the oxide layer thickness is limited to mere nanometers. This layer would be quite beneficial, as it can ban the adhesive wear. At high temperatures, the oxide layer thickness grows unlimitedly. When each oxide layer reaches critical thickness, they cannot withstand the load and they will be destroyed totally or partially. Figure 20 shows the generation of oxidative wear and consequently the wear debris from it.

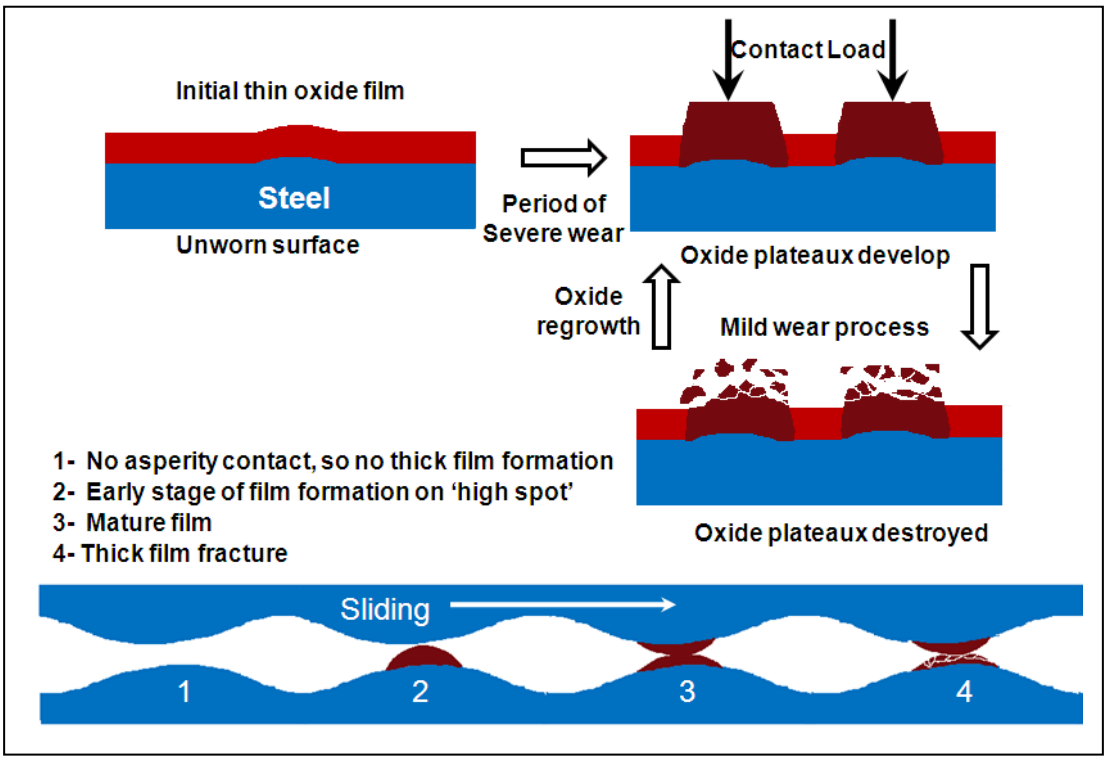

Figure 20. A schematic view of different possible mechanisms that lead to oxidative wear. (Inspired by Stachowiak and Batchelor, 2007.)

Fatigue wear occurs when contact between asperities is accompanied by a repeated number of high local stresses. The rolling contact or sliding contact initiates these kinds of stresses and propagates cracks.

Figure 21 shows how the deformation in different layers of a material happens. Repetition of these deformations can cause cracks in the weak cell boundaries, and the convergence of those cracks leads to fatigue wear.

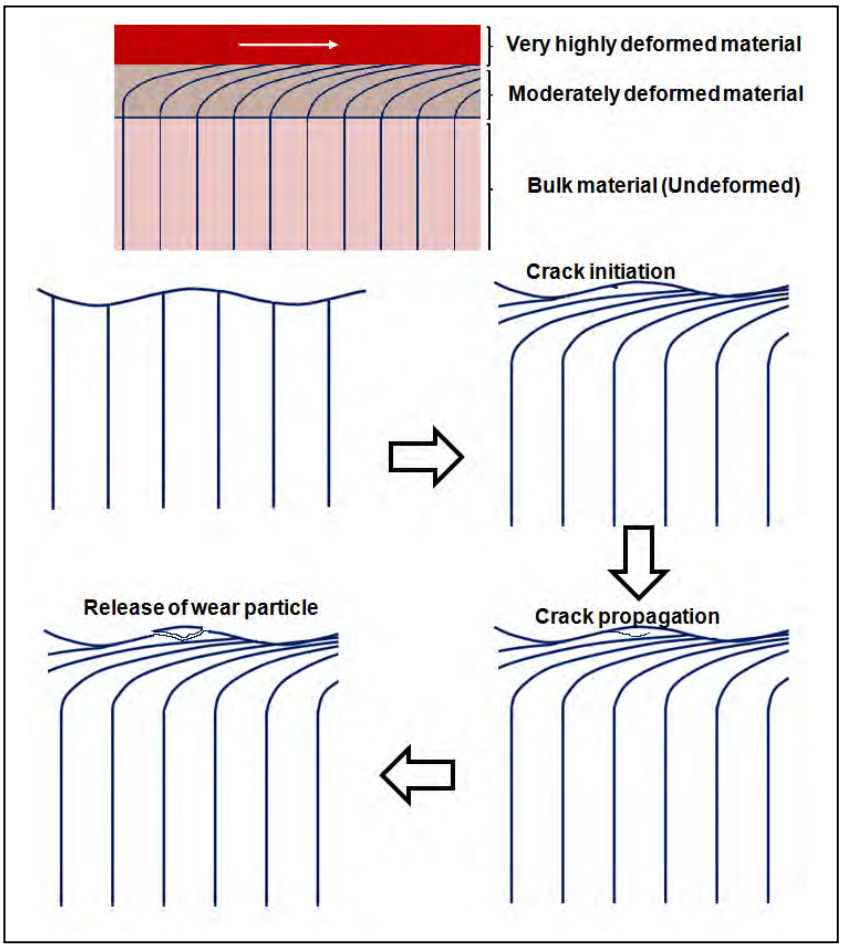

Figure 21. A schematic view of different possible mechanisms that lead to fatigue wear. (Adopted from Stachowiak and Batchelor 2007.)

There is no model to describe how and how much of wear debris can convert to airborne particles. However, there are different end results for the resulting wear debris from abrasive, erosive, fatigue, and adhesive wear:

- They can leave mating surfaces and transfer to the airborne.

- They can stick to the regions of the mating surfaces where it is not interacting with the wear process.

- They can stick to the regions of mating surfaces in the interacting wear process.

In the last case, wear debris has the potential to repeat the above scenario and contribute to the generation of particles.

Until this moment no model has been provided to consider all of the forces that may affect detached wear debris or particles. Recently, effects of Brownian diffusion, drag force, gravitational force, thermophoresis force, electrostatic drift, and turbophrosis have been studied by Sippola and Nazaroff (2002) to predict particle suspension possibilities in ducts. According to their work, other forces have negligible effects for the particle-air system. Nearly almost all of those forces can affect detached wear debris. However, the initial velocity of the detached wear debris during detachment and surface forces are other factors that exist during the wear process and must be taken into account. The overall effects of affected forces can result in fluidised particles converted into airborne particles. Therefore, we expect the particle characteristics, air properties, airflow conditions, and temperature on contacts to affect the wear debris and influence the possibility of transferring to airborne particles.

The study of airborne wear particles from road transport was seriously started during the 1970s (Subramani, 1971). This part is quite well-known in road transport and referred to as non-exhaust emission. It deals with airborne particles from tire and braking material and road surface wear. Recently, the different methods and results of emissions from these sources have been reviewed in the EEA report 2009 (EEA website, 2011). The fractions of total particles are provided in mg/km according to the defined test conditions for a specific vehicle. Table 6 shows a typical result of measurement for different vehicles in different conditions based on an average speed of 80 km/h (UK Informative Inventory Report, 2011).

Table 6. A typical result of PM10 per km for tire, brake and road surface wear, which resulted from different cars.

mg PM10/km		Tire	Brake	Road surface wear
Car (passenger)	Urban	8.74	11.68	
	Rural	6.80	5.53	7.5
	Motorways	5.79	1.30	
LGVs	Urban	13.80	18.22	
	Rural	10.74	86.2	7.5
	Motorways	9.15	21.2	
Rigid HGVs	Urban	20.74	51.00	
	Rural	17.39	27.14	38
	Motorways	13.98	8.44	
Artic HGVs	Urban	47.07	51.00	
	Rural	38.24	27.14	38
	Motorways	31.49	8.44	
Buses	Urban	21.18	53.60	
	Rural	17.39	27.14	38
	Motorways	13.98	8.44	
Motorcycle	Urban	3.76	5.84	
	Rural	2.92	2.76	3
	Motorways	2.49	0.68	

3. RESEARCH METHODOLOGY

A brief introduction about different particle instruments, the test train and the modified pin-on-disc laboratory tests are presented in this chapter.

3.1 Particle measurement instruments

In this thesis, four different types of particle instruments were used. The main instrument was a GRIMM 1.109 aerosol spectrometer. This instrument measured airborne particles 0.25–32 μm in diameter in 31 size intervals and at concentrations from 1 to 2 x 10^6 particles L^{-1} (Peters et al., 2006). The instrument registered number concentrations with a time resolution of 6 seconds. As GRIMM is an optical counter, its stated particle sizes are approximate and dependent on the particle shape and refractive index (Liu and Daum, 2000).

The second device was a TSI™ P-TRAK (Model 8525, referred to hereinafter as P-Trak) condensation nuclei particle counter that measured the number concentration of airborne particles of 0.02–1 μm in diameter with no size resolution (Zhu et al., 2006). Number concentrations were registered with a time resolution of 1 second.

The third instrument was a TSI™ DustTrak (Model 8520, referred to hereinafter as DustTrak) photometer that reported the mass concentration as mg m^{-3}. This is a laser photometer and measures particle concentration roughly corresponding to respirable size fractions. Thus, it registered mainly particles in the 0.1–10 μm diameter range. The instrument is factory calibrated using a test dust (with a density of 2650 kg m^{-3}), which has a size distribution, density and refractive index different from those of the particles measured here. Though the results could only be used as relative measures, they were useful in describing the changes in generated particle mass over time (Cheng, 2008).

The fourth instrument was a scanning mobility particle sizer (SMPS) combining an electrostatic classifier (TSI™ 3071) with a particle counter (TSI™ CPC 3010). The particles are charged in a controlled manner and thereafter sequentially classified according to their electrical mobility. Electrical mobility is transformed to a corresponding particle size (Fissan et al., 1983). The counter was a condensation nuclei counter that, by means of condensation, optically counted particles down to 10 nm in diameter. The size distribution was divided into 110 size classes in the 10-520 nm range. Number concentrations down to a few particles per cm^3 could be registered. The SMPS gave a particle number concentration size distribution every 5.5 min.

3.2 Instrumented test train

In Papers A and B, a series of full-scale field tests was performed using the ~~"~~Gröna Tåget test train Regina 250" (Bombardier Regina) on the regular Swedish intercity tracks (grona tåget website, 2011). The train followed normal traffic operation when it was on main tracks. Parts of the test runs were conducted on a low trafficked track, where the maximum operational speed was only 90 km h^{-1} and the electrical brake was intentionally deactivated. The test train was instrumented to measure and record the speed and the total electrical and mechanical

brake forces on each axle. The data acquisition frequency was 10 Hz. Two sampling points were deployed in these tests.

One sampling point was located 145 mm far from the main brake pad. During braking, it was highly exposed to the particles generated by the main brake pad. The effect of particles from the wheel and rail was also traceable in this sampling point when the train was in an accelerating condition or curve negotiating. We refer to this point as the brake pad sampling point. The other point was located in the middle of the axle. The effect of generated particles from concrete sleepers and ballast was more traceable in it. We refer to this point as the global sampling point. This study used the GRIMM 1.109, DustTrak and P-Trak on each sampling point, and the number and mass concentration of particles recorded every 6 seconds.

In this study, the two-sheet *Prescale*™ films were used to investigate mean contact pressure between brake disc and brake pad. The two-sheet films are composed of A-Film and C-Film. A-Film is coated with a microencapsulated colour-forming material, and a C-Film, which is coated with a colour-developing material (Figure 23a). The A-Film and C-Film must be positioned with the coated sides facing each other. The changes of colour density in the film are dependent on the magnitude of pressure levels in the contact and can be interpreted by manufacturers guideline (Figure 23b).

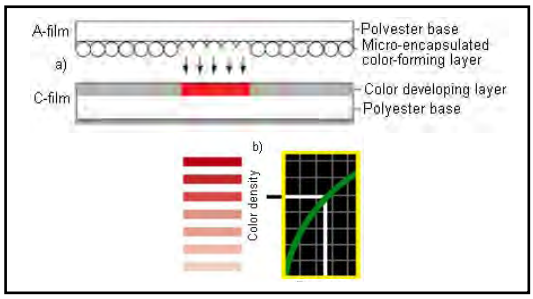

Figure 23. An illustration of how prescale films work.

3.3 Modified pin-on-disc laboratory tests

The laboratory tests were performed using a pin-on-disc machine in a sealed box with a horizontal rotating disc and a dead-weight-loaded pin (Figure 24). The sealed box allowed us to control the cleanliness of the supply air and sampling of air containing only wear particles. The machine could run under stationary conditions with constant applied normal forces of up to 100 N and at constant rotational speeds of up to 3,000 rpm.

A load cell was used to measure the tangential force acting on the pin. The feature of using a displacement sensor in order to measure wear rates of specimens during test running time or measuring the weight of samples before and after the test in order to evaluate the average wear rates of specimens was not used in the achieved tests.

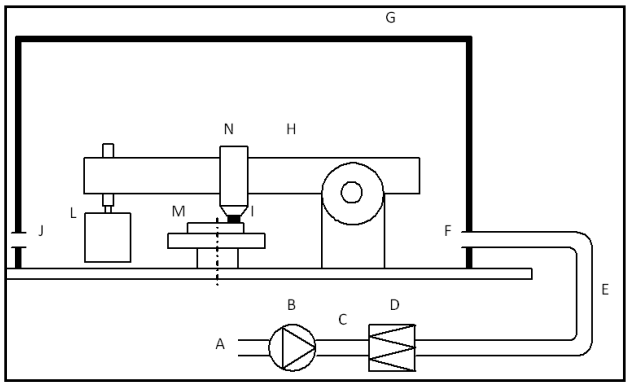

Figure 24. Schematic of the test equipment. A: Room air; B: Fan; C: Flow rate measurement; D: Filter; E: Flexible tube; F: Inlet for clean air, measurement point; G: Sealed box; H: Pin-on-disc machine; I: Pin sample; J: Air outlet, measurement points; L: Dead weight; M: Rotating disc sample, N: Air inside chamber.

The fan (B) took the air from the room (A) and passed it into the chamber (G) via a flow measurement system (C) a filter (D) and through the air inlet opening (F). The connections between the fan, measurement system, filter and chamber were flexible tubes (E). In the sealed box the air was well mixed (N) due to the complicated volume of the pin-on-disc machine (H) and the high air exchange rate. This mixing was verified by registering particle concentrations from the box. The air in the sealed box transported the generated particles to the air outlet (J), where sampling points for the particle measurement devices were situated.

The supply air was set to a flow rate of 7.7 m^3 h^{-1} (2.1 L s^{-1}). The sealed box volume was 0.135 m^3, and the volume of the pin-on-disc machine was approximately 0.035 m^3, giving an approximate air change rate of 77 h^{-1} corresponding to a time constant of 47 s. The measured flow rate varied somewhat during the tests, from 7.7 to 9.2 m^3 h^{-1}. The flow rate measurement system consisted of a straight calibrated tube with separate connections for total and static pressure, measured using an ordinary U-tube manometer. The system was calibrated in the flow interval 2–50 m^3 h^{-1}. The filter used to ascertain a particle-free inlet air was of class H13 (according to the EN 1822 standard) with a certified collection efficiency of 99.95% at maximum penetrating particle size (MPPS).

All of the particle instruments‘ pipes were mounted in point (J). Another P-Trak device was used in the inlet point and its pipe was inserted into the flexible tubes near the inlet opening point (F) in order to measure the cleanliness of inlet air and control the functionality of filter during test running time.

The laboratory simulation in the modified pin-on-disc used the GRIMM 1.109, DustTrak, P-Trak, and SMPS. The number and mass concentration of particles were recorded in the minimum available time of each instrument.

4. SUMMARY OF RESULTS AND APPENDED PAPERS

This chapter summarises the results from the appended papers and the division of works for each paper is presented.

4.1 Summary of appended papers

Paper A
This paper attempted to check the validity of generating airborne wear particles in a laboratory condition with their characteristics in real conditions.

In this regard, we conducted field tests with a running train, instrumented with two sets of P-trak, DustTrak and Grimm devices connected with the two sampling points. The P-Trak® 8525 is an optical particle measurement device that can measure particle diameter in the size interval of 20 nm up to 1 micrometer. The DustTrak® was used to measure particle mass concentration. The Grimm 1.109 is an aerosol spectrometer that counts number of particles from 0.25 micrometer to 32 micrometer in 31 intervals. The Millipore filters were mounted in the Grimm outlets to capture particles for further studies on morphology and matter of particles.

That train was equipped with Becorit 950-1 brake pads and steel disc brakes. The effects of different brake levels on a running train with the speed of 70 km/h in particles size distribution and number concentration were recorded. The particles were collected in the Millipore filters of Grimm device. Furthermore, the activating and deactivating electrical brake on particles characteristics were investigated.

The laboratory simulation used a pin-on-disc machine in a sealed box with a horizontal rotating disc and a dead-weight-loaded pin. The sealed box allowed us to control the cleanliness of the supply air and sampling of air containing only wear particles. The pins were prepared from Becorit 950-1 brake pad and discs were cut from railway steel brake disc similar to field test materials. We used the same particle instruments as a scanning mobility particle sizer (SMPS) in laboratory simulations. This device allowed us to measure particle size distribution for particles with the size 10-520 nm in diameter in 110 intervals.

The SEM and EDX were used to investigate particles morphologies and element composition. The recorded results from particle instruments and SEM images from both tests were in agreement. Both results show a dominant fine peak for particles with a size of around 350 nm in diameter, and a coarse peak with a size of 3-7 μm in diameter. Furthermore, the effects of increasing applied loads in both systems resulted in higher particle concentration in both systems. However, the particle size distribution was independent of the applied loads.

Paper B
Most of the existing railway particle studies were mainly on the stationary measurement, evaluating the particle mass concentration. As the coarse particles have the main contribution in the total particles mass, a few information was documented for the submicron-sized particles. However, new studies show ultrafine particles can cause more severe health effects. In this paper, we investigated particle characteristics near their sources with an on-board measurement.

A series of full-scale field tests was performed using the ―Gröna Tåget test train Regina 250". Four test runs on a part of a Swedish intercity track were performed, where the maximum operational speed was 200 km/h. We considered a special set-up in that train to investigate particle generation in different operational conditions (e.g., activating/deactivating electrical brakes or negotiating curves). Investigating particles sizes, morphology, element composition, and particle size distributions were the main objective of that study.

We designated two airborne particle sampling points: one near a pad–rotor disc brake contact and a second under the frame, but not near a mechanical brake or the wheel–rail contact. The numbers and size distributions of the particles detected were registered.

Two sampling points for airborne particles were designated in the train under the frame. One of the sampling points was near a pad to rotor disc brake contact, and a second global sampling point was chosen under the frame, but not near a mechanical brake or the wheel-rail contact. The first one was highly influenced by brake pad wear debris and the other one was influenced by all of the brake pads, wheel and rail wear debris, as well as re-suspension. In each sampling point, three tubes were linked to three particle measurement devices. Two sets of P-TRAK®, DustTrak® and Grimm devices were used. The P-TRAK® 8525 is an optical particle measurement device that can measure particle diameter in the size interval of 20 nm up to 1 micrometer. The DustTrak® was used to measure particle mass concentration. The Grimm 1.109 is an aerosol spectrometer which counted number of particles from 0.25 micrometer to 32 micrometer in 31 intervals. These two Grimm devices were equipped with Millipore filters in the devices‘ outlets to capture particles for further studies on morphology and matter of particles.

The total number and size distribution of the particles for these two sampling points were registered and evaluated in different situations, including activating and deactivating the electrical brake or train curve negotiating.

During braking, three speed/temperature-dependent particle peaks were identified in the fine region, representing particles 280 nm, 350 nm, and 600 nm in diameter. In the coarse region, a peak was discerned for particles 3–6 μm in diameter. Effects of brake pad temperature on particle size distribution were also investigated. Results indicate that the 280 nm peak increased with increasing temperature, and that electrical braking significantly reduced airborne particle numbers.

A FESEM was used to capture the images from collected particles on filters. Its images captured particles sizing down to 50 nm. Both EDS and ICP-MS methods were used. According to ICP-MS investigation of the filters, the particulate matter mainly comprised Fe, Si, Al, Ca, Cu, and Zn. The higher amounts of some elements—such as Ca, Si, Na, and Al—in the global sampling point filters indicated that ballast and concrete sleepers were the main sources of these particles, although some originated from rails, wheels, brake discs, and brake pads.

Paper C

In this paper, we investigated the particle characteristics generated by organic brake pad-steel brake discs, sintered brake pad-steel brake discs, cast iron brake block-railway wheels, and organic brake block-railway wheels in laboratory conditions. We also attempted to introduce a new index and methodology to compare airborne particles from different material.

In this regard, we used a pin-on-disc machine in a sealed box with a horizontal rotating disc and a dead-weight-loaded pin. The sealed box allowed us to control the cleanliness of the supply air and sampling of air containing only wear particles. The pins were prepared from brake pads, and brake blocks and discs were prepared from steel brake discs and railway wheels, respectively.

The mean contact pressures and sliding velocities were similar to the real operational conditions. Four different types of particle instruments were used, and particle size, particle number concentration, and particle size distributions were investigated. Two P-Trak® devices, one Grimm, one DustTrak® and one SMPS, were employed in a particular set-up. A manual pump was also used to collect particles on Nuclepore® polycarbonate filters. The changes of volume size distributions over time were also investigated. The morphologies of particles were investigated by FESEM and EDX.

According to the results, the relationships between increase of sliding velocity or contact pressure, and the increase of particles concentration, were detected. The number of fine and ultrafine particles generated from sintered brake pads was lower than those for organic brake pads in a similar test condition. The number of ultrafine particles from cast iron brake blocks was higher than those for organic brake blocks in a similar test condition.

In the ultrafine particle region, we recorded a peak at around 70-120 nm in diameter. In the fine particle region, we recorded two peaks at 300-400 nm and at 500-600 nm in diameter. And in the coarse particle region, we recorded a peak at around 3-6 μm in diameter. The fraction of this peak is highly dependent on material composition and test conditions. The effect of material composition on the particle morphologies were also discussed

The new index, AWPER, was introduced in this paper, which was suggested to be used in legislations for the non-exhaust emissions.

Paper D

In this paper, we reviewed most of the recent documented studies about exhaust-emission and non-exhaust emission in rail transport. This work consists of studying adverse health effects, particles size, morphology, chemical compositions, suggested solutions to reduce particles, current legislations, and recorded PM_{10} and other PM values on platforms and compartments. Since the adverse health effects from rail traffic particles are one of the most questionable issues, it was discussed in this work. Furthermore, lung cancer, neurobehavioural impairment, heart attacks, and exacerbated respiratory diseases were recorded for exposure to the diesel exhaust. As it has been discussed, the new legislations in the US and EU were aiming to tighten the limit values for exhaust emissions. A summary of these legislations has been provided.

It has been recorded that the particles from non-exhaust emission are more genotoxic than road particles, as they can affect the amount of chromium, manganese and iron in the commuters‘ blood. The higher rates of mortality, higher tuberculosis notification, and lower life expectancy have been recorded for the residents near high-trafficked railroads. The biomarkers among subway drivers and subway workers were higher than bus drivers. But surprisingly, the incident of heart attacks or cancer was not higher among male subway drivers in comparison to other occupations among men working in subways. For the non-exhaust emission, there is no legislation, although the high mass concentrations of these kinds of particles were recognised before 1909. In this regard, we provided new legislations for outdoor air quality in the US and EU, and also presented a part of the current legislations for the exposure limits for some of materials related to the rail traffic particles.

In this study, we summarised the amount of PM_{10} and $PM_{2.5}$ for both above ground and underground rail traffics. For the above grounds, we made a subclassification for rail traffic with diesel locomotives.

The element compositions of the non-exhaust emission particles were also discussed based on the differences in the results. However, iron was the dominant one among all of the studies. It was interesting that in the oldest investigation, which was conducted during 1910s, the amount of iron in the particles was around 60%, and over these years no significant differences occurred for this fraction.

Some of the recent images from diesel particles and wear particles from railway wheels, organic brake pads, sintered brake pads, organic brake blocks, and cast iron brake blocks are presented in the current study. The differences between wear particle morphologies were more likely attributable to the difference in material compositions and the dominant wear mechanisms.

Finally, we reviewed the current alternatives that impact the exhaust emission and non-exhaust emissions. For the non-exhaust emission, we considered those papers that aimed to reduce wear among components, which are usually subjected to a wear process in rail traffic.

5. DISCUSSION

The results are discussed in this chapter.

In this thesis, we investigated some aspects of airborne particle characteristics from rail traffic. We checked the feasibility of reproducing operational real situations in laboratory conditions and validated our results. Particle characterisation (i.e., size in diameter, mass concentration, number concentration, and morphologies) were investigated for different brakes against steel brake discs and different brake blocks against railway wheels. The particle mass concentration from the sintered brake pads was lower than organic brake blocks, whereas the particle mass concentration from organic brake blocks was higher than cast iron brake blocks. These differences were attributed to different material compositions in these components. The differences in abrasivity and wear mechanisms were investigated in the particle morphologies.

A part of the results in this thesis was investigating the particle sizes. The three size regions were identified and dominant peaks were distinguished respectively. According to the results, a similar dominant peak around 280-350 nm was recognised for all test conditions. We separated peaks for 280 nm and 350 nm when we conducted our tests with organic brake pads and steel disc brakes in the sliding velocity 12.4 m/s. In other cases, there was no peak in the 280 nm. However, one peak in that region was quite obvious. It must be noted that when we used two different devices with the two different measurement principles, we received the same results. Meanwhile, those results were in agreement with similar studies by other researchers. Thus, these similarities are independent to measurement techniques or particle instruments.

However, there were some limitations in our particle instruments, which influenced our results. One of particle instruments that was used to investigate size distribution had a 6 s time resolution, and the lower limit of that device was 250 nm, which was close to the detected peak. In another particle instrument, the lower limit was 10 nm but the size distribution evaluated every 5.5 min. Currently, there is no explanation for these similarities in the results. We plan to apply particle instruments with higher time resolutions in the future in order to check factors that can result in this phenomenon. Studying the changes of particle morphology is another technique that may shed more light on this issue. Furthermore, we plan to measure particles‘ shape factors (i.e., sphericity, convexity and elongation) at the same time. Hopefully, the simultaneous measurements of wear rate, particle morphology and particle size distributions in a low time resolution assist us in understanding the unclear characteristics of airborne particles.

In the field of non-exhaust emission (non-combustion or non-tailpipe emission), a few studies have been conducted and consequently some limited legislations can be addressed. However, this part is quite well-known in road transport, and it deals with airborne particles from tires, braking material and roads. One of the existing legislations prohibits or limits the use of studded tires. The adverse health effects of using studded tires and their effects on PM10 are documented in Dahl et al. (2006), Lindbom et al. (2007) and Gustafsson et al. (2009). These kinds of results are motivations to ban or limit using studded tires. The use of studded tires is prohibited in the UK, Germany and 10 states in the US (Götzfried, F., 2008). There are seasonal restrictions for using them in Austria, Switzerland, Sweden, Norway, and most states in the US.

There is lack of similar methodology for non-exhaust emission in rail transport. The suggested airborne wear emission rate (AWPER) in this thesis is suggested to be used as an applicable index in this context. It can be used by clients to rank their sub-contractors during outsourcing products. Also, It can be used in legislation to force different manufacturers to optimise their products by considering the AWPER indices in their products. Furthermore, it can be used as a factor to evaluate emission tax for non-exhaust sources in rail traffic. In that case, the train operators and wagon owners will be willing to retrofit their systems (e.g., applying braking materials with lower particle emission rates) or even use bogies with higher steering performance. All of these efforts will result in lower airborne particles emission in rail transport.

As it was mentioned in Paper C, our results were based on the used set-up and the first 600 s of the sliding time. It is also suggested to control the effects of different particle density in the calibration of the measurement. One applicable solution is to use five or six different calibrations to avoid any biased results or conclusions. The particle instrument can be calibrated for different pair materials such as: organic brake pad-steel disc brakes, sintered brake pad-steel disc brakes, wheel-rails, organic brake block-railway wheels, and cast iron brake block-railway wheels. These kinds of calibrations help us obtain more reliable values for AWPERs.

Studying the adverse health effect of airborne particles was not the objective of this thesis. Yet, we have commented about the prioritisation in concerning iron in the studies. In fact, iron is the main dominant element in our study and the studies of other researchers. However, if we compare the $\frac{Mn}{Fe}$ or $\frac{Cu}{Fe}$, $\frac{Cr}{Fe}$ and the cumulative concentration of copper, iron, manganese, silicon, and chromium to the proposed OELs for these materials, we will understand the risk of those non-ferrous compound are higher.

6. CONCLUSIONS AND FUTURE WORK

This chapter presents answers to the research questions and future work is suggested.

6.1 Answers to the research questions

- *What is the state-of-the-art knowledge of airborne particles generation mechanisms, characteristics and sources?*

  We created an information survey and reviewed almost all of the documented research and studies. A part of that review is presented in Chapter 2.3. We classified the main particle sources to the exhaust emission and non-exhaust emission (Table 4). That review is summarised in paper D.

  These data were the backbone for further studies. Almost all of the documented studies were achieved based on stationary measurements by focusing on PM values and tracing some limited elements. We conducted field tests to distinguish particle sources and obtained some information about particle morphology and their sizes (Paper A and B).

  The generation mechanism for airborne particles is partly described in Chapter 2.4. We also suggested a schematic model in Paper A, which shows the interactions between different affective factors leading to airborne particles. However, this information is the first step towards a robust model. We suggest some future work (Chapter 6.2) with the aim of helping us understand the causes for the observed phenomena and results.

- *What is the element composition of airborne particles generated by a running train?*

  We investigated 32 elements during our field tests. We applied two sampling points during field tests and attempted to recognise the more likely sources of those elements. The detailed information of those results is presented in Paper B.

- *How can the composition of airborne particles be classified with respect to their health effects?*

  We presented some fundamental information about adverse health effects of airborne particles in Chapter 2.1. We also discussed the adverse health effects from exhaust emission and non-exhaust emission in Paper D. In that paper, we made critical comments on the single focus on iron in many research papers. It seems that the high amount of iron has fascinated many researchers and made them skip materials such as manganese, copper, nickel and chromium. The cumulative effects of particles and their adverse health effect on more sensitive people, such as children and people with pre-existing health problems, must be studied deeply. Future work in that area is suggested in Section 6.2.

- *What are the effects of different operational conditions on the airborne particles characteristics?*

  The effects of curve negotiating, accelerating, decelerating, activating, and deactivating electrical brakes were studied and reported on in Paper B.

- *Is it feasible to study the generation of airborne particles with reduced testing in a controlled laboratory environment?*

  In Paper A, we checked the feasibility to generate airborne wear particles in laboratory conditions. Those laboratory tests were limited to representing the condition of sliding contacts. In Chapter 6.2, we suggest further work to investigate the effect of rolling contact fatigue by using proper laboratory test benches.

- *How large a portion of the total amount of non-exhaust particles originates from wear processes?*

  As it was described in Chapter 2.4, there are numerous parameters that influence both the wear process and the conversion process, where wear debris are converted to airborne particles. According to Table 4, there are also a number of factors, besides wear, that affect the non-exhaust emission rate. The maintenance level, the operational condition, the applied technology in rail vehicles and infrastructures, the commuter cultural levels, and the traditional habits are all factors that affect the non-exhaust emission rate.

- *What is the best criterion to quantify airborne particle emission factors?*

  In Paper C, we introduced the airborne wear particle emission rate (AWPER) and described the set-up to measure and calculate this factor. This factor can, for example, be used in legislations as a measure for evaluating and controlling the amount of airborne particles generated by wear.

  And finally the main question:

- *How can the emission of airborne particles from a running train be efficiently controlled?*

  This question was the main objective of the entire project, and it is only partly addressed by this thesis. In Paper D, we reviewed the different suggested solutions to reduce the particle emission in rail transport. We have also emphasised the lack of legislations in this issue. In Section 6.2, we suggested future work with two approaches. In one approach, we propose to investigate other angles of particle generation mechanisms and attempt to simulate these mechanisms. In the other approach, our efforts would be focused on how to affect the number and size of the generated particles.

6.2 Future work

Almost all of the research about the changes in the contact surfaces are limited to studying the differences between specimen before and after testing. We are attempting to create knowledge on particle characteristics and to relate that to wear regimes and mechanisms in order to develop methods and tools to control the effect of these causes.

This thesis does not consider the following items and subjects that are proposed for future work:

- Particle emission from rolling contact of wheel and rails.

- Particle emission from wheel and switches (tongue blade).

- Particle emission from overhead line or third rail with electric collectors.

- Particle emission by erosion caused by piston effect, spraying sand or wind.

- The effect of electrical discharge from third rail or overhead lines in the characteristics of generated particles.

- Computer simulations to predict temperature, pressure, wear, and airborne particles generation from the non-exhaust sources, particularly wheel-rail contact and braking materials.

- Investigation of tribochemical films during contact of braking materials against brake discs or railway wheels.

- Creating innovative devices that collect airborne wear particles.

- Investigation on fluidising particles during the wear process.

- Investigation of the morphology of wear particles and its relation to transitions from one wear regime to another.

- Investigating disc radial groove effects on the particle characteristics from brake discs and brake pads.

- Investigating the relation between wear coefficients, friction coefficients, particles shape factors, flash temperatures, particle size distributions, and AWPERs for different materials.

7. REFERENCES

Barghini, F., Bruni, S., and Lewis, R., 2009, Railway wear, Chapter 6, Eds, Lewis., R, Olofsson, U., Wheel-rail interface Handbook, CRC

Batchelor, A.W., Stachowiak, G.W., and Cameron, A., 1986, The Relationship between Oxide Films and the Wear of Steels, Wear, Vol. 113, 1986, pp. 203-223.

Blanchi, C. and Blanchi T., 2007, Malignant Mesothelioma: Global Incidence and Relationship with Asbestos, Industrial Health, 45 (3), Pages:379-387

Cheng, Y. H., 2008, Comparison of the TSI model 8520 and Grimm Series 1.108 portable aerosol instruments used to monitor particulate matter in an iron foundry. Journal of Occupational and Environmental Hygiene 5(3) (2008) 157-168

Clarke, M., 2008, Wheel rolling contact fatigue (RCF) and rim defects investigation to further knowledge of the causes of RCF and to determine control measures, Rail Safety and Standards Board.

Cheremisinoff, N. P, 2002, Handbook of Air Pollution Prevention and Control, Butterworth-Heinemann.

Dahl, A., Gudmundsson, A., Swietlicki, E., Bohgard, M., Blomqvist G., and Gustafsson, M., 2006, Size-Resolved Emission Factor for Particle Generation Caused by Studded Tires – Experimental Results. 7th International Aerosol Conference, American Association for Aerosol Research (AAAR), St. Paul, Minnesota, USA (2006).

EPA NAAQS, (2011). 40 Code of Federal Regulation part 50., Online ‹http://www.epa.gov/air/criteria.html› (accessed 2011.04.18)

EPA PM Research, (2011). Online ‹http://www.epa.gov/airscience/quick-finder/particulate-matter.htm› (accessed 2011.04.03)

EPA RIN 2060-AM06, (2008). Online ‹http://emerginglitigation.shb.com/Portals/f81bfc4f-cc59-46fe-9ed5-7795e6eea5b5/lm-preamble.pdf› (accessed 2011.03.03)

EU Directive 2008/50/EC, (2008). On ambient air quality and cleaner air for Europe, 2008. Online ‹http://eur-lex.europa.eu/LexUriServ/LexUriServ.do?uri=OJ:L:2008:152:0001:0044:EN:PDF› (accessed 2011.03.03)

EU Directive 2008/232/CE, (2008). Concerning a technical specification for interoperability relating to the „rolling stock‘ sub-system of the trans-European high-speed rail system. Online ‹http://eur-lex.europa.eu/LexUriServ/LexUriServ.do?uri=OJ:L:2008:084:0132:0392:EN:PDF› (accessed 2011.04.03)

EU Directive 2000/53/EC,(2000). On end-of life vehicles. Online ‹http://eur-lex.europa.eu/LexUriServ/LexUriServ.do?uri=CONSLEG:2000L0053:20050701:EN:PDF› (accessed 2011.04.03)

Elliott, B. 2006, Compressed Air Operations Manual, McGraw-Hill Professional; 1 edition

Elstorpff M., and Mathieu, M., 2008, Development, Testing and TSI-Certification of the New Bogie Mounted Tread Brake Unit for Freight Cars, Tagung Moderne Schienenfahrzeuge, 132, Pages 106-114

Fissan, H.J., Helsper, C., and Thielen, H.J, 1983, Determination of particle size distribution by means of an electrostatic classifier, J. Aerosol Sci. 14 (1983), pp. 354–359.

Ford, R., 2007, Regenerative braking boosts green credentials, Railway Gazette International, 02 July 2007

Gfatter, G., Berger, P., Krause, G., Vohla, G., 2007, Basics of brake technology, 3rd edition, Knorr-Bremse

Goodal, R. M., Brunib, S., Mei, T. X., 2006, Concepts and prospects for actively controlled railway running gear Vehicle System Dynamics: International Journal of Vehicle Mechanics and Mobility, 44(S1), Pages 60 – 70

Gustafsson, M., Blomqvist, G.,Anders Gudmundsson, Dahl,A., Jonsson, P., and Swietlicki, E., 2009, Factors influencing PM10 emissions from road pavement wear, Atmospheric Environment, 43(31), Pages 4699-4702

Golhd, D.R., 2008, Vulnerability to Cardiovascular Effects of Air Pollution in People with Diabetes, Current Diabetes Reports, 8(5), 333-335,

Guy, R.H., 1999, Metals and the Skin: Topical Effects and Systemic Absorption, Informa Healthcare

Götzfried, F., 2008, Policies and Strategies for increased Safety and Traffic Flow on European Road Networks in Winter. In: The Proceedings of the Final Conference of the COST Action 353 - Winter Service Strategies for Increased European Road Safety - Bad Schandau (Dresden), Germany, 26-28th May 2008

Hawley JK., 2005, Assessment of health risk from exposure to contaminated soil. Risk Anal, 5, Pages 289-302

Hawthorne V. T.1996, Recent improvements to three-piece trucks, Proceedings of the ASME/IEEE joint railroad conference, p 151-161.

Hecht M.,2001, European freight vehicle running gear: today‘s position and future,demands, Proc. of the Inst. of Mech. Engrs., Part F, Journal of Rail and Rapid Transit, 215, p 1-11.

Hinds, W, 1999, Aerosol Technology: Properties, Behavior, and Measurement of Airborne Particles, Wiley-Interscience; 2 edition

Hopke, P. K. 2009, Contemporary threats and air pollution, Atmospheric Environment, 43, Pages 87-93.

Hostynek, JJ, 2004,Chapter 6, Permeability of Human Skin to Metals And Paths for Their Diffusion, Dermatotoxicology, Sixth Edition, CRC

Jönsson Per-Anders, 2002, Freight wagon running gear- a review, Report 2002:35, KTH Railway Technology, Stockholm

Krech S, J.R. McNeill, J. R., Carolyn Merchant, C.,2003, Encyclopedia of World Environmental History, Routledge; 1 edition (July 1, 2003)

Lee, W. R. ,1973,Emergence of occupational medicine in Victorian times, British Journal of Industrial Medicine,30, 118-124.

Li, W. and Hopke, P.K. 1993, Initial Size Distributions and Hygroscopicity of Indoor Combustion Aerosol Particles, Aerosol Science and Technology, 19(3) Pages 305 – 316

Lindbom, J., Gustafsson, M., Blomqvist, G., Dahl, A., Gudmundsson, A., Swietlicki, E., Ljungman, AG., 2007, Wear particles generated from studded tires and pavement induces inflammatory reactions in mouse macrophage cells, Chem Res Toxicol. 20(6), pages 937-46.

Liu, Y., and Daum, P.H., 2000, The effect of refractive index on size distribution and light scattering coefficient derived from optical particle counters, J. Aerosol Sci. 31(8) (2000) 945-957

Liudvinavičius, L., Lingaitis, L.P., 2007, ELECTRODYNAMIC BRAKING IN HIGH-SPEED RAIL TRANSPORT, TRANSPORT, XXII(3), pages 178–186

Ludema, K.C., Meng, H.C., 1995, Wear models and predictive equations: their form and content, WEAR, 181-183, Pages 443-457

Nadal MJ, Théorie de la stabilité des locomotives, Part 2: Mouvement de lacet. Annls Mines Vol. 10 (1896), p. 232.

Nielsen GD, Ovrebø S. 2008, Background approaches and recent trends for setting health-based occupational exposure limits: a mini review, Regul Toxical Pharmacol. 51(3), Pages 253-69.

Oberdörster. G., Fitzpatrick, J., Maynard, A., Donaldson, K., Castranova, V., Ausman K.,Carter, J., Karn, B., Kreyling, W., Lai, D., Olin, S., Monteiro-Riviere, N., Warheit, D., Yang, H., and A report from the ILSI Research Foundation/Risk Science Institute Nanomaterial Toxicity Screening Working Group, 2005, Principles for characterizing the potential human health effects from exposure to nanomaterials: elements of a screening strategy, PARTICLE AND FIBRE TOXICOLOGY, 2(8), Pages: 1-35

Peters, T., Ott, D., and Shaughnessy, PT., 2006, Comparison of the Grimm 1.108 and 1.109 portable aerosol spectrometer to the TSI 3321 aerodynamic particle sizer for dry particles, J. Annals of Occupational Hygiene 50 (2006) 843-850

Podol'skii, A., Kitanov, S.,2008, Analysis of Eddy-Current and Magnetic Rail Brakes for High-Speed Trains, The Open Transportation Journal, 2008, 2, 19-28

Ruzer, S. and Naomi H., 2005, Aerosols Handbook: Measurement, Dosimetry and Health Effects, CRC

Schenk, L., Hansson, S.V., Rudén, C., and Gilek,M., 2008, Occupational exposure limits: a comparative study, Regulatory toxicology and pharmacology, 50(2), Pages: 261-270

Schenk, L., 2011, Setting occupational exposure limits, Doctoral thesis, KTH, Stockholm, Sweden

Schofield, K., 2002, Overview of magnetic brakes, Interfleet Technology ltd, RSSB, UK

Sippola, M. R., and Nazaroff, W. W. ,2002, Particle deposition from turbulent flow: Review of published research and its applicability to ventilation ducts in commercial buildings. Rep. No. LBNL-51432, Lawrence Berkeley National Laboratory, Berkeley, Calif.

Stachowiak, G.W.,Batchelor, A.W., 2007, Engineering Tribology, Elsevier, 3rd ed.

Stachowiak, G.W., 2005, Wear: Materials, Mechanisms and Practice, Wiley,

Subramani, J. P. 1971. PhD thesis, University of Cincinnait, OH, 1971. Cited in Councell et al. (2004). Tire wear particles as a source of zinc to the environment', Environmental Science and Technology, 38, pp. 4206–4214.

Sundell, J. 2004, On the history of indoor air quality and health, Indoor Air, 14, Pages 51-8.

Tager I. B., 2005, Ch. 24 Health effects of aerosols*:* mechanisms and epidemiology, Eds Ruzer L. S., Aerosols Handbook: Measurement, Dosimetry and Health Effects, CRC

Wickens, A. H., 2009, Comparative stability of bogie vehicles with passive and active guidance as influenced by friction and traction Vehicle System Dynamics: International Journal of Vehicle Mechanics and Mobility, 47(9), Pages 1137 – 1146

Williams, T.I.,Schaaf, Jr,Burnette, E., 2000, A History of Invention: From Stone Axes to Silicon Chips, Checkmark Books

Xue J, Zartarian V, Moya J, Freeman N, Beamer P, Black K, Tulve N, Shalat S., 2007, A meta-analysis of children's hand-to-mouth frequency data for estimating nondietary ingestion exposure, Risk Anal. 27(2), Pages 411-20.

Yamaguchi, Y., 1990, TRIBOLOGY OF PLASTIC MATERIALS, ELSEVIER SCIENCE PUBLISHERS B.V.,

Zhu, Y., Yu, N., Kuhn, T. and Hinds, WC., 2006, Field comparison of P-Trak and condensation particle counters, J. Aerosol Sci. 40 (2006) 422-430

Website addresses:

AAR website; http://www.aar.org/

ACGIH website; http://www.acgih.org/home.htm

ASTDR website; http://www.atsdr.cdc.gov/

EEA; http://www.eea.europa.eu/publications/emep-eea-emission-inventory-guidebook-2009

Gröna Tåget website; http://www.gronataget.se

IARC; http://monographs.iarc.fr/ENG/Classification/index.php

Railway-technical website, www.railway-technical.com

UIC website; http://www.uic.org/

http://uk-air.defra.gov.uk/reports/cat07/1103150849_UK_2011_CLRTAP_IIR.pdf

A

A study of airborne wear particles generated from organic railway brake pads and brake discs

Saeed Abbasi,
Jens Wahlström,
Lars Olander,
Christina Larsson,
Ulf Olofsson,
Ulf Sellgren

Accepted for publication in

Wear Journal, special issue Nordtrib 2010

A study of airborne wear particles generated from organic railway brake pads and brake discs

Saeed Abbasi[1], Jens Wahlström[1], Lars Olander[2], Christina Larsson[3], Ulf Olofsson[1], Ulf Sellgren[1]
1-KTH Machine Design, SE 10044, Stockholm, Sweden
2-KTH Building Service Engineering, SE 10044, Stockholm, Sweden
3-Bombardier Transportation Sweden AB, SE-721 73 Västerås, Sweden
Corresponding author's email: sabbasi@md.kth.se

Abstract: Brake pads on wheel-mounted disc brakes are often used in rail transport due to their good thermal properties and robustness. During braking, both the disc and the pads are worn. This wear process generates particles that may become airborne and thus affect human health. The long term purpose of 'Airborne particles in Rail transport' project is to gain knowledge on the wear mechanisms in order to find means of controlling the number and size distribution of airborne particles. In this regard, a series of full-scale field tests and laboratory tests with a pin-on-disc machine have been conducted. The morphology and the matter of particles, along with their size distribution and concentration, have been studied. The validity of results from the pin-on-disc simulation has been verified by the field test results. Results show an ultra-fine peak for particles with a diameter size around 100 nm in diameter, a dominant fine peak for particles with a size of around 350 nm in diameter, and a coarse peak with a size of 3-7 μm in diameter. Materials such as iron, copper, aluminium, chromium, cobalt, antimony, and zinc have been detected in the nano-sized particles.

Key words: Railway brake pads, airborne particles, wear.

1. INTRODUCTION

The main concerns about airborne wear particles are environmental. Health effects of the inhaled nano-sized particles have been studied extensively but most studies have been focused on combustion processes [1]. Only a few studies have been carried out to investigate the emission of wear particles in rail transport.

Gustafsson recently presented a review of these works [2]. Furthermore, investigations in the Stockholm [3], London [4] and Budapest [5] underground systems have shown particle mass concentrations in the range of 300-1000 μg/m³ much higher than the upper limit for urban traffic in the EU, which is 50 μg/m³ per day [6].

The purpose of the research presented in this paper is to experimentally evaluate the number, concentration, size distribution, morphology, and element analysis of airborne wear particles from typical organic brake pads. A series of field tests and their simulations on a pin-on-disc machine using the same sliding velocity and contact pressure have been performed.

2. EXPERIMENT SET-UP

Two different set-ups were considered for the experiments. A series of full-scale field tests were performed with a Regina X54 test train. The main reason for conducting the pin-on-disc laboratory tests was to clarify the results from the field test (e.g., to be able to distinguish the airborne wear particles that originate from the brake disc from other particles in the surrounding environment).

In both field and laboratory tests, typical organic brake pads (Becorit 950-1) were tested against steel brake discs. The chemical compositions of these braking components are reported in [7]. Airborne wear particles were collected on filters during testing and subsequently analysed with a scanning electron microscope (SEM) and energy-dispersive X-ray spectroscopy (EDX).

2.1. Field tests

A Regina X54 train was equipped with particle measurement instruments at two different sampling points. The field tests were conducted in normal traffic conditions on a regular Swedish inter-city track over the course of three days.

The test route is shown in Figure 1. The maximum allowable operational speed of the train was 200 km/hr when both mechanical and electrical brakes were active (although the speed was reduced to 180 km/h when the electrical brake was deactivated on purpose). The train followed normal traffic operation when it was on the main track. Some tests were conducted on an industrial track, where the maximum operational speed was only 90 km/h. As that area was rather isolated from disturbance and noise, most of the data was gathered from that region. The climatic conditions of this route during test runs are reported in [7].

The compact brake caliper used was RZS, and Becorit 950-1 was used as the brake pads. The brake disc was made from steel. The train's weight was 62,500 kg and the brake percentage was 150% during operation. The test train was equipped with measurement devices to measure and record speed, and total electrical and mechanical brake force on each axle. The data acquisition frequency was 10 Hz. Figure 2 shows four K-type thermocouples inserted in the main brake pad. Particles generated from pad-disc contact were investigated by particle measurement devices (see Figure 3).

Figure 1. Field test route, with the industrial track between Nyköping and Flen highlighted.

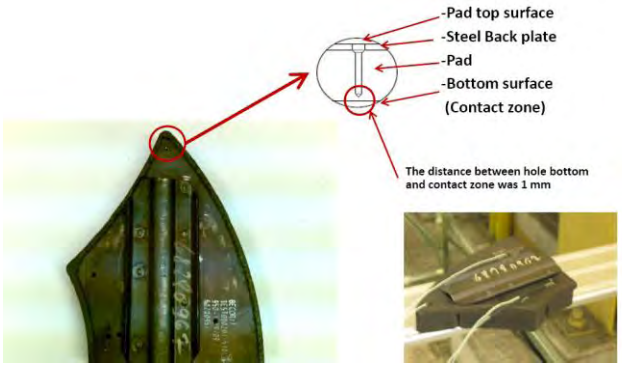

Figure 2. Thermocouples position in brake pad.

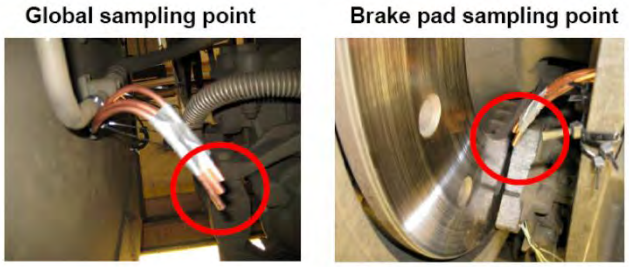

Figure 3. Particle measurement devices, along with connecting tubes arrangement.

Two sets of DustTrak ,Grimm and P-Trak were used in two different sampling points (see Figure 3). One sampling point was located 145 mm far from the main brake pad. During braking, it was highly exposed to the particles generated by the main brake pad. We refer to this point as the brake pad sampling point. The other point was located in the middle of the axle. The effect of generated particles from concrete sleepers and ballast was more traceable in it. We refer to this point as the global sampling point.

2.2. Laboratory tests

The laboratory tests were performed using a pin-on-disc machine with a horizontal rotating disc and a dead-weight-loaded pin (Figure 4). The machine ran under stationary conditions with constant applied normal forces of up to 100 N and at constant rotational speeds of up to 3,000 rpm. A load cell was used to measure the tangential force acting on the pin. Each pin was also equipped with a K-type thermocouple inserted by drilling, and placed 1 mm from the nominal contact area between the pin and the disc.

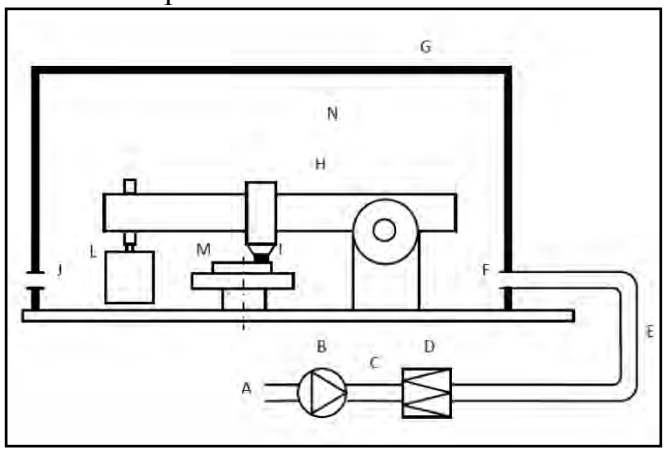

Figure 4. Schematic of the test equipment [8]. A: Room air; B: Fan; C: Flow rate measurement; D: Filter; E: Flexible tube; F: Inlet for clean air, measurement point; G: Closed box (Chamber); H: Pin-on-disc machine; I: Pin sample along with thermocouple; J: Air outlet, measurement points; L: Dead weight; M: Rotating disc sample, N: Air inside chamber,

The pin-on-disc machine was operated in a sealed box in order to control the cleanliness of the incoming air. This setup was previously used by Sundh [8], Olofsson [9,10] and Wahlström et al. [11] to study the airborne particles generated by simulated wheel-rail contact and passenger car brakes.

The filter used to ensure particle-free inlet air was of class H13 (according to standard EN 1822), with a certified collection efficiency of 99.95 percent at maximum penetrating particle size.
The 110 mm diameter disc specimens were cut from a used piece of wheel-mounted steel brake disc from a Regina X54 train by using a water jet, while the 10 mm diameter pins were sawn out mechanically from a Becorit brake pad. Before testing, the disc specimens were cleaned ultrasonically for 20 min with both heptane and methanol. The test conditions are presented in Table 1.

Table 1. Contact conditions in the laboratory tests

No.	Load(N)	Sliding Velocity(m/s)	Time(min)
1	60	12.4	20
2	40	12.4	20
3	20	12.4	20

2.3 PARTICLE MEASUREMENT DEVICES

In this study, four different types of particle measurement instrument were used. The main instrument was a Grimm 1.109 aerosol spectrometer. The second device was a PTRAK particle counter. The PTRAK was a condensation nuclei counter that measured the number concentration of airborne particles between 0.02 and 1 μm in diameter. The third instrument was a scanning mobility particle sizer (SMPS) which used only on laboratory tests. The SMPS combined an electrostatic classifier (TSI 3071) with a particle counter (TSI CPC 3010). The fourth instrument was a DustTrak counter, which reported the mass concentration in mg/m³. It was used to measure particles between 0.1 and 10 μm.

The technical specification and set-up of all of the measuring devices were akin to those in previous studies by Olofsson et al. [8,9]

3. RESULTS

Figures 5, 6 and 7 show field test results based on applying different brake conditions. Different brake levels and deactivating electrical brakes on purpose were the main concern of these series of field tests. All of these results were registered by running the test train on the aforementioned industrial track (Figure 1) at an operational speed of 70 km/h. Every six seconds, the total number of particles was recorded by the Grimm spectrometer and the concentration was recorded by DustTrak. In all of these graphs, the magnitude of train speed, brake force, brake pad temperature and particle concentration have been illustrated as a normalised value in the vertical axis. The maximum values of these factors in the illustrated time interval have been presented using the number 1, and other values are scaled proportionally.

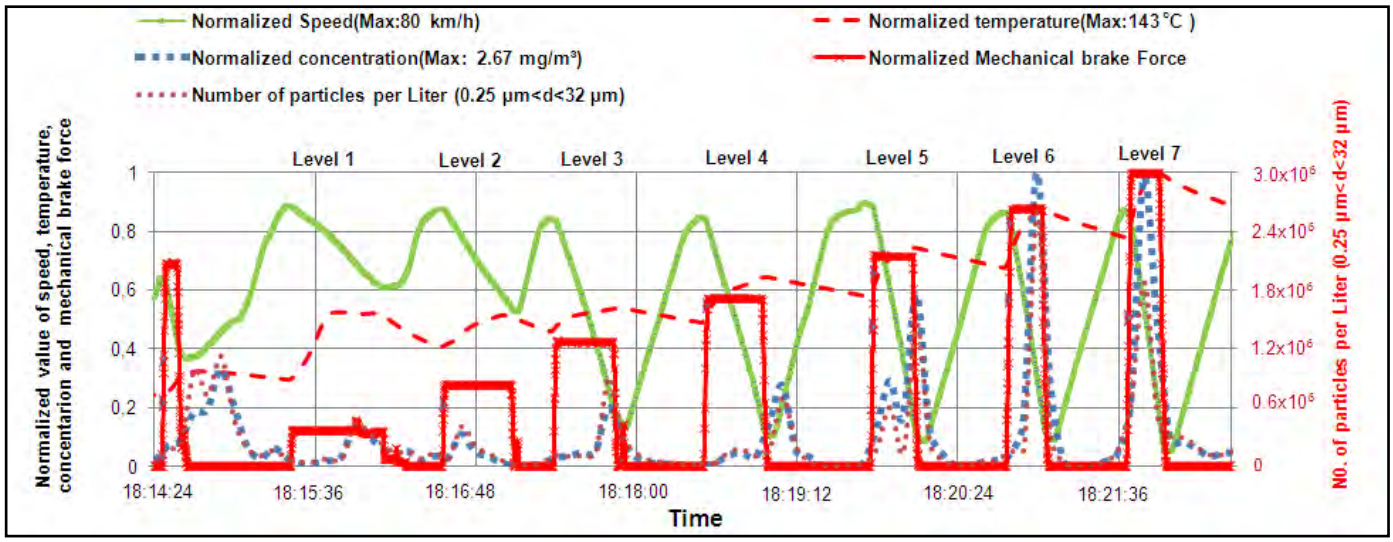

Figure 5. Effects of the different brake levels on the concentration and total number of the recorded particles, brake pad temperature and train speed reduction in normal traffic (brake pad sampling point). The train speed was 70 km/h and the electrical brake was deactivated on purpose.

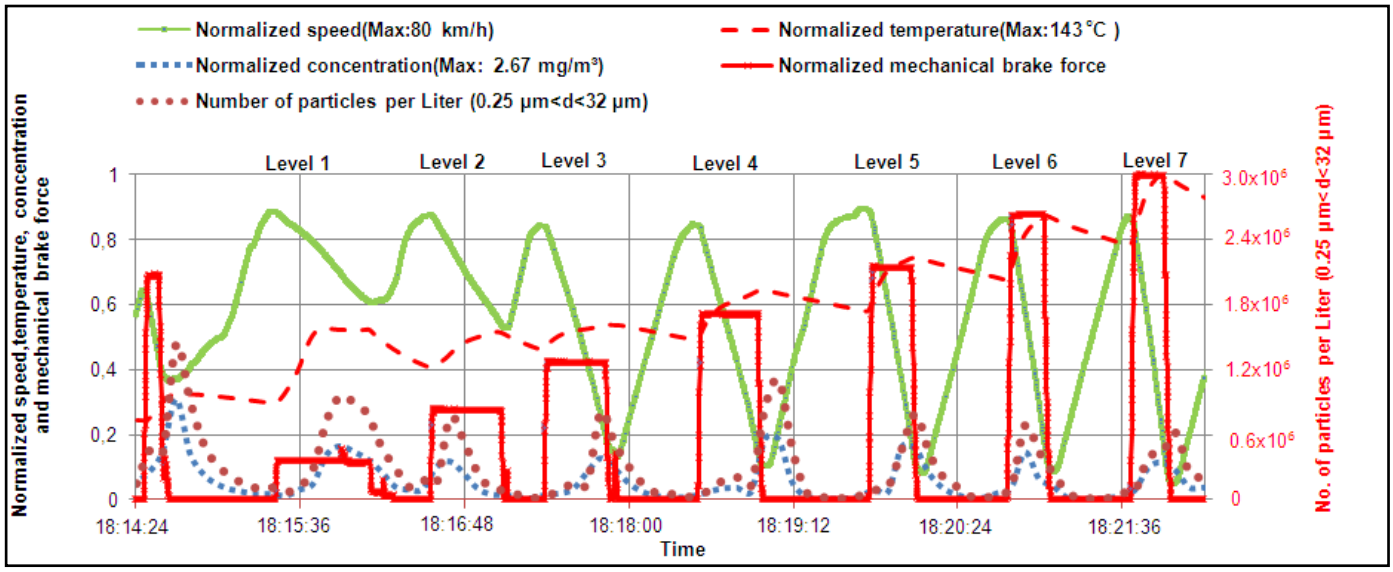

Figure 6. Effects of the different brake levels on the concentration and total number of the recorded particles, brake pad temperature and train speed reduction in normal traffic (global sampling point). The train speed was 70 km/h and the electrical brake was deactivated on purpose.

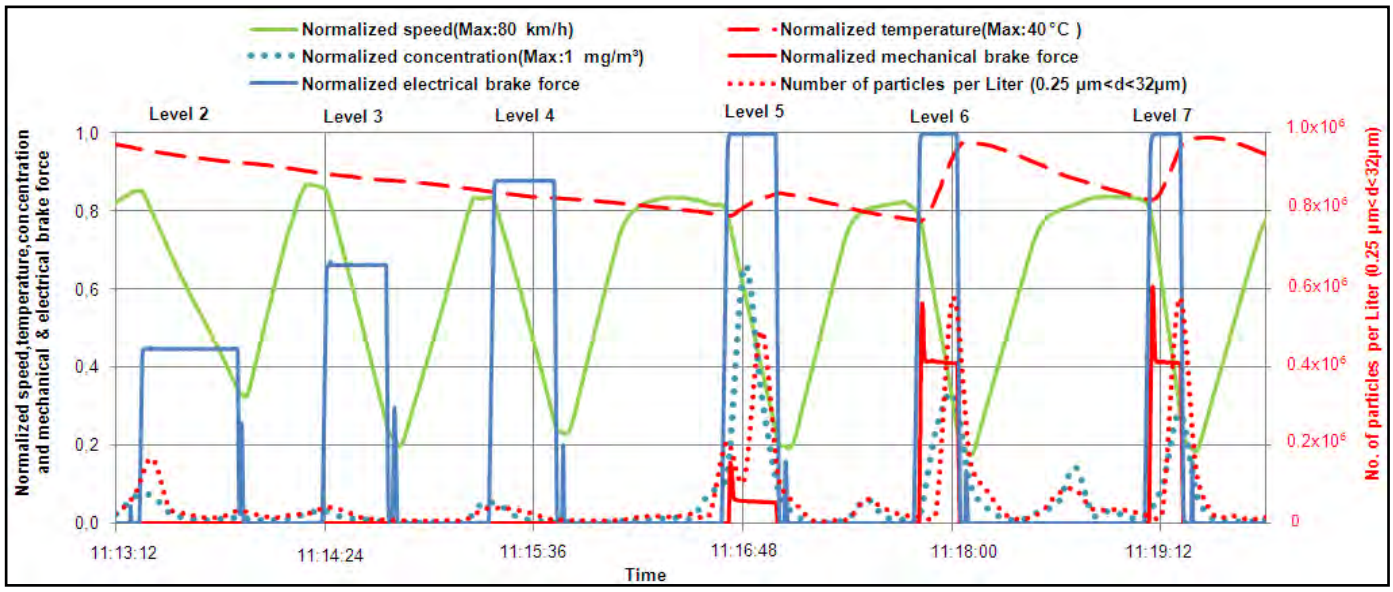

Figure 7. Effects of the different brake levels on the concentration and total number of the recorded particles, brake pad temperature and train speed in normal traffic (brake pad sampling point). The train speed was 70 km/h and the electrical brake was activated.

An elements analysis by EDX from a piece of the new brake pad is depicted in Figure 8. Figures 9 and 10 present the SEM images for typical particles. A typical result by SMPS from a pin-on-disc test is shown in Figure 11. Figures 12 and 13 show particle size distribution based on Grimm measurement results. In Figures 13, 14, 15 and 16 the pin-on-disc machine had been used to simulate braking force. Loads 60 N, 40 N and 20 N reproduced brake levels 7, 5 and 3, and a sliding velocity of 12.4 m/s in pin-on-disc simulated a speed of 70 km/h in a train, according to disc size and wheel and brake radius in a train. One repetition was conducted for each test condition during pin-on-disc simulation. The particle volume distributions in Figure 15 were based on an assumption of a spherical shape for the particles.

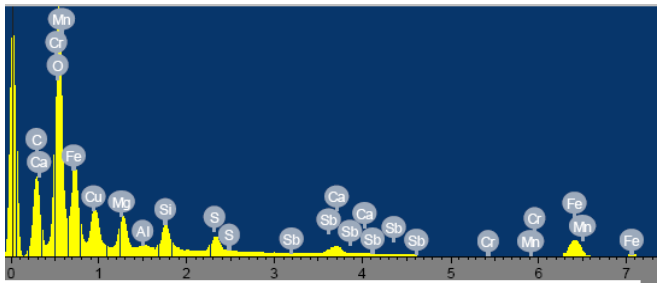

Figure 8. A typical spectroscopy result from a part of Becorit brake pad by EDX.

Figure 9. A typical image by SEM from particle that was collected during the field tests in the local sampling point filter.

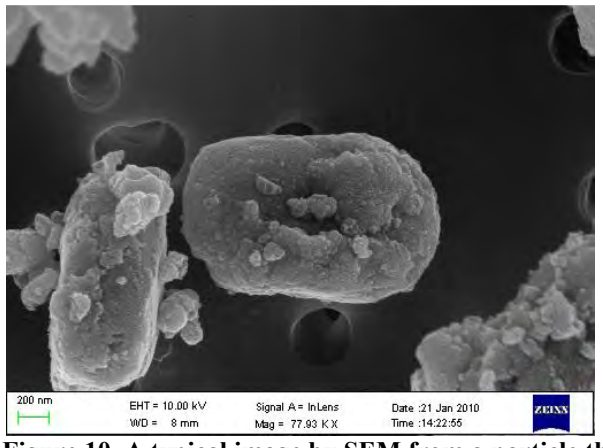

Figure 10. A typical image by SEM from a particle that was collected during pin-on-disc simulation.

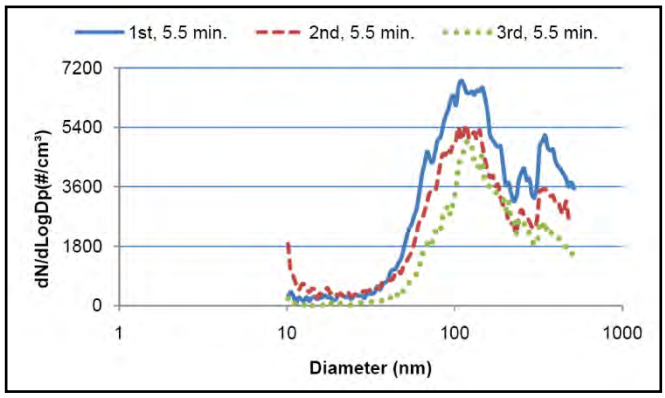

Figure 11. A typical size distribution for particles sized less than 520 nm in diameter by SMPS (Load: 60 N , Sliding velocity: 12.4 m/s).

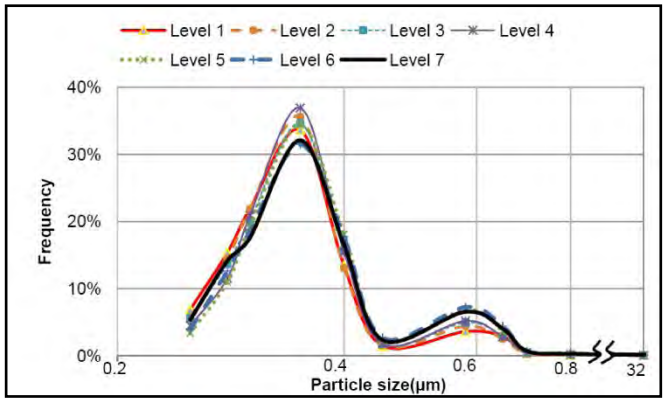

Figure 12. Particle size distribution in different brake levels when the electrical brake was deactivated on purpose. Results were recorded by Grimm (brake pad sampling point).

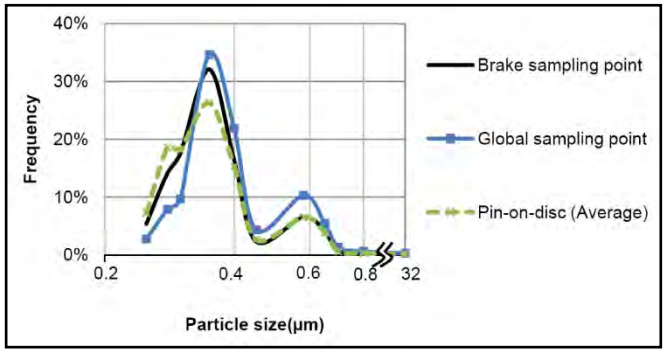

Figure 13. A comparison between particle size distribution in field test sampling points and pin-on-disc simulation (results were recorded by Grimm).

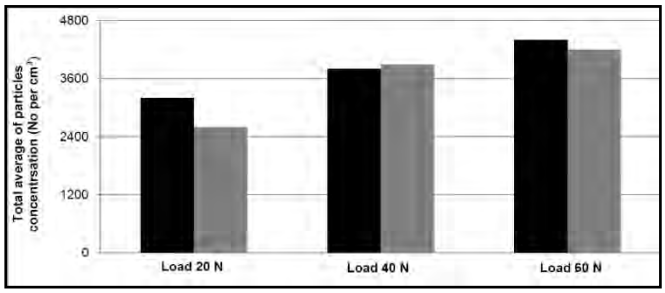

Figure 14. The total average number of particles when different loads were applied in 2 repetitions (the grey and black column) during pin-on-disc simulation. Results were recorded by Grimm. (Sliding velocity: 12.4 m/s, Time: 20 minutes.)

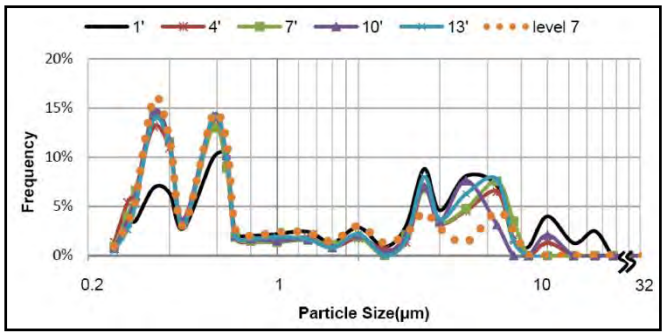

Figure 15. A comparison between volume distribution in field tests and pin-on-disc simulations every three minutes. Results were recorded by Grimm (Load: 60 N, Sliding velocity: 12.4 m/s).

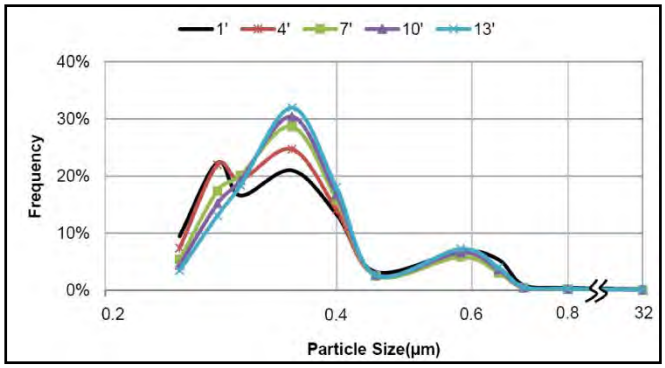

Figure 16. A typical running-in effect on the size distribution of particles in pin-on-disc simulations every three minutes. Results were recorded by Grimm. (Load: 60 N, Sliding velocity: 12.4 m/s).

4. DISCUSSION

In any unlubricated contact, the loss of material is associated with frictional heat, vibration, wear debris, and tribochemical reactions in the contacting surfaces. Actually, these factors have

the potential to interact each other and even influence the wear process [13]. A fraction of the wear debris can be transformed into the airborne particles . Figure 17 shows a schematic view of a mechanism which lead to the generation of airborne particles in wear processes. Concerning these factors and providing a model to predict the particle formation is a long-term objective of the current project which needs further studies.

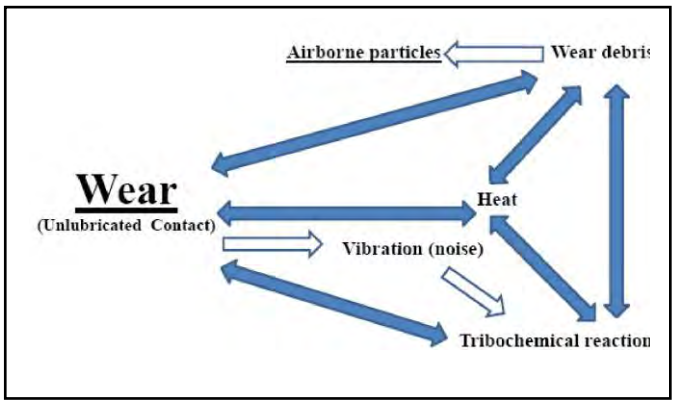

Figure 17. A schematic illustration of mechanisms which lead to generation of the airborne particles in the unlubricated contacts wear processes.

As depicted in Figures 5 and 13, both field tests and laboratory tests confirm that wear rate and particle generation increases with increasing braking force. This result is in line with previous studies by Olofsson et al. [9,10]. Figures 5 and 6 illustrate particle generation and concentration during mechanical braking. Effects of different mechanical brake levels are evident in Figure 5. As only one sampling point was located near the brake pad, and the fact that the apparent contact area was only a portion of the nominal brake pad contact surface and also moved in the nominal contact area during braking, the discrepancies were small. In contrast, the global point (Figure 6) shows no considerable changes between the total amount of the detected particles and their concentration during the application of different mechanical brake levels. Re-suspension and dilution were believed to be the main reasons for this phenomenon.

Figure 7 presents a comparison between different brake levels when both mechanical and electrical brakes were used simultaneously. For the first four levels, there was no particle generation and the brake force applied by the electrical system was sufficient to stop the train. However, in levels 5, 6 and 7, the mechanical forces were added to the total brake system in order to satisfy the requested deceleration rate. Although the driver dictated the magnitude of the deceleration rate manually by using different brake levels, the train computer struck a balance among electrical brake force, mechanical brake force, and the speed and weight of the train. This process caused only slight differences in the magnitudes of the applied mechanical brake forces for levels 6 and 7. Obviously, applying mechanical brake forces caused particle generation at these levels. As four brake pads were mounted on each train axle, we assumed the total amount of the brake force in each brake pad was one quarter of the total recorded applied brake force on that axle.

Figures 9 and 10 illustrate a typical particle from the field test and the laboratory test. Besides their similarity in appearance, iron and copper were the main elements in both particles. The element analysis results of brake pads, in particles and in bulk (Figure 8), detected metals such as: iron, copper, cobalt, chromium, molybdenum, aluminum, antimony and zinc, which is in line with results in [2, 12].

A typical result of SMPS is shown in Figure 11. According to the tri-modal distribution, a peak occurred near the ultra-fine region around 100 nm in diameter, and two other peaks occurred around 280 and 350 nm in diameter in the fine particle region. These two peaks in the fine particle region were also detected by Grimm (Figures 12 and 16), although SMPS and Grimm used different principles in measuring particles. It is also noteworthy to mention the indecency of the particle size distributions at different brake levels, as shown in Figure 12.

Figure 13 presents a typical comparison between size distribution of two sampling points during both the field test and laboratory simulation. Although the coincident of their peaks are

acceptable, there are some discrepancies between their frequencies. This can be explained by particle characteristics. Airborne particles are a mixture of liquid droplets or solid particles in the air. As the laboratory conditions were set up to provide air flow without any solid particles or droplets, these discrepancies are reasonable. Besides, according to Hind [14], sub-micron-sized particles are susceptible to size enlargement due to a high magnitude of surface-to-volume ratio and van der Waals forces. During field tests, the probability of size enlargement was higher than in laboratory conditions due to drawing in unfiltered air and using longer tubes. Two peaks in the fine region, of around 350 nm and 600 nm in diameter, have been illuminated in Figures 15 and 16. These observations are in agreement with Wahlström's work [11], although his studies focused on automobile brake pads.

Typical volume distributions from a field test and a pin-on-disc test are presented in Figure 15. All results confirm that coarse particles with sizes of 3-7 μm in diameter are generated during the application of similar braking force.
Figures 15 and 16 show typical particle size and volume distributions over time. The size distribution started from a tri-modal distribution and ended with a bimodal distribution. This time-dependency may be explained by a mild-severe transition and the brake pad material stabilisation process during operation. This process was treated in the field test by first running the train on the test tracks and applying the brakes before starting the

field tests. As these changes can affect laboratory simulations, the average values of these data have been used in Figures 13 and 14.

5. CONCLUSION

The following general conclusions can be made based on an analysis of the test results:
1. The pin-on-disc test is a robust method for studying airborne particle generation, based on the similarity of morphology and size distributions, with the prerequisite that the same contact conditions are used in the laboratory tests as in the field tests.
2. Deactivating electrical brakes or applying higher levels of mechanical brakes increase particle generation from brake pads.
3. Three particle size regimes were identified:
    a. In the ultra-fine particle region, a peak of around 100 nm in diameter,
    b. In the fine particle region, three peaks of 280 nm, 350 nm and 600 nm in diameter, with the 350 nm peak dominating.
    c. In the coarse particle region, a peak of around 3-6 μm in diameter.

6. ACKNOWLEDGMENT

This work formed a part of the activities of the Railway Group of the Royal Institute of Technology. The author acknowledges the valuable assistance from Dr Wobushet Sahle of the Royal Institute of Technology, and Dr Anders Jansson from Stockholm University.

7. REFERENCES

[1] **A. Madl, K. Pinkerton**, Health effects of inhaled engineered and incidental nanoparticles, *Critical Reviews in Toxicology, 2009, Vol. 39, No. 8, 629-658*

[2] **M. Gustafsson,** Airborne particles from the wheel–rail contact. In: **R. Lewis, and U. Olofsson,** (eds.), *Wheel–Rail Interface Handbook, pp. 550–575. CRC Press; 2009*.

[3] C. **Johansson, P. Johansson**, Particulate matter in the underground of Stockholm *Atmospheric Environment, 2003, Vol.37*

[4] **A. Seaton, J. Cherrie,M. Dennekamp, K. Donaldson, J. Hurley, C Tran**. The London underground: Dust and Hazard to health. *Occup Environ Med 2005; 62(6), 355-362*

[5] **I. Salma, T. Weidinger, and W. Maenhaut**, Time-resolved mass concentration, composition and sources of aerosol particles in a metropolitan underground railway station, *Atmospheric Environment 2007, Vol 41*

[6] European Commission (EC), *Air quality stds. 2008-07-01*

[7] **S. Abbasi, U. Olofsson, L. Olander, C. Larsson, U. Sellgren, and A. Jansson.** A field test study of airborne wear particles From a running train. *J. Rail Rapid transit., 2011, In press*

[8] **J. Sundh, U. Olofsson,** Wear testing in relation to airborne particles generated in a wheel-rail contact, *Lubr. Sci., 2009, 135-150*

[9] **U. Olofsson, L. Olander, A. Jansson,** Towards a model for the number of particles generated from a sliding contact, *Wear, 2009, Volume 267, Issue 12, 2252-2256*

[10] **U. Olofsson, L. Olander**, On the identification of wear modes and transition using airborne wear particles generated from sliding steel-on-steel contact, 2006

[11] **J. Wahlström, A. Söderberg, L. Olander, L. Olofsson L and A Jansson**, Airborne wear particles from passenger car disc brakes, *Engineering Tribology, 2010, Vol:224, 179-188*

[12] **E. Fridell, M. Ferm, A. Björk, and A. Ekberg,** On-board measurement of particulate matter emissions from a passenger train. *J. Rail Rapid Transit., 2010, In press*

[13] **I. Hutching,** *Tribology: Friction and Wear of Engineering Materials, CRC Press 1992*

[14] **WC**,**Hinds,** *Aerosol Technology: Properties, Behavior, and Measurement of Airborne Particles*, 2nd ed., Wiley, NY, 1999.

B

A field test study of airborne wear particles from a running regional train

Saeed Abbasi,
Lars Olander,
Christina Larsson,
Anders Jansson,
Ulf Olofsson,
Ulf Sellgren

Accepted for publication in

IMechE, Part F: Journal of Rail and Rapid Transit

A field test study of airborne wear particles from a running regional train

Saeed Abbasi[1], Lars Olander[2], Christina Larsson[3], Anders Jansson[4], Ulf Olofsson[1], Ulf Sellgren[1]

1-KTH Machine Design, SE 10044, Stockholm, Sweden
2-KTH Building Service Engineering, SE 10044, Stockholm, Sweden
3-Bombardier Transportation Sweden AB, SE-721 73 Västerås, Sweden
4-Stockholm University Applied Environmental Science, SE 106 91, Stockholm, Sweden

Corresponding author's email: sabbasi@md.kth.se

Abstract

Inhalable airborne particles have inverse health affect. In railways, mechanical brakes, the wheel–rail contact, current collectors, ballast, sleepers, and masonry structures yield particulate matter. Field tests examined a Swedish track using a train instrumented with particle measurement devices, brake pad temperature sensors, and speed and brake sensors. The main objective of this field test was to study the characteristics of particles generated from disc brakes on a running train with an on-board measuring set-up.

Two airborne particle sampling points were designated, one near a pad–rotor disc brake contact and a second under the frame, not near a mechanical brake or the wheel–rail contact; the numbers and size distributions of the particles detected were registered and evaluated under various conditions (e.g. activating/deactivating electrical brakes or negotiating curves).

During braking, three speed/temperature-dependent particle peaks were identified in the fine region, representing particles 280 nm, 350 nm, and 600 nm in diameter. In the coarse region, a peak was discerned for particles 3–6 µm in diameter. Effects of brake pad temperature on particle size distribution were also investigated. Results indicate that the 280 nm peak increased with increasing temperature, and that electrical braking significantly reduced airborne particle numbers.

FESEM images captured particles sizing down to 50 nm. The ICP-MS results indicated that Fe, Cu, Zn, Al, Ca, and Mg were the main elements constituting the particles.

Keywords: *airborne particles, elemental content, morphology, rail transport.*

Nomenclature / Abbreviations

BoBo:	In this axle arrangement, all two-axle bogies are driving
Bo2:	In this axle arrangement, one two-axle bogie is driving while the other is trailing
DMA:	First driving motor car in an electric multiple unit
DMB:	Last/second driving motor car in an electric multiple unit
EDX:	Energy-dispersive X-ray spectroscopy
EC:	European commission
FESEM:	Field emission scanning electron microscope
IARC:	International agency for research on cancer
ICP-MS:	Inductive coupled plasma mass spectrometry
NRMM:	Non-road mobile machinery
PM:	Particulate matter (PM_{10} ,$PM_{2.5}$, and PM_1)
RZS:	Compact brake calliper unit for wheel-mounted brake disc (from Knorr-Bremse)
SMPS:	Scanning mobility particle sizer
UIC:	International union of Railways
OPC:	Ordinary Portland cement

1. Introduction

Particle emission is of concern for the inverse effects on both environment and human health. Most of the research in this field has been focused on engine-emission. In this regard, many different legislations have been directed. Euro VI emission, Tier 4 and 97/68/EC NRMM directive are some of the latest legislations which introduced some limitations for the amount of NOx, HC, CO and PM value in the engine exhaust. Soot particles from engine emission, which are mainly carbon-based, are reported as carcinogen by IARC [1]. They are consequently regarded as a major health issue. The airborne particles generated by electric railways and subways, originate from other sources than combustion engines. Examples of such other sources are wear in the wheel-rail contact and in mechanical brakes. Particles from these sources are of a different character than soot particles, in terms of size distribution and composition, since they contain a significant amount of metals and minerals. According to IARC, particles containing asbestos, talc, nickel, and *hexavalent chromium* compounds are regarded as carcinogens [1]. This implies that the mechanisms that generate these particles must be better understood, in order to be able to control them.

Olofsson [2] and Abbasi et al. [3, 4] studied the size and morphology of airborne particles from different brake pads and brake blocks by simulating real operational conditions on a modified pin-on-disc machine. Sundh et al. [5] used the same set-up and reported the size and morphology of airborne particles from wheel and rail contact.

Recently, Samla [6] and Gustafsson [7] have reviewed most of the latest works in the field of non-engine emission from railway traffic based on stationary measurements. Particle morphology, particle toxicology, particle element composition, PM values and also size of coarse particles were special issues which were investigated by different authors in their stationary measurements.

One of the few published on-board measurements was conducted by Fridell et al. [8], who reported particle characteristics and emission factors for wear particles from a running Regina train. They investigated particles size in 7 intervals and aimed to investigate 27 elements among collected particles. The curve negotiation effects were not traceable in his work as they used one sampling point that was located between the two coaches.

As it has been presented, most of the research on airborne particles was based on measures of the PM value. The PM value is, however, a mass-based criterion. This means that it contains no information of characteristic particle properties that are important from a health effect point of view [9]. The fact that we are obliged to use an average particle value by operating on the PM with a factor, makes it problematic to evaluate the effect from different operating conditions, such as braking, accelerating, and curve negotiation, on the size distribution and material content of the airborne particles that are generated in these cases. The lack of information of the sub-micron sized particles generated by a running train was the main motivation for performing the presented study.

The present study investigates the comparative number and size distribution of airborne wear particles from a running regional train. The train was instrumented by two sets of three different particle measurement devices which collected particles from two different sampling points. The distance difference from the sampling points to the main particles sources caused different effects on the recorded results. The morphologies and elemental compositions of the collected particles were also studied. Various real operational conditions, such as train acceleration, train deceleration, or train curve negotiating, were taken into account.

2. Experimental set-up

A series of full-scale field tests was performed using the ~~–~~Gröna Tåget test train Regina 250" (Bombardier Regina) [10]. The 340 km test route is presented in Fig. 1. Four tests runs were conducted under normal traffic conditions on this regular Swedish inter-city tracks over the course of three days.

Fig. 1. The field test route, with the low trafficked track between Nyköping and Flen

The climatic conditions and train operational speeds are presented in Table 1. The train's maximum allowable operational speed was 200 km h^{-1} when both mechanical and electrical brakes were active (the speed was reduced to 180 km h^{-1} when the electrical brake was intentionally deactivated). The train followed normal traffic operation when it was on main tracks. Parts of the test runs were conducted on a low trafficked track, where the maximum operational speed was only 90 km h^{-1}. That area was green and less influenced by other man-made particles. It was fairly isolated from disturbances and artifacts; therefore most data related to mechanical braking was gathered from this part of the test route.

The train unit weighed 62,500 kg and the braking ratio was 150% during operation. The braking ratio denotes the ratio of brake force to vehicle mass. The axle arrangement of the test train was BoBo–Bo2 and it was equipped with two kinds of bogies. The DMA was equipped with FLEXX passive Regina 250 soft bogies and the DMB with standard Regina bogies. The test train was instrumented to measure and record the speed and the total electrical and mechanical brake forces on each axle; the data acquisition frequency was 10 Hz. The compact brake calliper used was RZS with Becorit 950-1 used as the brake pads. The brake disc was made of steel.

Table 1 . The climatic conditions and train operational speeds on four test runs

Test runs and Date	Positions and conditions	Part 1	Part 2	Part 3	Part 4	Part 5
		Västerås–Stockholm	Stockholm–Nyköping	Nyköping–Flen	Flen–Eskilstuna	Eskilstuna–Västerås
	Approximately distance (km)	100	110	50	40	45
Test run 1 Date: 2009-09-28	Dry bulb (°C)	11–14	9–12	9–12	8–11	6–10
	Relative humidity	52 ± 5%	55 ± 5%	57 ± 5%	71 ± 5%	75 ± 5%
	Weather	Sunny	Sunny	Sunny	Rainy	Rainy
	Max. train speed (km h^{-1})	200	200	90	200	200
Test run 2 Date: 2009-09-29	Dry bulb(°C)	4–9	4–9	5–10	5–10	5–10
	Relative humidity	55 ± 5%	53 ± 5%	55 ± 5%	55 ± 5%	55 ± 5%
	Weather	Sunny	Sunny	Sunny	Sunny	Sunny
	Max. train speed (km h^{-1})	200	200	90	200	200
Test run 3 Date: 2009-09-29	Dry bulb(°C)	5–10	5–10	6–12	4–10	4–10
	Relative humidity	55 ± 5%	55 ± 5%	50 ± 5%	52 ± 5%	55 ± 5%
	Weather	Sunny	Sunny	Sunny	Sunny	Sunny
	Max. train speed (km h^{-1})	200	200	90	200	200
Test run 4 Date: 2009-09-30	Dry bulb(°C)	5 –10	5–10	6–12	4–10	4–10
	Relative humidity	56 ± 5%	55 ± 5%	55 ± 5%	52 ± 5%	52 ± 5%
	Weather	Sunny	Sunny	Sunny	Sunny	Sunny
	Max. train speed (km h^{-1})	200	200	90	200	200

K-type thermocouples were used to measure the temperature in the brake pads. Fig. 2 shows four K-type thermocouples inserted into one of the brake pads. We refer to this as the main brake pad, and it was mounted in the bottom, outer brake disc of the third axle of the first car.

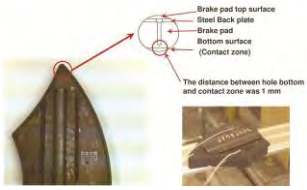

Fig. 2. Detailed specifications of the k-type thermocouples mounted in the brake pad

Table 2 presents briefly information about technical specifications and material composition of

brake pads, brake discs and wheels in the test train. The similar information is also presented for overhead lines, concrete sleeper OPC and rails of the aforementioned route track.

Table 2. The technical specification and elemental composition of key parts in this study

Name	Standard	Main element	Some other elements
Wheels	Luccini, Grade superlose	Fe	C, Si, Mn, Cr, V, Ni,
Brake discs	-	Fe	C, Si, Mn, Cr, V, Mo
Organic brake pads	UIC 541-3	C	Fe, Cu, Zn ,Si, Al, Ti, Pb, Ca, Sb, Ba, Mn, Mg, Co, Cr, Mo, V
Rails	UIC 861-3, Grade 900	Fe	C, Si, Mn, Cr
Overhead lines	DIN EN 50149	Cu	Ag, Mg
Concrete sleeper(OPC)	BS EN 13230	Ca	Al, K, Na, Mg

Two sampling points were deployed in these tests (Fig. 3). One sampling point was located 145 mm away from the main brake pad. During braking, it was highly exposed to the particles generated by the main brake pad. The effect of particles from wheel and rail was also traceable in this sampling point when the train was in accelerating condition or curve negotiating. We refer to this point as the brake pad sampling point.

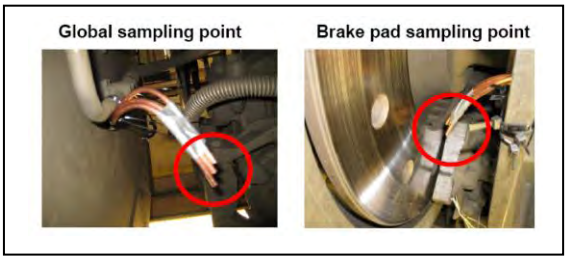

Fig. 3. Two sampling points, brake pad sampling point (right) and global sampling point (left)

The other point was located in the middle of the axle. The effect of generated particles from concrete sleepers and ballast was more traceable in it. We refer to this point as the global sampling point.

This study used three types of particle measurement instruments on each sampling points. The main particle measurement instrument was a GRIMM 1.109 optical aerosol spectrometer. This instrument measured airborne particles 0.25–32 μm in diameter in 31 size intervals and at concentrations from 1 to 2 x 10^6 particles L^{-1}. The GRIMM instrument worked at a flow rate of 0.072 m^3 h^{-1} [11]. Millipore filters were mounted in the GRIMM devices to collect airborne particles during runs; these filters were changed after each run. The particles collected on filters were analyzed using FESEM, EDX, and ICP-MS methods.

The second device was a TSI's P-TRAK® (Model 8525, referred to hereinafter as P-TRAK) condensation nuclei particle counter that measured the number concentration of airborne particles 0.02–1 μm in diameter. There was no size resolution between the upper and lower limits [12].

The third instrument was a TSI's DustTrak® (Model 8520, referred to hereinafter as DustTrak) counter that reported the mass concentration in mg m^{-3}. This was a laser photometer that could

measure particle concentrations corresponding to respirable size fractions; it thus measured particles 0.1–10 μm in diameter. The instrument had a factory calibration with standardized test dust (with a density of 2650 kg m^{-3}), which had a size distribution, density, and refractive index different from those of the particles measured here. Though the results could only be used as a relative measure, they were useful in discerning the changes in generated particle mass over time [13].

3. Results

The GRIMM devices were also used to collect particles on filters; the elemental compositions of these particles are presented in Table 3.

Table 3. The comparative percentile weights of 35 elements detected in the filters determined using the ICP-MS method; all values in percent

	Run	Fe	Cu	Zn	Ca	Mg	Al	Sb	Na	Ni	Mn	Ba	Cr
Brake Pad	1	65	10.1	4.4	2.9	2.2	1.8	1.4	0.5	7.1	0.6	2.6	0.8
Global	1	60.2	9.7	3.9	5	4	5.7	1.8	3.2	1.1	0.6	0.2	1.2
Brake Pad	2	66.2	10.7	4.5	3.5	3.7	1.6	2.8	0.5	3.6	0.7	0.8	0.6
Global	2	63.9	7.4	3.1	5.3	4.8	5.3	2.3	3.4	0.6	0.7	0.3	0.6
Brake Pad	3	65.8	9.5	3.8	4.2	3.4	3.7	2.4	1.2	1.3	0.7	0.8	0.5
Global	3	62.8	8.5	3.3	5.4	4.1	6	2.6	2.2	1	0.7	0.3	0.7
Brake Pad	4	64.7	9.9	3.9	4.9	4	2.6	2.9	1.6	0.7	0.7	0.4	0.7
Global	4	59	8.1	3	6	4.9	6	2.6	3.7	0.5	0.7	0.2	0.5
Notes:													
a. The amounts of K, Si, As, and U were above the detection limit only in the global filters.													
b. The amounts of B, Be, Se, Cd, P, S, Th, and Tl were under the detection limit in all filters in both locations.													
c. The percentile weights of Li, Ag, As, U, Bi, Co, Rb, Pb, V, Sn, Sr, Ti, and Mo were under 0.5%.													
d. Regarding limitations of the ICP-MS method, C, F, O, H, and N were not investigated, so all presented percentile weights were comparative values.													
e. The unused Millipore filters contain Ca in addition to C, H, F, and O; the amounts of other elements in the filters were negligible. The filter composition has no effect on the results as the relative comparative weights were discussed.													
f. The amounts of Ti and Sn were above the detection limit in the global filters when *whole* filters from the fourth run were digested.													
g. Hydrofluoric and nitric acids were applied to all filters in the digestion process.													

Hydrofluoric and nitric acids were used in digesting the filters; after digestion, the ICP-MS was

used to determine the amounts of 35 elements contained in the remaining particles. The amounts of B, Be, Se, Cd, P, S, Th, and Tl were under the detection limit in all filters in both locations. Some other elements, such as K, Si, As, and U were above the detection limit only in the global filters which meant the amount of these elements in the global filters were higher than their amount in the brake pad filters. It should be noticed that the detection limits in ICP-MS method varies among different elements. For instance, the ICP-MS detection limit for Si is thousands times higher than the ICP-MS detection limit for U [14]. In order to have a fair judgment in the results of both filters, the weight results of elements which were detectable in both filters were taken into account in order to calculate each element percentile weight. As some elements such as C, H, F, N and O were not measurable in the ICP-MS, we used the comparative percentile weight and summarized data in Table 3 for elements. The comparative percentile weight of each element represents the weight ratio of that element to the summation weight of all of detected elements in both filters. Fe, Cu, Zn, Ca, Mg, and Al were the main elements constituting the particles.

In the filters collecting particles from the sampling point near the brake pad, the amounts of Fe, Cu, and Zn were higher than in the filters collecting particles from the global sampling point. In contrast, the amounts of Ca, Al, Mg, Na, Si, As, U, and K in the filters from the global sampling point were higher. The differences in percent between the sampling points in the amounts of other elements were too small and random to be significant.

The morphologies of the collected particles were investigated using an FESEM. Figs. 4–8 present a representative selection of images of those particles. Most coarse particles have geometrical diameters of approximately 3–6 μm (Figs. 4 and 5). Some of the fine and ultrafine particles were agglomerated with other particles (Figs. 5-8).

Figs. 9 illustrate the EDX mapping results of a small portion of investigated filters. Fig. 9(a) shows the EDX result of brake pad filter; corresponding to Fig. 4(a). Fig. 9(b) shows the EDX result from collected particles in global filter corresponding to Fig. 4(b). It should be noted that Ni was detected in only the brake pad filter where as K was detected only in the global filter.

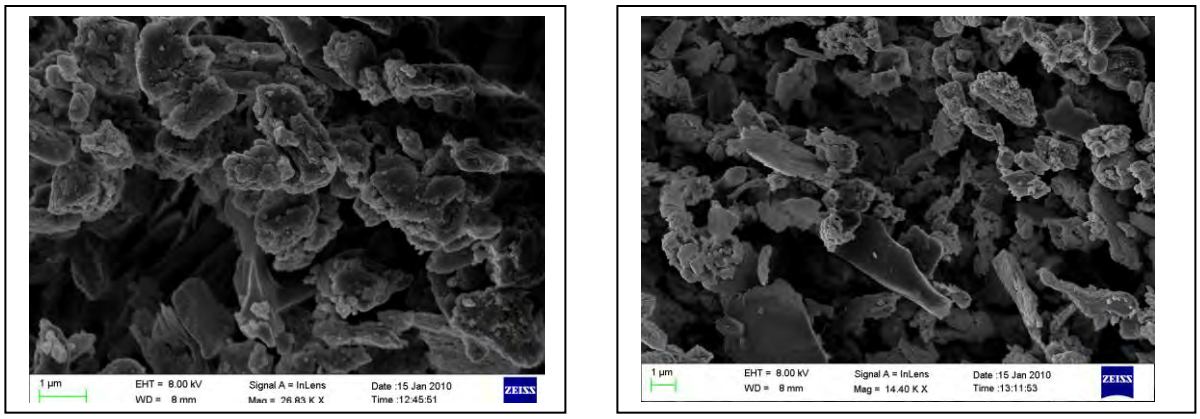

Fig. 4. Overview of particles collected on the second run; most coarse particles have a geometrical diameter of approximately 3–6 µm; (a) in the brake pad filter and (b) in the global filter

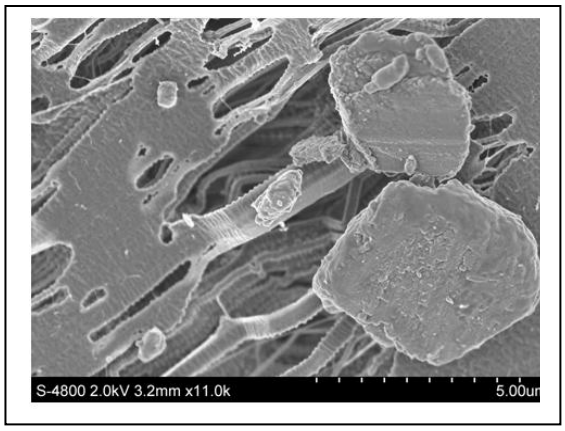

Fig. 5 Another image of particles collected in the brake pad filter on the second run, showing both coarse and fine particles against the porous texture of the filter, and the agglomeration of fine and ultrafine particles with the coarse ones.

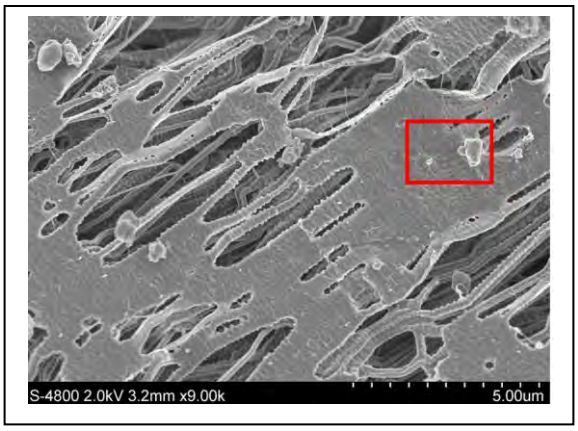

Fig. 6. Image of fine particles collected in the brake pad filter on the second run; highlighted portion is magnified 5× in Fig. 7.

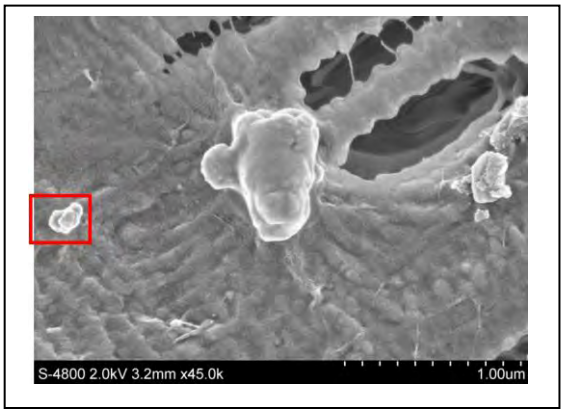

Fig. 7. Image of particles under 300 nm in diameter collected in the brake pad filter on the second run; highlighted portion is magnified 5× in Fig. 8

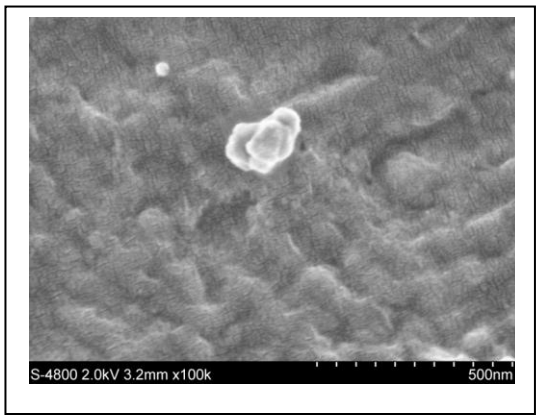

Fig. 8. Image of ultrafine collected particles under 100 nm in diameter collected in the brake pad filter on the second run.

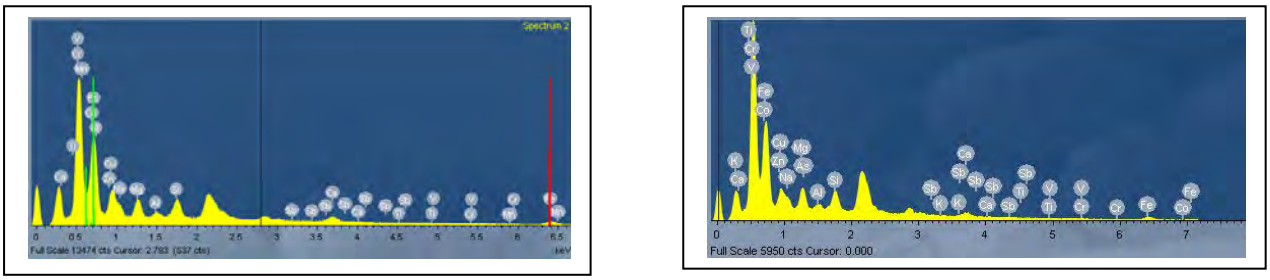

Fig. 9. EDX results from collected particles; (a) in the brake pad filter; corresponding to Fig. 4(a), and (b) in the global filter; corresponding to Fig. 4(b)

Figs. 10–12 present test results under different braking conditions. Different braking levels and intentionally activating or deactivating the electrical brakes were the main differences considered.

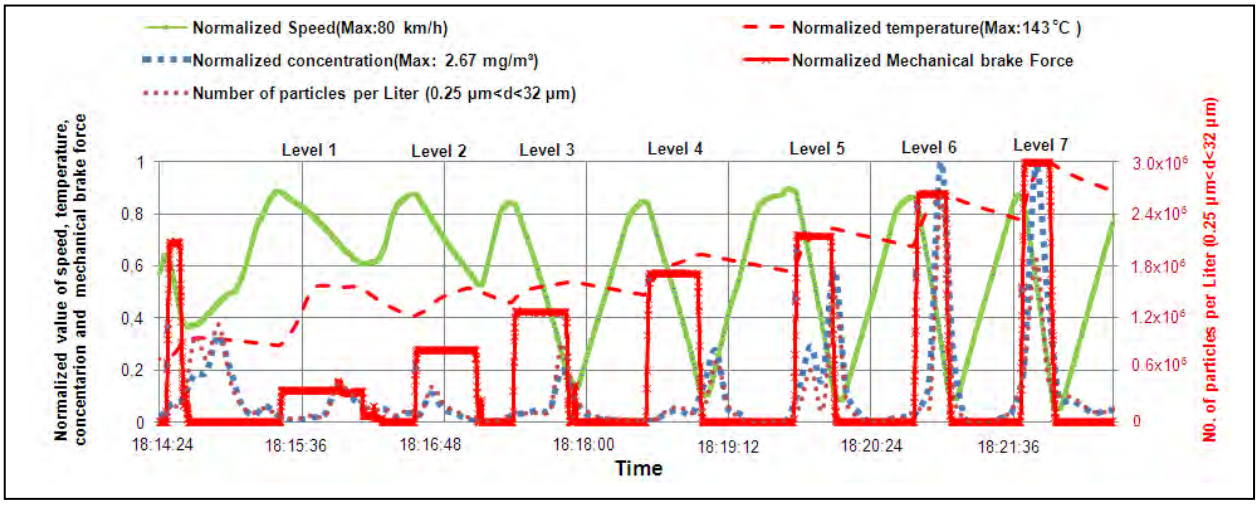

Fig. 10. Effect of braking level on the concentration and number of recorded particles, brake pad temperature, and train speed (brake pad sampling point); train speed 70 km h^{-1} and electrical brake intentionally deactivated.

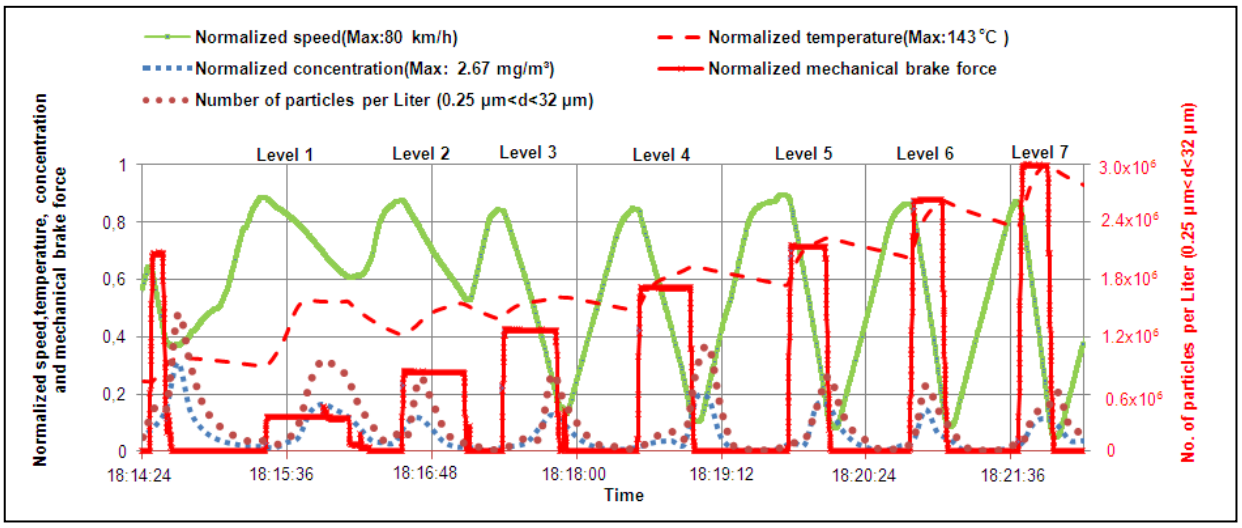

Fig. 11. Effect of braking level on the concentration and number of recorded particles, brake pad temperature, and train speed reduction (global sampling point); train speed 70 km h^{-1} and electrical brake intentionally deactivated.

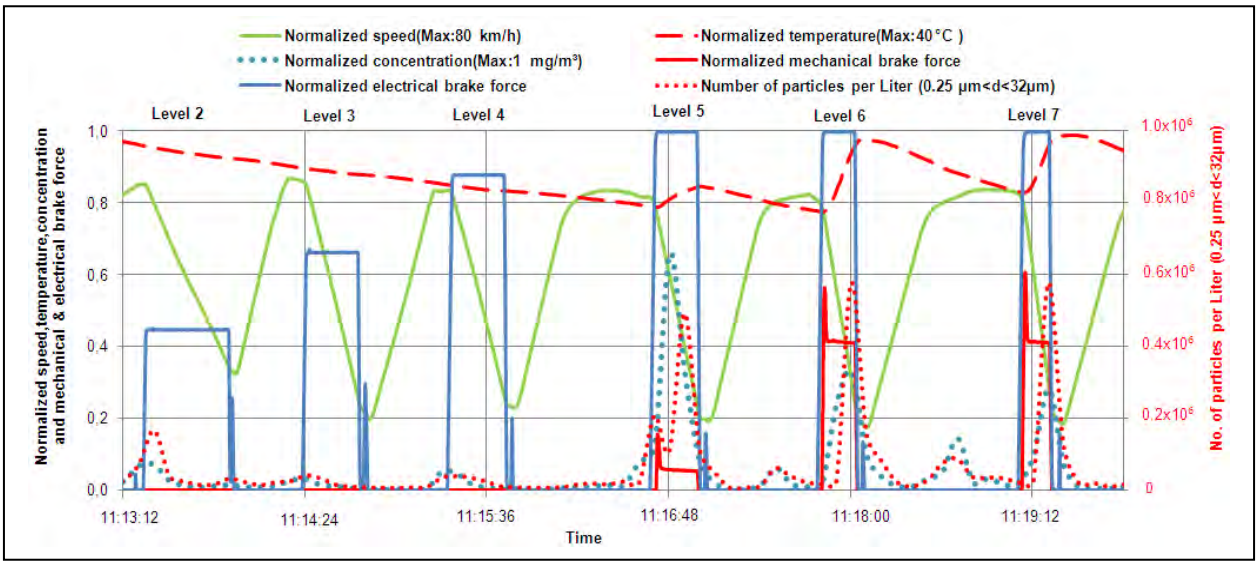

Fig. 12. Effect of braking level on the concentration and number of recorded particles, brake pad temperature, and train speed (brake pad sampling point); train speed 70 km h^{-1} and electrical brake activated.

These results were registered by running the test train on the aforementioned low-trafficked track (Fig. 1) at an operational speed of 70 km h^{-1}. In all of these graphs, the magnitudes of train speed, brake force, brake pad temperature, and particle concentration are depicted as normalized values in the vertical axis. The maximum values of these factors are set to 1, and the other values are scaled proportionally; this normalization procedure is used in Figs. 13-15 as well.

Figs. 13 and 14 present particle characteristics under normal traffic conditions with the active electrical brake. Fig 13 depicts the effect of train deceleration from 180 km h^{-1}. Such a sudden deceleration increases the temperature in the brake pad drastically which leads to abrupt increase in the number of generated particles. Fig. 14 shows the train acceleration effects on number of particles and particle concentration.

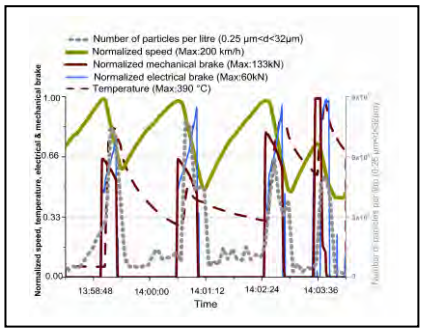

Fig. 13. Effects of increasing brake pad temperature on the concentration, number of recorded particles; numbers of particles were recorded using P-TRAK and GRIMM devices and particle concentration was recorded using a DustTrak device.

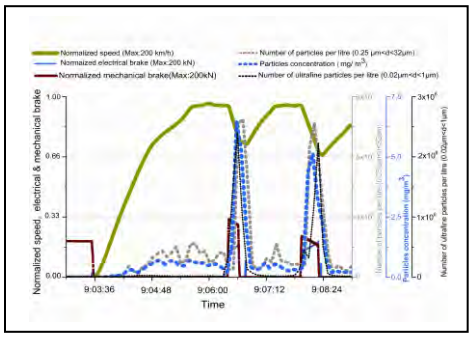

Fig. 14. Effects of train acceleration on the concentration, number of recorded particles, brake pad temperature, and train speed reduction in normal traffic (brake pad sampling point); numbers of particles were recorded using P-TRAK and GRIMM devices and particle concentration was recorded using a DustTrak device.

Figs. 15 (a) and (b) show the effect of train curve negotiation; intuitively, the process of wear between rail and wheel is considerably more severe during curve negotiation.

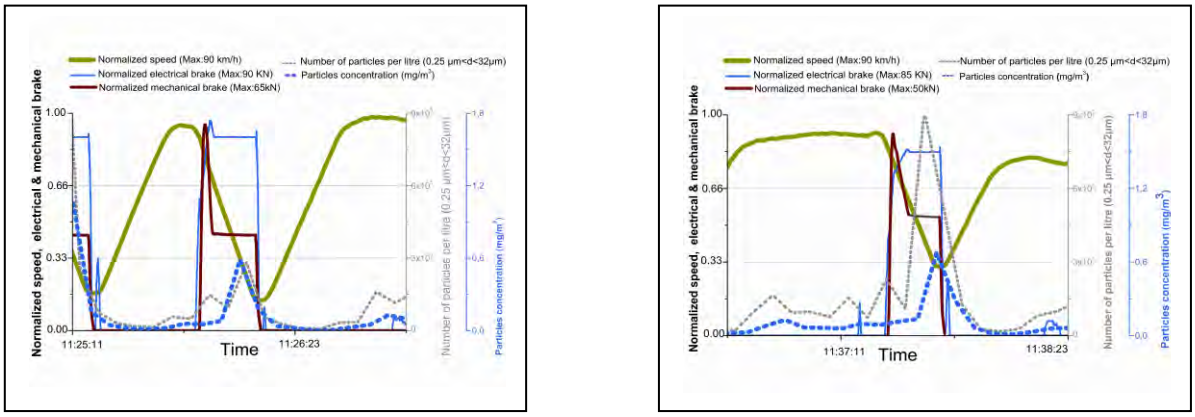

Fig. 15 Effects of curve negotiation on the concentration, number of recorded particles, and train speed (brake pad sampling point); numbers of particles were recorded using P-TRAK and GRIMM devices and particle concentration was recorded using a DustTrak device; (a) right curve negotiation and (b) left curve negotiation.

Figs. 16 (a) and (b) present particle number size distributions from the brake pad sampling point during braking from 70 km h^{-1}, Fig. 16 (a) with the deactivated electrical brake and Fig.16 (b) with the active electrical brake. In these figures, the recorded particles number size distributions are distributed semi-trimodally. Although the concentration and number of particles were highly dependent on the applied force (i.e. different braking levels effect in Fig. 10), no significant discrepancy was observed between Fig. 16 (a) and Fig.16 (b) in the number size distribution of particles.

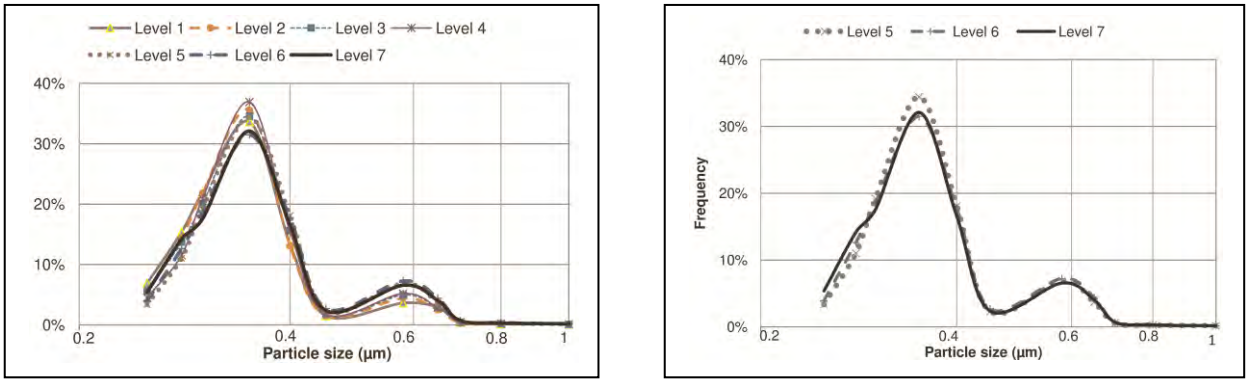

Fig. 16 Comparison of particle number size distribution between braking levels (corresponding to Fig. 10 and Fig. 12), semi-trimodal curves with three peaks for fine particles recorded using a GRIMM device; (a) electrical brake deactivated and (b) electrical brake activated.

Figs. 17 and 18 present particle number size distributions in four occasions of train acceleration and deceleration corresponding to Figs 13-14.

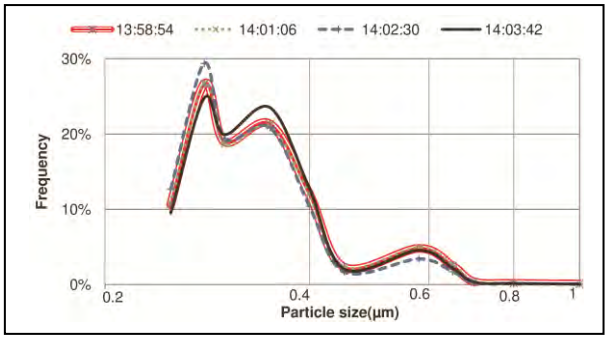

Fig. 17. Particle number size distribution results on four sampling occasions; corresponding to Fig. 13 (recorded using GRIMM device).

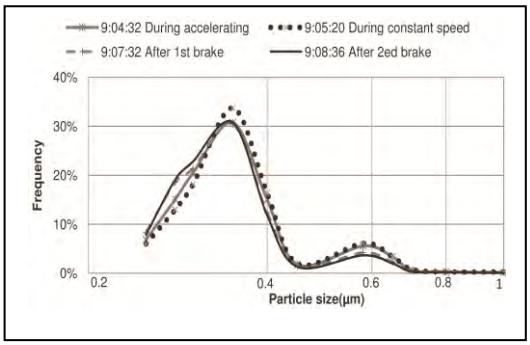

Fig. 18. Particle number size distribution results on four sampling occasions corresponding to Fig. 15 (recorded using GRIMM device).

4. Discussion

Figs. 9(a), 9(b) and table 3 show some element composition of investigated filters. As it has been presented there is good agreement between the results of EDX and ICP-MS for the most of the main elements. It must be noted that the investigated filter areas are quite different in these two methods. In EDS, we investigated particles composition locally where as in the ICP-MS we investigated the whole part of digested area.

Table 3 indicates that Cu, Fe, Ni, Zn, Al, Ba, Ca, Ti, Mg, Mn, and Na were the main detected elements. Some of these elements were also reported in the recent review by Gustafsson [7], according to which, Fe, Cu, Zn, Ca, Al, Cr, Ni, and Mn are the main elements constituting particles, as indicated by stationary measurements in train traffic studies. Iron-based particles were dominant in all of the aforementioned studies, composing 60–70% of total particles by weight. However, there were some discrepancies in the concentration percentage of other elements, such as Cu, Cr, Mn, Al, Si, and Ca [7]. These differences can be explained by the following differences:

- material composition of main wearing components, such as wheels, rails, brake pads, brake blocks, third rail shoes, brake discs, and masonry structures

- monitoring system and measurement setup

- ventilation system and air-quality management in subway stations

- operational conditions

- climatic condition and humidity effects

The amounts of Fe, Cu, Ni, and Zn detected at the brake pad sampling point were definitely higher than at the global sampling point; in contrast, the amounts of Al, Ca, Mg, K, As, Si, Na, and U detected at the global sampling point were higher. These results suggest that the main sources of particles containing Fe, Cu, Ni, and Zn must be nearer the brake pad sampling point and the main sources of particles containing Al, Ca, Mg, K, As, Si, Na, and U are likely nearer the global sampling point. This difference allows us to consider the railway brake pads, rails, wheels, and brake discs as the main sources of the first group of elements, and concrete sleepers and ballast as the main sources of the second group. This conclusion is in line with Gehrig's results [15]. He reported that Fe, Cu, Zn, Ni, Cr, and Mn were the main elements found in particles from rolling stock; he also hypothesized that Al, Ca, Mg, and K, which made smaller contributions, resulted from erosion, abrasion, and re-suspension.

The ratio of Mn to Fe found in the present study was close to 0.01, which is akin to the elemental composition of steel wheels and brake discs. This result is in agreement with those of Gehrig [15], Aarino [16], Chillrud [17] and Ripunucci [18] though some of those studies were conducted in underground stations.

The amount of the copper found in the global sampling point filter was 14-31% higher in the first run than in the others (Table 3). Overhead electric wire and brake pads are the main sources of copper-based particles. However, the greater variation found at the global sampling point led us to investigate overhead electric wire characteristics. As indicated in Table 1, ambient humidity increased abruptly along the first run because of rainy weather. In rainy weather, two phenomena could increase the material loss from the overhead electrical wire and the contact strip. One of these is the corona effect in which ionized air changes water pH by giving rise to nitric acid. The other is the effect of humidity on the sparking between the electrical wire and the contact strip. In this regard, Ostlund et al. reported a higher contact strip consumption rate in rainy months [19]. The significant effect of electric discharge on copper wear rate was studied by Kubo as well [20]. Shing [21] considered relative humidity a factor affecting the consumption rate of contact strips. Notably, Bukowiecki [22] also found a similar anomaly in the amount of the detected copper in the collected particles from aboveground train traffic. The author concluded that relative humidity has a crucial effect on the amount of copper-based particulate matter generated from an overhead electrical wire.

According to Fig. 4(a) and 4(b), no distinctive difference was obtained between particle morphologies in two different sampling points and most coarse particles were approximately 3–6 μm in diameter. Besides, this result was similar to the previous studies by Sundh et al. [5] and Abbasi et al. [3, 4]. They derived the volume size distribution from the number size distribution by simulating wheel-rail contact and brake pad-brake disc contact in the laboratory conditions. It is also in agreement with others studies in the field test measurements [6, 7, 23].

Coarse particles of flake shape seem to be generated mechanically, though ultrafine and some fine particles (Figs. 4–5) of semi-spherical shape seem to be generated through a thermal

process, such as melting or partial melting. Note that wear-generated airborne particles are often associated with particle sizes from 300 nm up to 15–20 μm. However, recent results [24] indicate that metallic particles in the 80 nm size range can also be generated when two metallic surfaces slide against each other, as in the wheel–rail contact or in disc brakes.

As depicted in Figs. 10–12, the wear rate and particle generation increase with increasing braking force, a result in line with that of Olofsson et al. [25]. Effects of different mechanical braking levels are evident in Fig. 10. Some slight differences between the effects of different braking levels can be explained by considering the thermo elastic instability characteristics [26]. Actually, the real contact area is a small portion of the entire brake pad surface, and it moves over the entire brake pad surface during braking. When the real contact area is close to the sampling point, more particles will be recorded than when it is further away. In contrast, at the global sampling point (Fig. 11), no significant changes were evident in the total amount and concentration of detected particles when applying different mechanical braking levels.

Fig. 12 presents a comparison between different braking levels on the particles characteristics when both mechanical and electrical brakes were used simultaneously (brake pad sampling point) . At the second, third, and fourth levels, there was no particle generation and the brake force applied by the electrical system was sufficient to stop the train. However, at the higher braking levels, mechanical forces were added to the total braking system to produce the required deceleration rate. Although the driver manually determined the magnitude of deceleration using different braking levels, the train computer ordered the balance between electrical brake force, mechanical brake force, and train speed and weight. This process caused only slight differences in the magnitudes of the applied mechanical brake forces at levels 5 and 6. Obviously, applying mechanical brake force caused particle generation at these levels.

Particle number size distributions are shown in Figs. 16 (a) and (b). In terms of the number of recorded particles, the particle size distribution at 70 km h^{-1} was independent of braking conditions. One possible explanation for this independency of the braking condition is that the same wear mechanism was dominant. During braking, three peaks at 280 nm, 350 nm, and 600 nm in diameter were identified in the fine particle region, the 350 nm peak being dominant. These results were reproduced under the laboratory test conditions by the present authors [3, 4]. Besides these peaks, another peak at approximately 100 nm in diameter was recorded using an SMPS under laboratory test conditions. Notably, Wahlström et al. reported similar peaks when investigating the wear between various car brake pads and cast iron brake disc [27].

In Fig. 17, one can see the effects of brake pad temperature on particle number size distribution. The deceleration at 180 km h^{-1} corresponds to the higher sliding velocity between the brake pad and disc. In addition, deceleration at this speed would dissipate more kinetic energy in the brake pad than at 70 km h^{-1}. By an increased temperature on the brake pad contact surface, more fine and ultrafine particles can be generated because of the higher probability of reaching the melting point in the asperity contacts. Note that the recorded temperature is not the flash temperature, which, among asperities, can considerably exceed the recorded temperature.

During curve negotiating, the wheel's conical shape is crucial. Figs. 19 (a) and (b) illustrate how

differences in wheel diameter affect curve negotiating. According to Andersson et al. [28], the lateral guiding force in the outer wheel is considerably higher than in the inner wheel. Consequently, higher creep and wear occur in the outer wheel. This phenomenon explains the higher recorded particle numbers and concentrations shown in Figs. 15 (a) and (b). In those figures, the train speed and applied braking forces were quite similar but the curve direction was completely different. In Fig. 15 (b), where the higher wheel–rail creep occurred, more wear and consequently particle generation resulted.

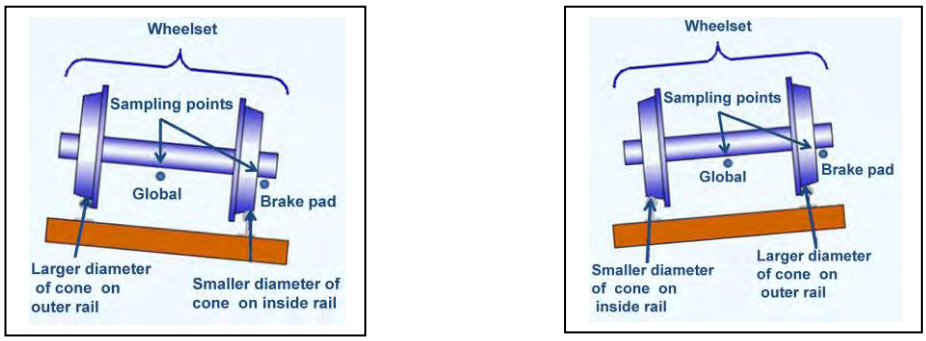

Fig. 19 Schematic showing position of sampling points, wheelset, and rail during curve negotiation: (a) right curve negotiation and (b) left curve negotiation

Fig. 18 illustrates the change of particle size distribution before and after braking. During mechanical braking, some particles stick to the brake pads; these could be released when the driver releases the mechanical brake, a moment when the brake pads and discs are not in contact. Airflow will remove some of the stuck particles generated from brake pads when they were applied to the brake disc. This characteristic could change the particle size distribution from a bimodal shape before mechanical braking to a semi-trimodal shape after releasing the brake, as presented in Fig. 18. The bimodal distribution of airborne particles from the wheel–rail contact was presented by Sundh et al. [5]; the trimodal shape of the airborne particles released from brake pads at high temperature is presented in Fig. 17.

Madl et al [9] introduced 31 different particles characteristics and exposure factors for evaluating health effects caused by particles. Particle mass, which was one of these particle factors, has been widely used in the researches and legislations. In contrast, other characteristic particle factors, such as size, shape, number and composition, have been poorly investigated and they are not considered in the present legislations. Möller et al. [29] reported a size-dependent toxicity effect from metal oxide particles. They showed that the toxicity of CuO particles increased, but that the toxicity of TiO2 particles decreased, when their sizes decreased to the nano scale. These issues can neither be understood nor controlled by relying exclusively on PM values.

The present study presented new data of airborne particles from a running train. These results are a first step in a more holistic study of the cause and effect of non-engine emissions from rail transport. The development of efficient and pro-active counter-measures necessitates further studies of particle characteristics, generation mechanisms, and exposure factors.

5. Conclusions

The following conclusions can be drawn from this study:

According to ICP-MS investigation of the filters, the particulate matter mainly comprised Fe, Si, Al, Ca, Cu, and Zn. The higher amounts of some elements, such as Ca, Si, Na, and Al, in the global sampling point filters indicated that ballast and concrete sleepers were the main sources of these particles, although some originated from rails, wheels, brake discs, and brake pads.

The amount of copper-based particles originating from overhead electrical wire is highly dependent on relative air humidity and can increase in rainy weather.

In the fine particle region, three peaks were identified at 280 nm, 350 nm, and 600 nm in diameter. The 350 nm peak was dominant for braking at 70 km h^{-1}, but at higher speeds corresponding to higher brake pad temperatures, particles 280 nm in diameter became dominant.

Particles as small as 50 nm were generated and captured on the filters.

Most coarse particles are approximately 3–6 μm in diameter according to FESEM images and the particle volume size distribution.

Wheel–rail creep during train acceleration and curve negotiation plays a crucial role in generating particles from wheel–rail contact.

6. Acknowledgments

This research was performed under the auspices of the Railway Group of the Royal Institute of Technology. The author acknowledges valuable assistance from Ms Minoo Arzpeima of the Royal Institute of Technology.

References

1 http://monographs.iarc.fr/ENG/Classification/index.php

2 **Olofsson, U.,** A study of airborne wear particles generated from the train traffic—Block braking simulation in a pin-on-disc machine, Wear,. 2010 in press

3 **Abbasi, S., Wahlström, J., Olander, L., Sellgren, U., Olofsson, U.,** and **Larsson, C.** A study of airborne wear particles generated from organic railway brake pads and brake discs,

Nordtrib conference 2010. Submitted to special issue of Wear.

4 **Abbasi, S., Jansson, A., Olander, L., Olofsson, U.,** and **Sellgren, U.** A pin-on-disc study of the rate of airborne wear particle emissions from railway braking material. Submitted to Wear.

5 **Sundh, J., Olofsson, U., Olander, L.,** and **Jansson, A.** Wear rate testing in relation to airborne particles generated in wheel–rail contact. Lubr. Sci., 2009, 21, 135–150.

6 **Salma, I.,** Air pollution in underground railway systems. In:Hester, R.E., and Harisson, R.M., Air quality in Urban environments, Royal society of chemistry, Cambridge, 2009, pp 65-85

7 **Gustafsson, M.** Airborne particles from the wheel–rail contact. In: Lewis, R. and Olofsson, U. (eds.), Wheel–Rail Interface Handbook, pp. 550–575. CRC Press; 2009.

8 **Fridell, E., Ferm, M., Björk, A., and Ekberg, A.** On-board measurement of particulate matter emissions from a passenger train. J. Rail Rapid Transit., 2010, In press

9 **Madl, K. A. and Pinkerton E. K.,** Health effects of inhaled engineered and incidental nanoparticles, Critical reviews in toxicology, 2009, 39, 629-658

10 http://www.gronataget.se

11 **Peters, T. M., Ott, D.,** and **O'Shaughnessy, P. T.** Comparison of the GRIMM 1.108 and 1.109 portable aerosol spectrometer to the TSI 3321 aerodynamic particle sizer for dry particles. Ann. Occup. Hyg., 2006, 50(8), 843–850.

12 **Zhu, Y., Yu, N., Kuhn, T.,** and **Hinds, W.** Field comparison of P-TRAK and condensation particle counters. Aerosol Sci. Technol., 2006, 40(6), 422–430.

13 **Cheng, Y. H.** Comparison of the TSI Model 8520 and GRIMM series 1.108 portable aerosol instrument used to monitor particulate matter in an iron foundry. J. Occup. Environ. Hyg., 2008, **5**(3),157–168.

14 **Nelms, S.M.,** Inductively Coupled Plasma Mass Spectrometry Handbook, CRC Press:2010

15 **Gehrig, R., Hill, M., Lienemann, P., Zwicky, C. N., Bukowiecki, N., Weingartner, E., Baltensperger, U.,** and **Buchmann, B.** Contribution of railway traffic to local PM10 concentrations in Switzerland. Atmos. Environ., 2007, 41(5), 923–933.

16 **Aarnio, P., Yli-Tuomi, T., Kousa, A., Makela, T., Hirsikko, A., Hameri, K., Raisanen, M., Hillamo, R., Koskentalo, T.,** and **Jantunen, M.** The concentrations and composition of and exposure to fine particles ($PM_{2.5}$) in the Helsinki subway system. Atmos. Environ., 2005, 39, 5059–5066.

17 **Chillrud, S., Epstein, N., Ross, J. M., Sax, S. N., Pederson, D., Spengler, J. D.,** and

Kinney, P. L. Elevated airborne exposures of teenagers to manganese, chromium, and iron from steel dust and New York City's subway system. Environ. Sci. Technol., 2004, 38, 732–737.

18 Ripanucci, G., Grana, M., Vicentini, L., Magrini, A., and **Bergamaschi, A.** Dust in the underground railway tunnels of an Italian town. J. Occup. Environ. Hyg., 2006, 3, 16–25.

19 Ostlund, S., **Gustafsson, A.**, **Buhrkall, L.**, and **Skoglund, M.** Condition monitoring of pantograph contact strip. Railway Condition Monitoring, 2008 4th IET International Conference, 18–20 June 2008, Derby, UK.

20 Kubo, S. and **Kato, K.** Effect of arc discharge on the wear rate and wear mode transition of a copper-impregnated metalized carbon contact strip sliding against a copper disk. Tribol. Int., 1999, 32, 367–378.

21 Shing, A. W. C. and **Wong, P. L.** Wear of pantograph collector strips. J. Rail Rapid Transit, 2008, 222, 169–176.

22 Bukowiecki, N., Gehrig, R., Hill, M., Lienemann, P., Zwicky, C. N., Buchmann, B., Weingartner, E., and **Baltensperger, U.** Iron, manganese and copper emitted by cargo and passenger train in Zurich (Switzerland): size-segregated mass concentrations in ambient air. Atmos. Environ., 2007, 41, 878–889.

23 Lorenzo, R., Kaegi, R., Gehrig, R., and **Grobety, B.** Particle emissions of railway line determined by detailed single particle analysis. Atmos. Environ., 2006, 40, 7831–7841.

24 Olofsson, U., Olander, L., and Jansson, A. A study of airborne wear particles generated from a sliding contact. J. Tribol.-T. ASME., 2009, 131(4), 044503.1–044503.4.

25 Olofsson, U., Olander, L., and **Jansson, A.** Towards a model for the number of airborne particles generated from a sliding contact. Wear, 2009, 267, 2252–2256.

26 Barber, J. R. Thermoelastic Instabilities in the Sliding of Conforming Solids. Proceedings of the Royal Society of London. Series A, Mathematical and Physical Sciences, 1969, 312, 381-394.

27 Wahlström, J., Söderberg, A., Olofsson, U., Olander, L., and **Jansson, A.** A pin-on-disc simulation of airborne wear particles from disc brakes. Wear, 2010, 268, 763–769.

28 Andersson, E., Berg, M., and **Stichel, S.** Rail Vehicle Dynamics. Division of Rail Vehicles, Dept of Aeronautical and Vehicle Engineering, KTH, Stockholm, 2007.

29 Möller, L., Karlsson, H. L., Cronholm, P., and Gustafsson, J. Size-dependent toxicity of metal oxide particles - A comparison between nano- and micrometer size. Toxicology letter, 2009, 188, 112-118

A pin-on-disc study of the rate of airborne wear particle emissions from railway braking materials'

Saeed Abbasi,
Anders Jansson,
Lars Olander,
Ulf Olofsson,
Ulf Sellgren

C

Submitted to Wear journal

A pin-on-disc study of the rate of airborne wear particle emissions from railway braking materials'

Saeed Abbasi[1], Anders Jansson[2], Lars Olander[3], Ulf Olofsson[1], Ulf Sellgren[1]

[1]*KTH Machine Design, SE 100 44, Stockholm, Sweden*
[2]*Stockholm University Applied Environmental Science, SE 106 91, Stockholm, Sweden*
[3]*KTH Building Service Engineering, SE 100 44, Stockholm, Sweden*

Corresponding author's email: sabbasi@md.kth.se

ABSTRACT

The current study investigates the characteristics of particles generated from the wear of braking materials, and provides an applicable index for measuring and comparing wear particle emissions. A pin-on-disc tribometer equipped with particle measurement instruments was used. The number concentration, size, morphology, and mass concentration of generated particles were investigated and reported for particles 10 nm to 32 μm in diameter. The particles were also collected on filters and investigated using EDS and SEM. The effects of wear mechanisms on particle morphology and changes in particle concentration are discussed. A new index, the airborne wear particle emission rate, is suggested be used in legislation to control non-exhaust emissions from transport modes, particularly rail transport.

Keywords: Airborne particles, Railway, Wear, Brake pad, Brake block

1. Introduction

The generation of airborne particles is a multi-faceted issue of interest to many researchers. Physicists and chemists are interested in the characteristics of these particles at the nano-scale, because of the huge property differences between nano-scale and bulk materials. Environmental researchers, physicians, and occupational health organizations study the mass, number, size, and morphology of these particles because of their possible adverse effects on human health.

Wear has been studied extensively with a focus on surface wear in various metallic and non-metallic materials [1]. In addition, wear particles are of great concern as they can be detrimental to sliding and other processes [2]. Unlike the case of exhaust emissions, concern about the effects of airborne wear particle characteristics on air quality has been limited in recent years. This matter is described as particle emissions from non-exhaust road transport sources, and brake pads, tyres, and the road surface are the main sources of such wear particle emissions. Methodologies for investigating such particles, along with the results so obtained, have recently been reported [3]. According to these results and methodologies, the mass of generated particles is measured in mg km^{-1} according to the size fractions of particles. The gross weight, operational

conditions, and functionalities of road vehicles affect the emission rate of particles from these sources, particularly from tyres and brake pads [4].

A century ago, the high mass concentrations of wear particles in subways attracted research interest, prompting the measurement of particle mass concentrations in the New York subway [5]. Since then, several studies have confirmed and characterized the high mass concentrations of particles in underground rail traffic and reviewed the adverse health effects of these particles [6,7]. However, none of them attempts to explore the actual mechanisms of wear particle generation. The braking materials (i.e., brake blocks against railway wheels and brake pads against brake discs) have been recognized as the sources of non-exhaust emissions in rail transport [6–9].

However, measurement noise and external disturbance are intrinsic to field testing; eliminating these problems calls for laboratory testing under controlled conditions. Sundh et al. [10] performed laboratory tests under selected loading conditions representing different contact conditions in a real wheel–rail contact. They found that the number of generated particles increased when the applied load increased, but that the particle size distribution was not dependent on the applied load. Abbasi et al. [11] simulated train mechanical braking at 70 km h^{-1} and reported a good correlation between particle size distribution in both field tests and laboratory simulations.

Notably, only a few studies have examined the characteristics of particles generated from railway components. Above all, no emission factor has been introduced to link airborne wear particle emissions from their source to real operational conditions. The main objective of this study is to investigate the characteristics of particles from various railway sources under controlled conditions. To this end, a series of laboratory tests has been conducted to investigate the number, size, size distribution, and morphology of particles generated from railway brake blocks, and brake pads. In addition, we have introduced a new factor that can be used to compare the particle emissions generated from various railway components. It can be extended to other industry as well.

Four particle measurement devices were used under different test conditions. To investigate particle morphology, we further used a field emission scanning electron microscope (FESEM) with energy dispersive spectroscopy (EDS).

2. Airborne wear particle emission rate

Note that some wear particles can become airborne during the wear process. We refer to this property as the airborne wear particle emission rate (AWPER). AWPER is defined as the ratio of the mass of generated airborne particles (in mg) to the length of time (in h) two objects are sliding against each other under controlled conditions. The sliding velocity (in m $s^{-1)}$ and mean contact pressure (in MPa) between the two objects remain constant in those conditions.

The relation between the registered particles concentration and AWPER in a sealed box equipped with an inlet/outlet and constant airflow can be modelled as follows: the rate of change of airborne particle mass in the test box is the difference between the outlet particle flow rate and the airborne particle generation rate in the box. Since no other airborne particles can enter the sealed box, due to the 99.95% efficiency of the filter used, we can assume that the particle

concentration at the outlet measurement point equals the concentration in the test box (Fig. 1). The mass balance for the airborne particles can then be formulated as follows:

$$\frac{d(CV)}{dt} = -qC + AWPER \quad \text{equation (1)}$$

where

V = box volume (m^3)

q = inlet airflow = outlet airflow ($m^3\ h^{-1}$)

C = concentration ($mg\ m^{-3}$)

$AWPER$ = airborne wear particle emission rate ($mg\ h^{-1}$)

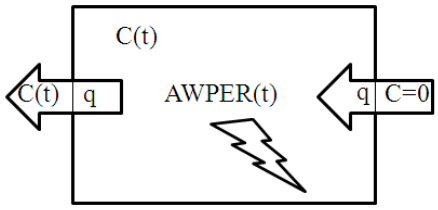

Fig. 1 An illustration of a box model. q is the inlet and outlet airflow; the inlet concentration is zero and the oulet concentration is C(t); the airborne particle emission rate in the box is AWPER(t).

By rewriting equation (1), we obtain:

$$\frac{dC}{dt} + \frac{q}{V}C = \frac{1}{V}AWPER \quad \text{equation (2)}$$

Since $AWPER$ and C are functions of time, while q and V are constant factors, the solution will be:

$$C = e^{\frac{-qt}{V}}\left(\int \frac{AWPER}{V} e^{\frac{qt}{V}} + C_0\right)dt \quad \text{equation (3)}$$

where C_0 is strongly related to the initial dust concentration in the box (in $mg\ m^{-3}$). Therefore, if we know the function of $AWPER$(t) and the initial conditions, we can obtain the concentration C at the outlet. As airborne particles are generated from wear debris, AWPER must be influenced by the changes in the contact state and by the transitions between different wear mechanisms.

As presented in equation (3), the registered concentration, C(t), is not linearly proportional to $AWPER$(t); nevertheless, equation (3) indicates that the concentration can change exponentially. This is the main reason why, when the applied load or sliding velocity changes, the recorded particle concentration is not directly proportional to the change in the applied load or sliding velocity. Fig. 2 shows the responses to five benchmark cases with different AWPER. These cases can be used to reason about the concentrations measured during testing. We can also use the average value of AWPER, $\overline{AWPER}$, to represent all these changes.

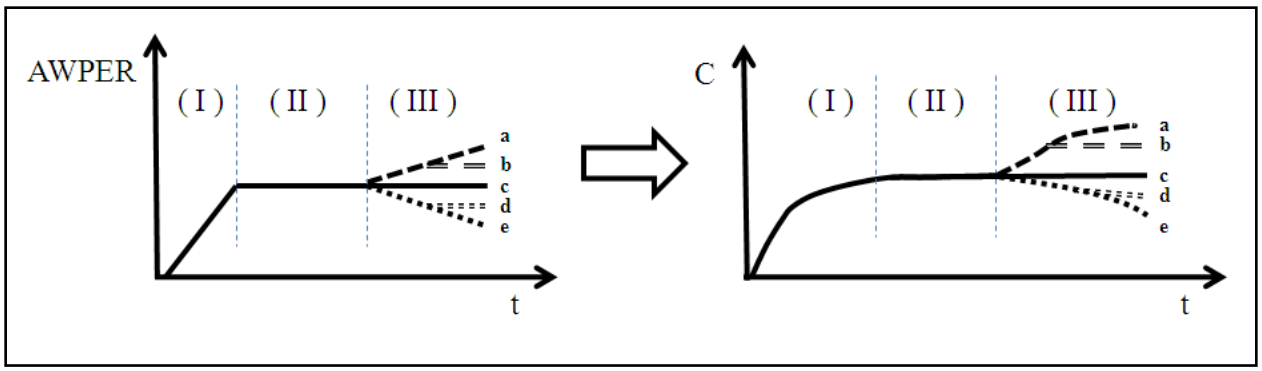

Fig. 2. Hypothetical model of AWPER changes and their effects on particle concentration changes.

In the other words, if we measure the concentration at the outlet for a predetermined period of time from the beginning of the test (before stopping the rotating disc) and then calculate the average concentration over that period, we can calculate an average value of AWPER, i.e., the mean wear airborne emission rate ($\overline{AWPER}$) (Fig. 3).

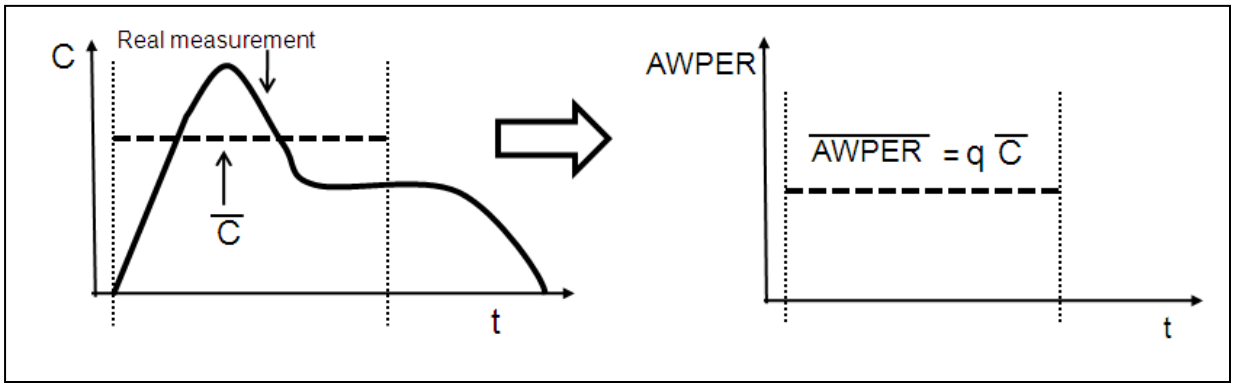

Fig. 3. An illustration of real measurement concentration, curve fitting and $\overline{AWPER}$

Notably, $\overline{AWPER}$ is similar to the non-exhaust emission rate of road vehicles. Both factors have been defined under specific load conditions and at a constant sliding velocity, even though the unit of the latter is mg km^{-1}. The concentration of particles size fractions such as PM_{10}, $PM_{2.5}$, PM_1 can be defined and used for the generated particles as well which was not the considered in this study.

3. Experimental set-up

3.1. Particle instruments

Four particle measurement instruments were used in this study. The main instrument was a GRIMM 1.109 aerosol spectrometer (hereafter "GRIMM"), which measured airborne particles 0.25–32 µm in diameter in 31 size intervals and at concentrations from 1 to 2 × 10^6 particles L^{-1} [14]. This instrument registered number concentrations with a time resolution of 6 s. As GRIMM is an optical counter, its stated particle sizes are approximate and depend on particle shape and refractive index [15]. The second device was a TSI P-TRAK condensation nuclei particle counter, model 8525 (hereafter "P-TRAK"), which measured the number concentration of

airborne particles 0.02–1 μm in diameter with no size resolution [16]. Number concentrations were registered with a time resolution of 1 s.

The third instrument was a TSI DustTrak photometer, model 8520 (hereafter "DustTrak"), which measured the mass concentration in mg m^{-3}. This is a laser photometer and measures particle concentrations roughly corresponding to respirable size fractions; it registered mainly particles in the 0.1–10 μm diameter range. The instrument is factory calibrated using a test dust (with a density of 2650 kg m^{-3}), the size distribution, density, and refractive index of which differ from those of the particles measured here. Though the results could be used only as relative measures, they were useful in describing the changes in generated particle mass over time [17].

The fourth instrument was a scanning mobility particle sizer (SMPS) combining an electrostatic classifier (TSI model 3071) with a particle counter (TSI CPC model 3010). The particles were charged in a controlled manner and thereafter sequentially classified according to their electrical mobility; electrical mobility was then transformed into corresponding particle sizes [18]. The particle counter was a condensation nuclei counter that, by means of condensation, optically counted particles down to 10 nm in diameter. The size distribution was divided into 110 size classes in the 10–520 nm range; number concentrations as low as a few particles per cm^3 could be registered. The SMPS produced a particle number concentration size distribution every 5.5 min.

3.2. Test equipment

The laboratory tests were performed using a pin-on-disc machine equipped with a horizontal rotating disc and a dead-weight-loaded pin (Fig. 4); the entire set-up was mounted in a sealed box. The sealed box allowed us to control the cleanliness of the supply air and to sample air only containing wear particles.

The machine could run under stationary conditions with constant applied normal forces of up to 100 N and at constant rotational speeds of up to 3000 rpm. A load cell was used to measure the tangential force exerted on the pin.The fan (B) took the air from the room (A) and passed it into the chamber (G) via the flow measurement system (C), filter (D), and air inlet opening (F). The connections between the fan, measurement system, filter, and chamber were flexible tubes (E). The air in the sealed box (N) was well mixed due to the complicated volume of the pin-on-disc machine (H) and the high air exchange rate. This mixing was verified by registering particle concentrations from the box. The air in the sealed box transported the generated particles to the air outlet (J), where sampling points for the particle measurement devices were situated.

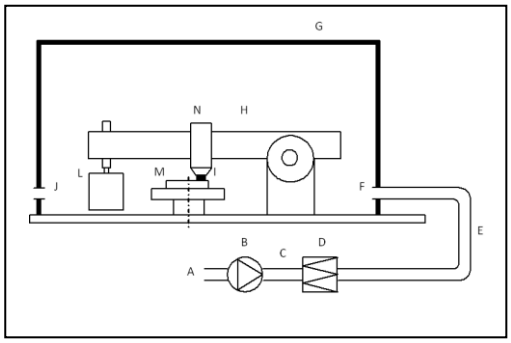

Fig. 4. Schematic of the test equipment. A: Room air; B: Fan; C: Flow rate measurement; D: Filter; E: Flexible tube; F: Clean air inlet, measurement point; G: Sealed box; H: Pin-on-disc machine; I: Pin sample; J: Air outlet, measurement points; L: Dead weight; M: Rotating disc sample, N: Air inside chamber.

The supply air was set to a flow rate of 7.7 m^3 h^{-1} (2.1 L s^{-1}). The sealed box volume was 0.135 m^3, and the volume of the pin-on-disc machine was approximately 0.035 m^3, giving an approximate air exchange rate of 77 h^{-1}, corresponding to a time constant of 47 s. The flow rate

measurement system consisted of a straight calibrated tube equipped with separate connections for total and static pressure, measured using an ordinary U-tube manometer. The system was calibrated in the 2–50 m^3 h^{-1} flow interval. The filter used to ascertain a particle-free inlet air was of class H13 (according to the EN 1822 standard) having a certified collection efficiency of 99.95% at maximum penetrating particle size (MPPS).

Two P-TRAK devices were used in this set-up, one connected to the sampling point at the inlet (F) and the other to the sampling point at the outlet (J).

This setup was previously used by Sundh et al. [10], Abbasi et al. [11], Olofsson et al. [19–20], and Wahlström et al. [21] to study the airborne particles generated from various materials under various test conditions.

During the tests, wear particles were collected from the box outlet air on filters. A volume of approximately 6 L of air was pumped through surface collecting filters (Nuclepore polycarbonate) with a pore size of 0.4 µm. The airborne wear particles collected on the filters were coated with gold and then analyzed using a FESEM with EDS.

All disc samples were made from a wheel and a brake disc, while the pins were made from brake pads, and brake blocks. The 110-mm-diameter disc specimens were cut, using a water jet, from a railway wheel and a used piece of wheel-mounted steel brake disc from a Regina X54 train, while the 10-mm-diameter pins were sawn mechanically from a brake pad, a sintered brake pad, a cast-iron brake block, and an organic brake block.

Table 1. The material characteristics of the test specimens.

Name	Specimen	Hardness	Roughness(Ra)
Railway wheel (R7)	Disc	270 HV	0.6 µm
Brake pad (Organic)	Pin, Flat head	-	9 µm
Brake pad (Sintered)	Pin, Flat head	-	3 µm
Brake block (Organic)	Pin, Flat head	-	1 µm
Brake block (Cast iron)	Pin, Flat head	270 HV	0.3 µm
Brake disc (Steel)	Disc	320 HV	0.6 µm

Table 1 presents the specimen characteristics. Before testing, the disc specimens were cleaned ultrasonically for 20 min using both heptane and methanol. The test conditions are presented in Table 2.

Table 2. The contact conditions of the laboratory tests.

Test No.	Pin material - Disc material	Load (N)	Sliding velocity (ms^{-1})	Mean contact pressure (Mpa)
1A	Organic brake pad-Steel brake disc	60	12.4	0.87
1B		60	8.9	0.87
1C		20	12.4	0.55
1D		40	12.4	0.27
2A	Sintered brake pad-Steel brake disc	60	12.4	0.87
2B		60	8.9	0.87
3A	Organic brake block-Railway wheel	60	12.4	0.87
3B		60	8.9	0.87
3C		20	12.4	0.27
3E		20	8.9	0.27
4A	Cast iron brake block-Railway wheel	60	12.4	0.87
4B		60	8.9	0.87
4C		20	12.4	0.27
4E		20	8.9	0.27

3.3. Test conditions

Most of the selected test conditions are representing real operational situations. For example, the 12.4 m s^{-1} sliding velocity represented the X54 train travelling at 70 km h^{-1}.

The whole system, including the pin-on-disc machine, was tested by starting all components simultaneously without any contact between the pin and disc. The measured particles concentration at the outlet became zero after 5–10 min, depending on earlier activity in the room and the box. Wear testing started after the concentration had reached zero. During the tests, the temperature was 20 ± 2°C and the relative humidity was 40 ± 5%. Two individual tests were run for each material combination.

4. Results

The effects of applying various loads, sliding velocities, and material combinations were investigated as specified in Table 2. Series of selected results obtained using P-TRAK, DustTrak, Grimm, and SMPS devices are presented in Figs. 5–12. Three particle size fractions were used, defined as follows: a *coarse* particle fraction comprising particles with diameters >1 μm, a *fine* particle fraction comprising particles with diameters between 100 nm and 1 μm, and an *ultrafine* particle fraction comprising particles with diameters <100 nm.

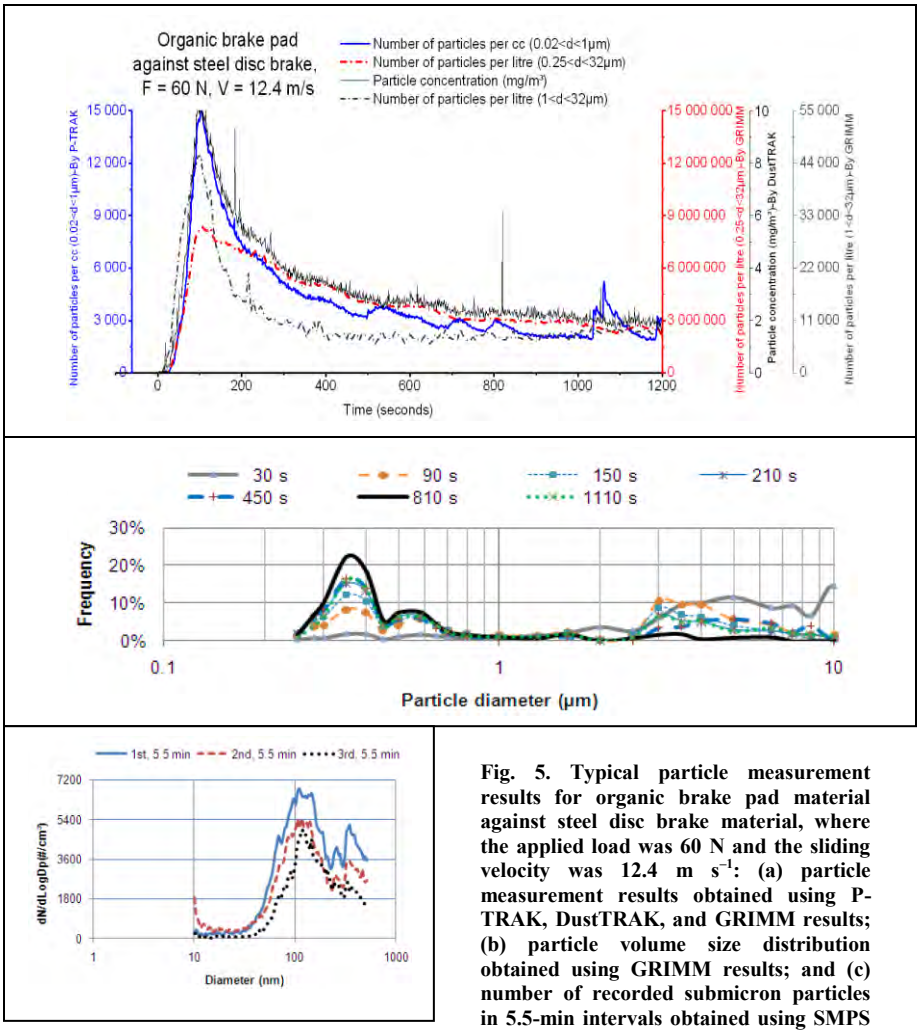

Fig. 5. Typical particle measurement results for organic brake pad material against steel disc brake material, where the applied load was 60 N and the sliding velocity was 12.4 m s^{-1}: (a) particle measurement results obtained using P-TRAK, DustTRAK, and GRIMM results; (b) particle volume size distribution obtained using GRIMM results; and (c) number of recorded submicron particles in 5.5-min intervals obtained using SMPS results.

Figs. 5–7 show the results associated with the particles generated from the organic brake pad material and the steel brake disc material using various loads and sliding velocities. A decrease in applied load (Fig. 6) or sliding velocity (Fig. 7) resulted in lower particle concentrations and lower number concentrations of ultrafine, fine, and coarse particles.

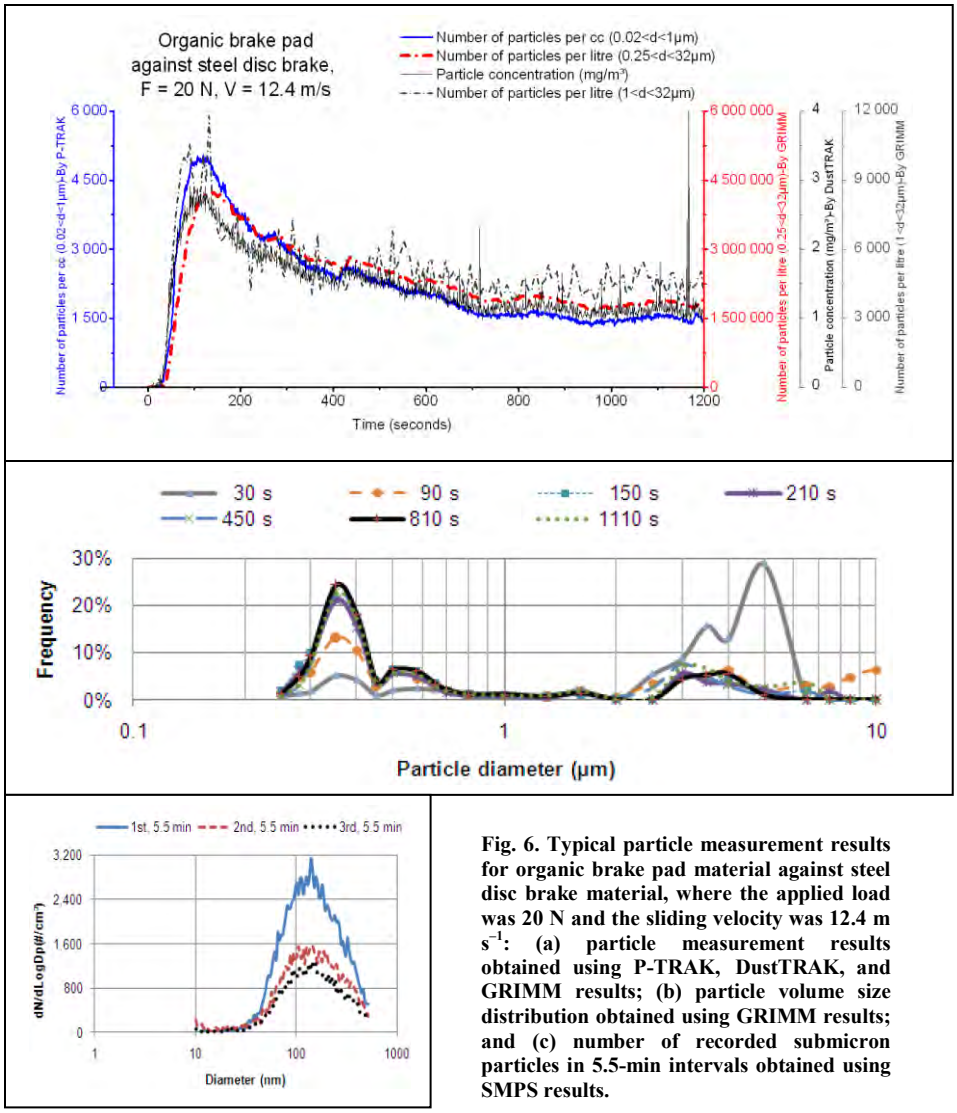

Fig. 6. Typical particle measurement results for organic brake pad material against steel disc brake material, where the applied load was 20 N and the sliding velocity was 12.4 m s^{-1}: (a) particle measurement results obtained using P-TRAK, DustTRAK, and GRIMM results; (b) particle volume size distribution obtained using GRIMM results; and (c) number of recorded submicron particles in 5.5-min intervals obtained using SMPS results.

These results were reproduced in both test replicates and under the other test conditions. In Figs. 5(b), 6(b), and 7(b), the GRIMM volume size distributions have been calculated from number size distributions assuming a spherical particle shape. Under all test conditions, the submicron particle fraction increased with time, whereas the fraction of particles with diameters over 1 µm decreased. A peak at approximately 3–6 µm in diameter in the coarse region, two peaks at 300–400 nm and 500–600 nm in the fine region (Figs. 5(b), 6(b), and 7(b)), and a peak at approximately 100 nm in the ultrafine region (Figs. 5(c), 6(c), and 7(c)) were recorded under all test conditions. Fig. 5(c) shows another peak in the fine region at a particle size of 280 nm.

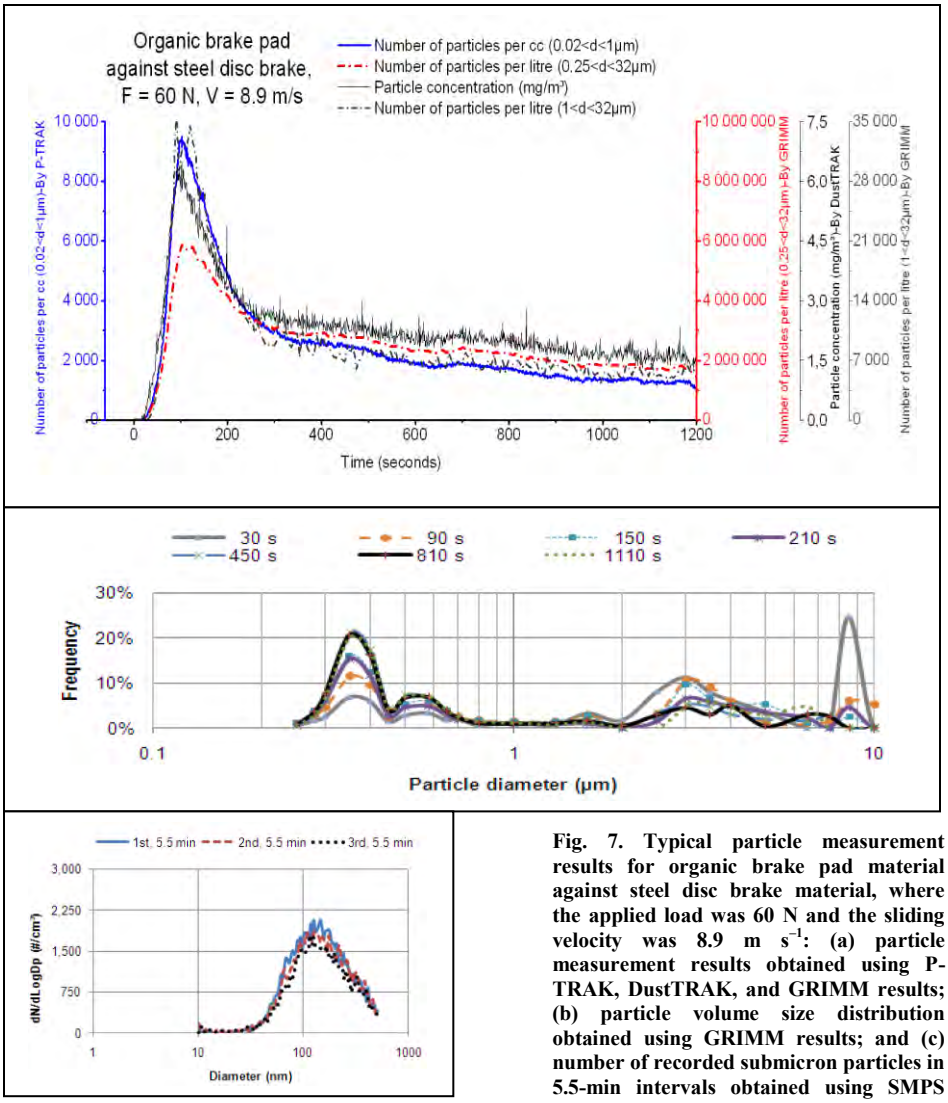

Fig. 7. Typical particle measurement results for organic brake pad material against steel disc brake material, where the applied load was 60 N and the sliding velocity was 8.9 m s^{-1}: (a) particle measurement results obtained using P-TRAK, DustTRAK, and GRIMM results; (b) particle volume size distribution obtained using GRIMM results; and (c) number of recorded submicron particles in 5.5-min intervals obtained using SMPS results.

The concentration characteristics of the particles generated from the sintered brake pad material over time (Fig. 8) were akin to those from the organic brake pad material; however, the submicron particle fraction of the total recorded number of particles was significantly smaller than for the organic brake pad particles.

A peak at approximately 3–6 µm in diameter in the coarse region, two peaks at 300–400 nm and at 500–600 nm in the fine region, and a peak at approximately 100 nm in the ultrafine region were also recorded under all these test conditions. The applied load was 60 N and the sliding velocity was 12.4 ms^{-1}.

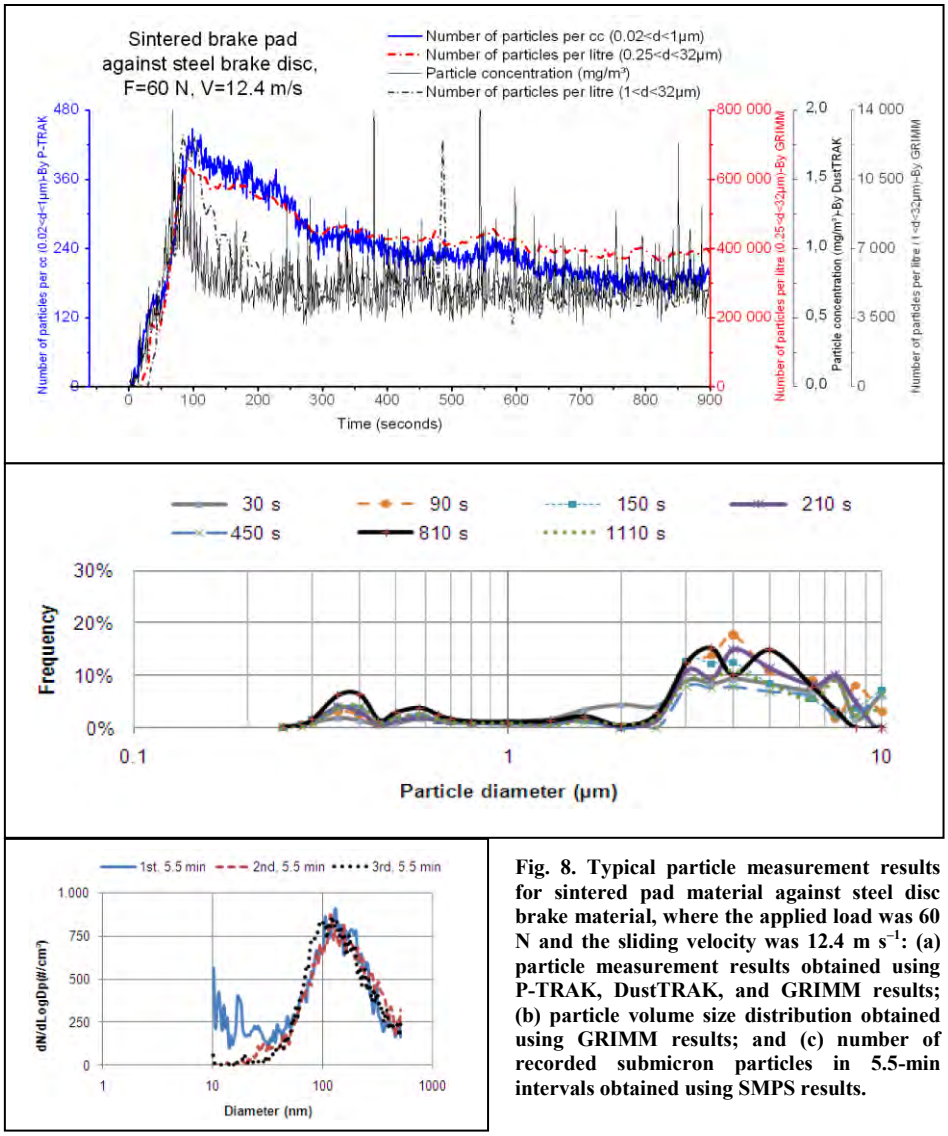

Fig. 8. Typical particle measurement results for sintered pad material against steel disc brake material, where the applied load was 60 N and the sliding velocity was 12.4 m s^{-1}: (a) particle measurement results obtained using P-TRAK, DustTRAK, and GRIMM results; (b) particle volume size distribution obtained using GRIMM results; and (c) number of recorded submicron particles in 5.5-min intervals obtained using SMPS results.

Fig. 9 presents the characteristics of particles generated from the organic brake block material against railway wheel material. Fig. 10 presents the corresponding characteristics of particles from cast iron brake block material. In both cases, the concentrations increase continuously from the start. For the organic brake block material, these trends continue, while the concentrations level off for the cast iron brake block material. For the latter, behaviour of the number concentrations of fine and ultrafine particles differ.

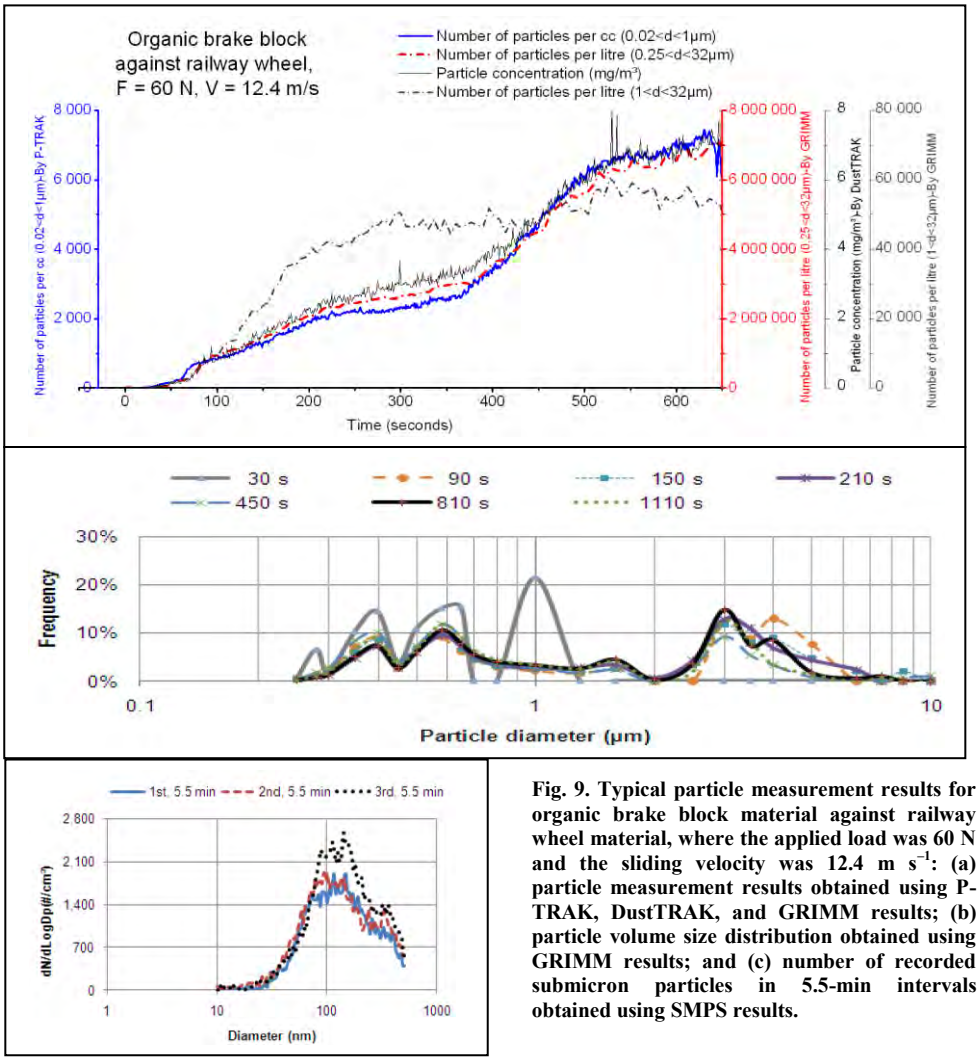

Fig. 9. Typical particle measurement results for organic brake block material against railway wheel material, where the applied load was 60 N and the sliding velocity was 12.4 m s^{-1}: (a) particle measurement results obtained using P-TRAK, DustTRAK, and GRIMM results; (b) particle volume size distribution obtained using GRIMM results; and (c) number of recorded submicron particles in 5.5-min intervals obtained using SMPS results.

According to Fig. 9(c), two peaks, at approximately 100 nm in the ultrafine region and at 300–400 nm in the fine region, were recorded for organic brake block material. A peak in the ultrafine region at approximately 70 nm for cast iron brake block material seemed to appear during the third 5.5 min of measurement.

Figs. 9(b) and 10(b) show a peak at approximately 3–6 µm in the coarse region and peaks at approximately 300–400 nm and 500–600 nm in the fine region.

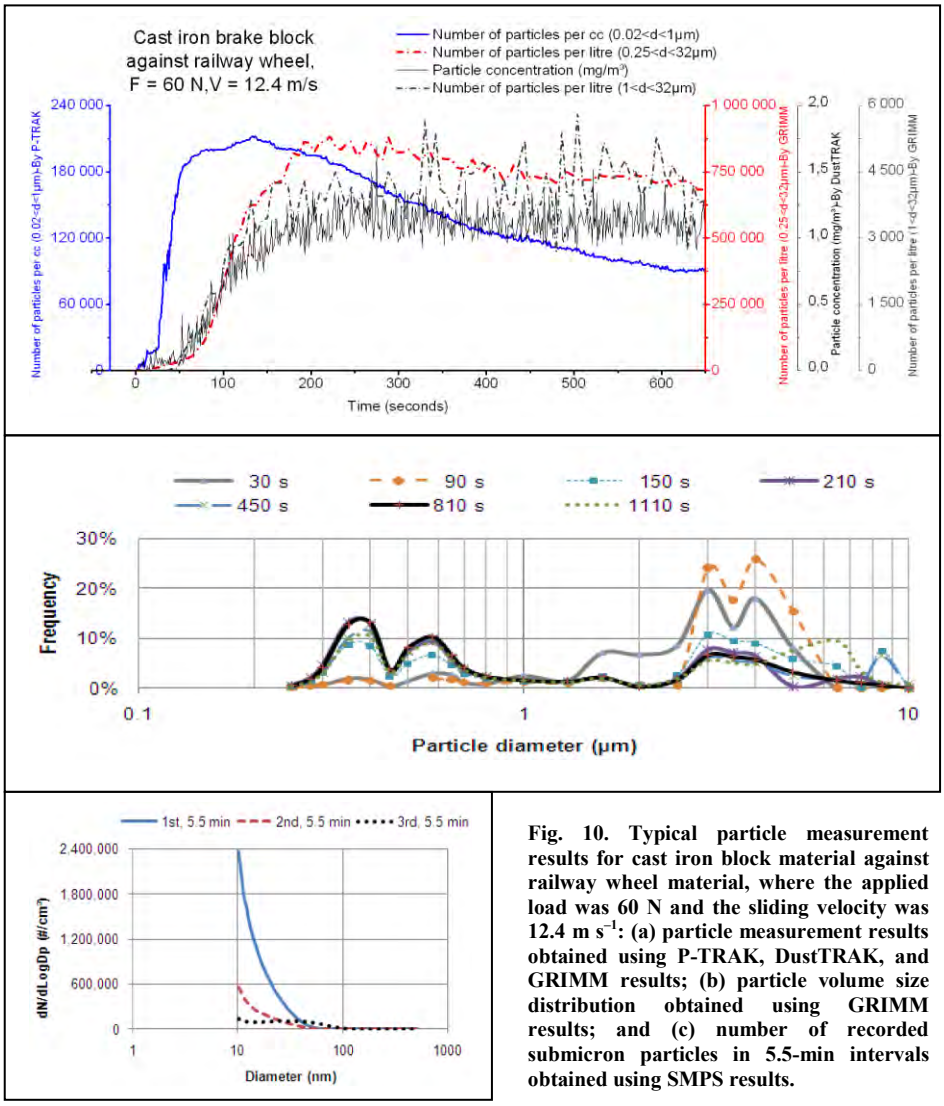

Fig. 10. Typical particle measurement results for cast iron block material against railway wheel material, where the applied load was 60 N and the sliding velocity was 12.4 m s^{-1}: (a) particle measurement results obtained using P-TRAK, DustTRAK, and GRIMM results; (b) particle volume size distribution obtained using GRIMM results; and (c) number of recorded submicron particles in 5.5-min intervals obtained using SMPS results.

According to Figs. 5–10, the particle concentrations and volume size distributions remained fairly constant after 7200 m under all test conditions presented in Table 2. We summarize the average number concentrations of fine and coarse particles over this distance under all test conditions in Fig. 11.

Figs. 11(a) and 11(b) show that the number concentrations of both the fine and coarse fractions increase with sliding velocity and applied load, although the relationship is not linear.

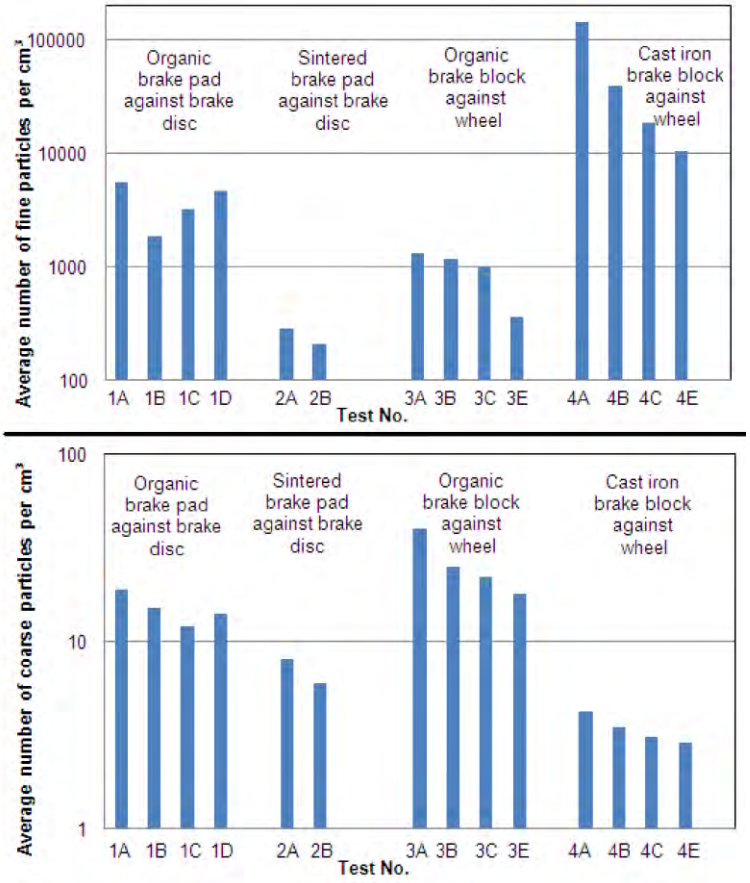

Fig. 11. Summary of the average number concentration in both the fine and coarse fractions over an equal sliding distance under all test conditions: (a) fine fraction particle number concentration for particles of 0.02–1 µm in diameter obtained using P-TRAK results; and (b) coarse fraction particle number concentration for particles of 1–32 µm in diameter obtained using GRIMM results.

According to Figs. 11(a) and 11(b), the particle number concentrations were lower in the sintered brake pad tests than in the organic brake pad tests. This result was obtained independent of size fraction and test conditions. However, we obtained quite different results from the brake block tests.

The fine particle fraction number concentrations obtained in the cast iron block tests were lower than those obtained in the organic brake block tests. In contrast, the coarse particle fraction number concentrations obtained in the cast iron block tests were lower than those obtained in the organic brake block tests.

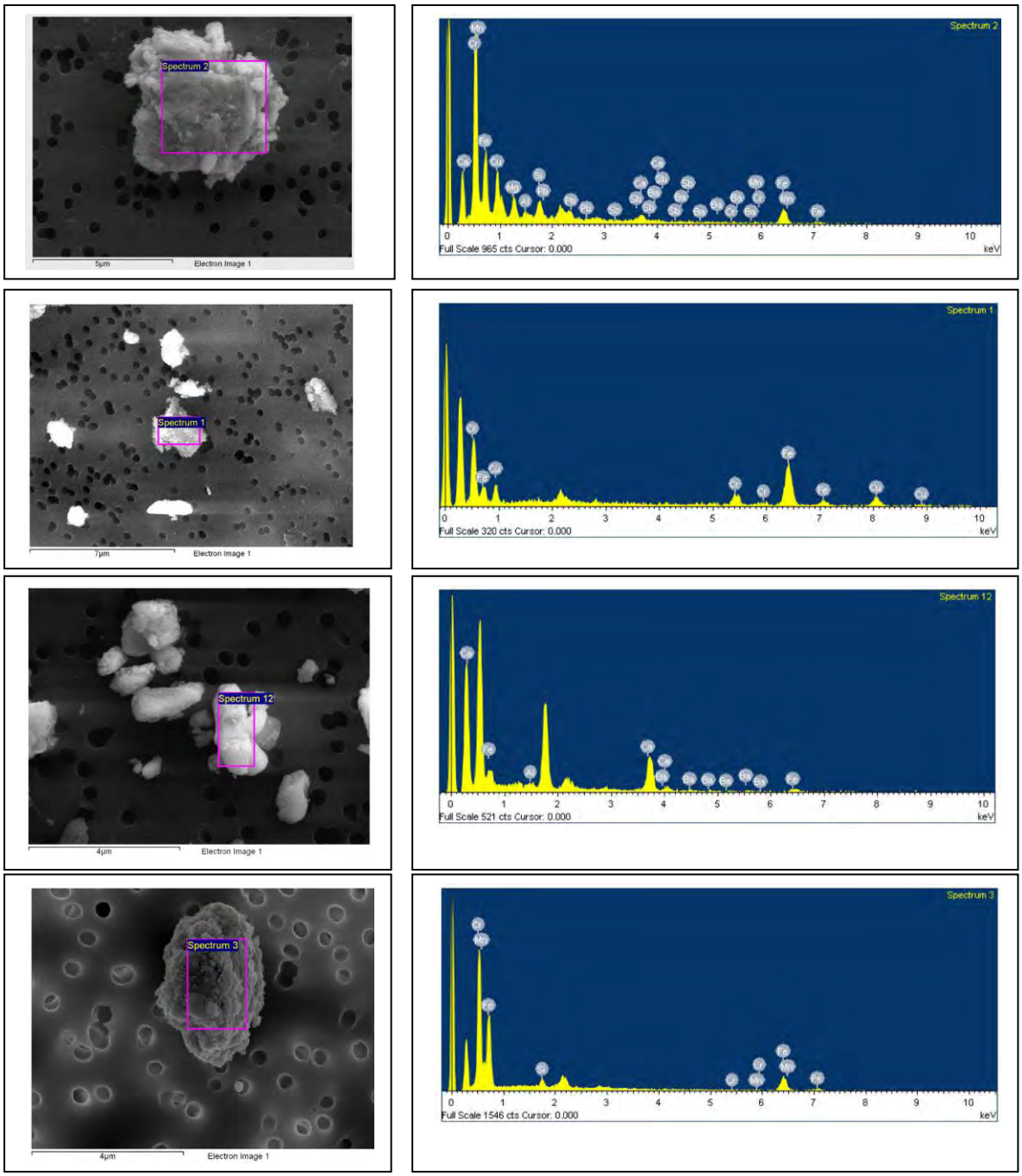

Fig. 12. Typical images of particles collected on Nuclepore filters: (a) morphology of particles generated from organic brake pad material; (b) EDS results for particles generated from organic brake pad material; (c) morphology of particles generated from sintered brake pad material; (d) EDS results for particles generated from sintered brake pad material; (e) morphology of particles generated from organic brake block material; (f) EDS results for particles generated from organic brake block material; (g) morphology of particles generated from cast iron brake block material; and (h) EDS results for particles generated from cast iron brake block material.

The morphologies and elemental compositions of the particles collected on Nuclepore filters were investigated using a FESEM equipped with EDS. Fig. 12(a)–(h) shows the morphologies and spectroscopy results for typical particles from various sources.

Fig. 13 illustrates the results of $\overline{\text{AWPER}}$ for all different braking materials. These results were calculated for the first 600 s of each test. The sintered brake pads had the lowest value of $\overline{\text{AWPER}}$ and the organic brake block had the highest value of $\overline{\text{AWPER}}$.

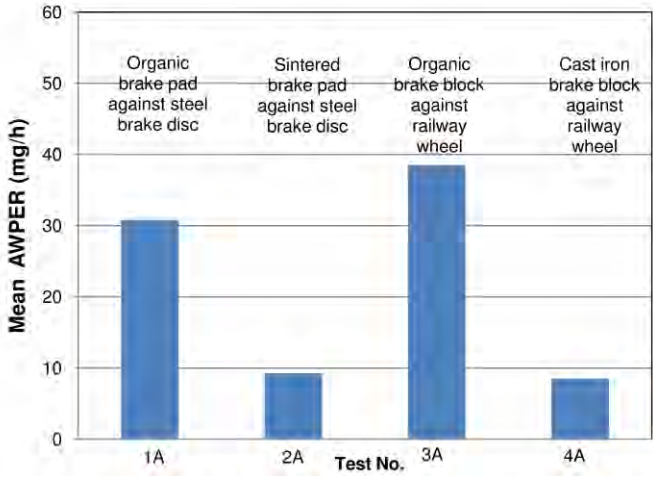

Fig. 13. Typical $\overline{\text{AWPER}}$ values for different braking materials.

5. Discussion

The three suggested regions in Fig. 2 can be explained by real situations in the conducted laboratory tests and by similar pin-on-disc studies [10,11,19–21]. Regions (I) and (II) correspond to the running-in of a sliding contact. In region (I), AWPER increases from zero to a constant value, which marks the start of region (II). The time interval in this region is dependent on two factors: first, the time it takes to accelerate the disc to the target rotational speed and, second, the time it takes for a steady-state particle concentration to be reached in the sealed box. Region (II) ends when contact surface changes, such as flash temperature, oxidation, and tribochemical film formation, start to influence the wear process. Case (c) presents the situation in which AWPER remains constant. In this situation, the cumulative effect on AWPER of changes in the contact surface state is neutral, so AWPER remains constant. Cases (b) and (d) represent situations in which the cumulative effect of changes in the contact state affects the AWPER level. In case (b), this effect is positive and increases AWPER, while in case (d), AWPER decreases. However, the increase in case (b) is not infinite, and AWPER approaches a constant value after a short while. Cases (a) and (e) represent unstable situations in which the effect is unlimited. In case (a), we assume that the AWPER keeps increasing linearly, resulting in an increase in the concentration. In contrast, in case (e), we assume a linearly decreasing rate, resulting in a decrease in the concentration.

At the beginning of all tests conducted in this and previous studies [10,11,21], the particle concentration suddenly increases, reflecting a burst of airborne wear particle emissions. This burst is followed by a decrease in emission and, in most tests, a levelling off (see Figs. 5(a),(c), 6(a),(c), 7(a),(c), 8(a),(c), and 10(a),(c)). These results are in agreement with the proposed model in cases (c) and (d). The results for the organic brake block material (see Figs. 9(a) and (c)) are exceptions. As depicted in Fig. 14, the particles generated from organic brake block material are more elongated; on the other hand, the amount of aluminium in this material is somewhat higher than in the brake pad material, whereas the amounts of antimony and copper are lower. According to Hutchings [1], particle composition and shape play crucial roles in determining the wear coefficient and hence directly affect the particle generation. Higher angularity in wear debris can increase the wear coefficient. In addition, the existence of more elongated particles among organic brake block particles can be used as an index to distinguish abrasive wear as the dominant wear mechanism [2]. Materials such as aluminium could cause higher abrasiveness, whereas materials such as copper and antimony compounds could reduce the wear rate. Materials such as alumina also follow the proposed model in cases (a) and (b). This result is also evident from the decreasing rate of generated particles greater than 1 μm in diameter and from the particle concentration results (see Figs. 5(a), 6(a), 7(a), 8(a), and 10(a)). Except for particles generated from the organic brake block material, the volume size distributions of particles increase in the submicron particle fraction (see Figs. 5(b), 6(b), 7(b), 8(b), and 10(b)). The increasing fraction of submicron particles might be explained by increasing temperature and the pulverizing of particles stuck to the disc. However, we see a decrease in the submicron particle fraction for organic brake block material, whereas the coarse particle fraction does not change markedly (Fig. 9(b)). The effects of the presence of more abrasive braking material on particle characteristics were also studied by Wahlström et al. [21]. They compared the particle concentrations in low-metalic (LM) brake pads, which wore at a higher rate than did in non-asbestos organic (NAO) brake pads. According to their report, the particle concentrations in LM brake pads increased continuously, whereas the particle concentrations reached a constant value in NAO brake pads. Further study is needed to determine the wear rate and investigate the mode of transition from mild to severe wear in such contacts.

Thuresson reported a higher average wear coefficient for organic brake block material than for cast iron brake block material [22]. His tests were conducted in a test rig mounted with a sample of railway wheel. He reported a higher average wear rate in the organic brake block material, in line with the current results, according to which higher particle concentrations are reported for organic brake block material.

The exponential decrease in concentration we observed is similar to that occurring at the end of tests reported by Sundh et al. [10] and Wahlström et al. [21], in which the disc reduced its rotating speed until it became stationary.

Nearly all of the submicron particles were spherical, a characteristic that was independent of the test conditions. Fig. 14(c), (e), (g), and (i) depict some of these spherically shaped particles. This phenomenon can be explained by the high temperature on the asperity tips [1] and high surface-to-volume ratio in submicron particles, which facilitates rapid heat transfer and may cause particle melting, in whole or in part. Such melting can lead to spherical or semi-spherical particles.

Most coarse particles generated from the brake pad and brake block materials were ellipsoid in shape, whereas most of the coarse particles from railway wheel and rail materials were flake shaped with sharp edges. Elongated wear particles were dominant in number among the particles generated from the organic brake pad material, while rounded particles were dominant in number for the other samples. These characteristics are attributable to the different wear modes occurring among different pairs of materials. In brake materials, abrasive and adhesive wear modes are dominant, whereas in wheel and rail materials, fatigue and delamination modes are the dominant wear mechanisms.

Several studies [6–8] report a similar dominant peak range in the coarse particle fraction. The dominant peak range in the fine particle fraction, which is reported to be 300–400 nm, is in line with field results presented by Abbasi et al. [8] and Fridell et al. [9]. These results were obtained by making stationary measurements in subways, except for studies in [8–9], who made on-board measurements in a train running aboveground, the particle size distribution being recorded during braking.

Based on field studies in three locations, Gustafsson [7] reports that the maximum frequencies of fine particles occur in three ranges, i.e., 10–20 nm, 20–50 nm, and 60–80 nm, which are higher than the values we obtained. In all three locations Gustafsson studied, the diesel locomotives did not use the main rail line; however, detailed information about the techniques used for measurement and to eliminate other possible particle sources was not mentioned [7].

The typical values of $\overline{\mathrm{AWPER}}$ depicted in Fig. 15 confirm that the proposed index can be obtained in real cases. However, those values are calculated based on the proposed test conditions, test setup, and selection of the first 600 s of sliding time. Any changes in those factors can affect the magnitude of calculated $\overline{\mathrm{AWPER}}$.

6. Conclusions

The following general conclusions can be made based on an analysis of the test results:

- A relationship between increased sliding velocity and increased particle concentrations was detected in the wear processes occurring in the braking materials.

- A relationship between increased contact pressure and increased particle concentrations was detected in the wear processes occurring in the braking materials.

- The rate of ultrafine particle emission from cast iron brake block material was significantly higher than from the organic brake block material.

- The rate of fine and ultrafine particle emission from the sintered brake pad material was significantly lower than the emission rate of the same-sized particles from the organic brake pad material under similar test conditions. There were negligible differences in coarse particle emissions between different pad materials.

- Three particle size regimes were identified:

In the ultrafine particle region, a peak occurred at diameters of approximately 70–120 nm

In the fine particle region, two peaks occurred at diameters of 300–400 and 500–600 nm

In the coarse particle region, a peak occurred at diameters of approximately 3–6 μm. The fraction of this peak is highly dependent on material composition and test conditions.

- A new index, airborne wear particle emission rate (AWPER), was introduced; this index is suggested to be used as a comparative index for non-exhaust emissions.

7. Acknowledgments

This research was performed under the auspices of the Railway Group at Royal Institute of Technology (KTH), Stockholm, Sweden. The author acknowledges valuable assistance from Dr. Wubeshet Sahle and Mr. Peter Carlsson at KTH.

References

[1] I. M. Hutchings, Tribology: Friction and Wear of Engineering Materials, Edward Arnold, Cambridge, UK, 1992.

[2] G.W. Stachowiak, G.P. Stachowiak, P. Posidalo, Automated classification of wear particles based on their surface texture and shape features, Tribology International 41 (2008) 34–43.

[3] P. G. Boulter, A review of emission factors and models for road vehicle non-exhaust particulate matter, PPR065 Project, TRL limited, UK. 2005. Online < http://uk-air.defra.gov.uk/reports/cat15/0706061624_Report1__Review_of_Emission_Factors.PDF >

[4] UK emission inventory team, AEA Group, UK informative inventory report (1980 – 2009), 2011 Online <http://uk-air.defra.gov.uk/reports/cat07/1103150849_UK_2011_CLRTAP_IIR.pdf>

[5] ANONYMOUS, Hygienische Forderungen für Untergrundbahnen. Internationale Wochenschrift für Wissenschaft, Kunst und Technik 38 (1909) 1205–1208.

[6] I. Salma, Air pollution in underground railway systems, in: R.E. Hester, R.M. Harisson (Eds.), Air Quality in Urban Environments, Royal Society of Chemistry, Cambridge, UK, 2009, pp. 65–85.

[7] M. Gustafsson, Airborne particles from the wheel–rail contact, in: R. Lewis, U. Olofsson (Eds.), Wheel–Rail Interface Handbook, CRC Press, USA, 2009, pp. 550–575.

[8] S. Abbasi, L. Olander, U. Olofsson, C. Larsson, A. Jansson, U. Sellgren, A field test study of airborne wear particles from a running regional train, Journal of Rail and Rapid Transit, 2011, In press

[9] E. Fridell, M. Ferm, A. Björk, A. Ekberg, On-board measurement of particulate matter emissions from a passenger train. Journal of Rail and Rapid Transit, 225 (2011), 99-106.

[10] J. Sundh, U. Olofsson, L. Olander, A. Jansson, Wear rate testing in relation to airborne particles generated in wheel–rail contact, Journal of Lubrication Science 21 (2009) 135–150.

[11] S. Abbasi, L. Olander, U. Olofsson, J. Wahlström, C. Larsson, U. Sellgren, A study of airborne wear particles generated from organic railway brake pads and brake discs, Wear, special issue Nordtrib 2010, In press

[12] http://delphi.com/pdf/emissions/Delphi-Passenger-Car-Light-Duty-Truck-Emissions-Brochure-2010-2011.pdf

[13] http://ec.europa.eu/environment/air/transport/road.htm

[14] T. Peters, D. Ott, P.T. Shaughnessy, Comparison of the Grimm 1.108 and 1.109 portable aerosol spectrometer to the TSI 3321 aerodynamic particle sizer for dry particles, Annals of Occupational Hygiene 50 (2006) 843–850.

[15] Y. Liu, P.H. Daum, The effect of refractive index on size distribution and light scattering coefficient derived from optical particle counters, Journal of Aerosol Science 31 (8) (2000) 945–957.

[16] Y. Zhu, N. Yu, T. Kuhn, W.C. Hinds, Field comparison of P-Trak and condensation particle counters, Journal of Aerosol Science 40 (2006) 422–430.

[17] Y.H. Cheng, Comparison of the TSI model 8520 and Grimm Series 1.108 portable aerosol instruments used to monitor particulate matter in an iron foundry, Journal of Occupational and Environmental Hygiene 5 (3) (2008) 157–168.

[18] H.J. Fissan, C. Helsper, H.J. Thielen, Determination of particle size distribution by means of an electrostatic classifier, Journal of Aerosol Science 14 (1983) 354–359.

[19] U. Olofsson, L. Olander, A. Jansson, Airborne wear particles generated from a sliding contact, Journal of Tribology 131 (2009) 044503-(1-4).

[20] U. Olofsson, A study of airborne wear particles generated from the train traffic: block braking simulation in a pin-on-disc machine, Wear 271 (2011) 86-91.

[21] J. Wahlström, L. Olander, U. Olofsson, A. Söderberg, A pin-on-disc simulation of airborne wear particles from disc brakes, Wear 268 (5–6) (2010) 763–769.

[22] D. Thuresson, Thermomechanic of block brakes, Ph.D. thesis, Chalmers University of Technology, Göteborg, Sweden, 2006.

Particle emissions from rail vehicles (A literature review)

Saeed Abbasi,
Ulf Olofsson,
Ulf Sellgren

Submitted to Atmospheric Environment journal

D

Particle emissions from rail vehicles: a literature review

Saeed Abbasi, Ulf Sellgren, Ulf Olofsson
KTH Machine Design, SE 10044, Stockholm, Sweden
Corresponding authors' email: sabbasi@md.kth.se

Abstract

Particle emissions are a drawback of rail transport. This work reviews recent research into particle emissions from rail vehicles. Both exhaust and non-exhaust particle emissions are considered when examining particle characteristics (e.g. size, morphology, composition, PM10, and PM2.5), adverse health effects, current legislation, and available and proposed solutions for reducing such emissions. We find that only a few limited studies have examined the adverse health effects of non-exhaust particle emissions and that no relevant legislation exists, warranting further research in this area.

Nomenclature / Abbreviations

ACGIH:	American Conference of Governmental Industrial Hygienists
ATSDR:	Agency for Toxic Substances and Disease Registry
BC:	Black carbon
CEN:	The European Committee for Standardization
DFG:	Deutsche forschungsgemeinschaft
DNA:	Deoxyribonucleic acid
DPM:	Diesel particulate matter
EC:	European Commission
EPA:	Environmental Protection Agency
EU:	European Union
EUROMOT:	The European Association of Internal Combustion Engine Manufacturers
IARC:	International Agency for Research on Cancer
MECA:	Manufacturers of Emission Controls Association
MMT:	Methylcyclopentadienyl manganese tricarbonyl
MMD:	Mass median diameter
MSHA:	Mine Safety and Health Administration
NIOSH:	The National Institute for Occupational Safety and Health
PAHs:	Polycyclic aromatic hydrocarbons
PM:	Particulate matter
UFP:	Ultrafine particles
UIC:	International Union of Railways
UNIFE:	The Association of the European Rail Industry
WHO:	World Health Organization

1. INTRODUCTION

Commercial rail transport appeared in the UK between 1804 and 1812, by means of steam locomotives running on cast iron rails. The London Underground, the oldest subway in the world, opened in 1863, 10 years before Carl Benz invented the first four-stroke gasoline engine for commercial vehicles used in road transport (Williams et al., 2000). Today, both of these transport modes are recognized as particle emission sources. However, the amount of research and legislations to limit particle emissions from rail transport is markedly small. Ever since the investigation of wear particles in rail transport began in 1909 (Anonymous, 1909), the high mass concentration of these particles has raised worries among researchers concerned with air quality. However, effective action has yet to be taken because of lack of relevant knowledge.

Rail transport involves various particle emission sources. Rail vehicles are one of the main sources of particles, primarily airborne ones. Exhaust and non-exhaust emissions are two categories of particle emissions from rail vehicles, and research has examined this area in recent years. The aim of the present review is to consider the following aspects of the selected studies:

current legislation and standards.
adverse health effects of particles.
particle characteristics (e.g., size, morphology, mass concentration, and composition).
current strategies for reducing emissions of these particles.

Table 1 summarizes the works selected for review; as shown, both exhaust and non-exhaust emissions were taken into account. It should be noted most studies of non-exhaust emissions have examined electric railways or subway systems, while most studies of exhaust emissions have examined railways systems with diesel locomotives, diesel multiple units (DMUs) or other diesel rail cars. However, both exhaust and non-exhaust emissions are traceable in all rail traffic, because even electric railways or subways use rail vehicles with diesel engines for shunting or maintenance purposes, while in locomotives and DMUs, wheels, rails, brake pads, and brake blocks, for example, contribute to non-exhaust emissions.

Table 1. Summary of topics and selected references covered in this review.

Selected topics	Publication year (number of studies)	
	Exhaust emissions	**Non- Exhaust emission**
Current legislation	2009(1) ; 2008(1); 2004(1);	We discussed several relevant literatures as there is no legislation.
Health effects	2009(1); 2008(1); 2006(1); 2005(1); 2002(1); 1989(1)	2010(2); 2009(2); 2008(2); 2007(2); 2005(1); 2004(1);2003(1); 2000(1), 1999(1)
PM levels in particular locations, such as stations, platforms, tunnels, and rail vehicles	2010(2)	2010(2); 2009(1); 2008(1); 2007(5); 2006(4); 2002(3); 2001(1); 1998(1)
Chemical composition of particles in rail transport	2007(1); 2006(1); 2004(1); 1998(1)	2010(2); 2009(1); 2007(2); 2005(2); 2004(1); 2001(1); 1909(1)
Particle morphology	2010(1); 2007(1); 2006(1); 2002(1); 1999(1); 1998(1)	2011(3), 2010(1); 2009(1); 2008(1)
Particle size	2010(1); 2007(1); 2006(1); 2002(1); 1998(1)	2011(2); 2010(3); 2009(1); 2006(2); 2004(1)
Current methods for reducing emissions of these particles	2011(1); 2010(1); 2007(2); 2006(2)	2009(1); 2006(2); 2005(1); 2002(1); 1993(1)

2. METHOD

We applied the integrative research review method of Cooper (1989), who suggested the following five stages for a research review:

I) defining a problem and hypothesis, resulting in an integrative research review
II) determining the data collection strategy and selecting multiple channels to prevent bias in coverage
III) evaluating retrieved data and deciding what data to include in the review
IV) analyzing the reviewed literature
V) reporting the results

Computerized key word searching was used in this review, as the technique is fast and efficient. However, this approach limits the search to electronically available studies, usually published after the 1980s. To compensate for this restricted coverage, we also performed some limited physical searches of the collection in the KTH library, searching technical magazines (not scientific journals), reports, and dissertations. That survey mainly included English documents. The key words used in the search were ~~–u~~nderground," ~~–s~~ubway," ~~–r~~ailway," ~~–t~~rain," ~~–l~~ocomotive," ~~–p~~latform," ~~–c~~ommuter," ~~–c~~ompartment," ~~–p~~article," ~~–v~~entilation," ~~–P~~M_{10}," ~~–P~~$M_{2.5}$," ~~–b~~rake block," ~~–b~~rake shoe," and ~~–b~~rake pad." Electronic documents in German,

Swedish, and Persian documents were also searched to a limited extent, using comparable keywords.
We reviewed 97 publications, comprising 81 articles in scientific journals and from conferences, five book and dissertation chapters, and 11 technical reports. In addition, we also examined various relevant pieces of legislation.

3. RESULTS

3.1 LEGISLATIONS

Both the USA and the EU have issued directives that set standards for exhaust emissions from diesel locomotives and railcars. These standards focus on controlling the mass of emitted HC, NO_x, CO, and PM (in g) per unit of power output (in kWh or bhph). Both sets of standards contain subcategories for the various applications or output powers of diesel engines.

In the USA, the EPA is using three approaches to controlling and reducing exhaust emissions from rail traffic: tightening emission standards for existing locomotives; specifying near-term engine-out emissions for newly built locomotives (TIER 3); and determining long-term standards based on applying high-efficiency exhaust gas treatment starting in 2015 (TIER 4). This regulatory framework is summarized in Table 2.

Table 2. Current US regulations covering emission factors (g bhph^{-1}) for line-haul and switching locomotives. All locomotives must be equipped with an automatic engine stop/start (AESS) idle control (EPA Locomotives, 2011).

Type	Tier	Year of manufacture	CO	HC	NOx	PM
Line-haul locomotives	Tier 0	1973-1992	5	1.00	9.5	0.22
	Tier 1	1993-2004	2.2	0.55[1]	7.40[1]	0.22
	Tier 2	2005-2011	1.5	0.30	5.5	0.10[2]
Power> 2300 hp	Tier 3	2012-2014	1.5	0.30	5.5	0.10
	Tier 4	2015	1.5	0.14[3]	1.3[3]	0.03
Switch locomotives	Tier 0	1973-2001	8	2.1	11.8	0.26
	Tier 1	2002-2004	2.5	1.2	11.0	0.26
	Tier 2	2005-2010	2.4	0.6	8.1	0.13[2]
Power>1006 hp Power≤2300 hp	Tier 3	2011-2014	2.4	0.6	5.1	0.10
	Tier 4	2015	2.4	0.14[3]	1.3[3]	0.03

[1]Without separate loop intake air cooling: NO_x, 8.0 g bhph^{-1}; PM, 1.0 g bhph^{-1}.
[2]Until January 2013: group (a), PM, 0.20 g bhph^{-1}; group (b), PM, 0.24 g bhph^{-1}.
[3]Manufacturers may elect to meet combined NO_x + HC standards: group (a), 1.4 g bhph^{-1}; group (b), 1.4 g bhph^{-1}.

In the EU, legislation regulating the exhaust emissions of locomotives came into force in 2004. In April 2004, EU Directive 97/68/EC was revised and Directive 2004/26/EC was introduced. This standard sets limit values for non-road mobile machinery (NRMM) engines, including DMUs and locomotives, based on their output powers. As Table 3 shows, these limit values were

implemented in two stages, the first (IIIA) effective 2005–2009 and the second 2011–2012. However, UNIFE has predicted that stage IIIB will not be completely realized before mid 2015 because of the recent economic crisis (Bönnen, 2009). This EU legislation is summarized in Table 3.

Table 3. Summary of EU Directive 2004/26/EC (2004).

Stage	Category		Propulsion by:	Approval from	Replacing on the Market	CO g kWh^{-1}	HC g kWh^{-1}	NO_x g kWh^{-1}	PM g kWh^{-1}
IIIA	RCA	P>130 kW	Railcar	01/07/2005	01/01/2006	3.5	4.0		0.2
	RLA	560kW≥P≥130kW	Locomotive	01/01/2006	01/01/2007	3.5	4.0		0.2
	RHA	P>560 kW	Locomotive	01/01/2008	01/01/2009	3.5	0.5	6.0	0.2
	RHA	P>2000 kW & SV>5 l/cylinder	Locomotive	01/01/2008	01/01/2009	3.5	0.4	7.4	0.2
IIIB	RCA	P>130 kW	Railcar	01/01/2011	01/01/2012	3.5	0.19	2.0	0.025
	RB	P>130 kW	Locomotive	01/01/2011	01/01/2012	3.5	4.0		0.025

Table 4 shows selected data on US and EU outdoor air quality regulations, which limit emissions of PM_{10}, $PM_{2.5}$, PAHs, and certain metal compounds. These emissions are considered independently of emissions of nitrogen dioxide, sulfur dioxide, ozone, and carbon monoxide, the limits for which are not shown in the table (EPA NAAQS, 2011; EU Directive 2008/50/EC, 2008).

Table 4. Comparison of US and EU outdoor air quality regulations and some of the parameters.

		$PM_{2.5}$ (µg m^{-3})	PM_{10} (µg m^{-3})	Lead (µg m^{-3})	Nickel (µg m^{-3})	Arsenic (µg m^{-3})	Cadmium (µg m^{-3})	PAHs (µg m^{-3})
US EPA website	Daily (24 h)	35	150	–	–	–	–	–
	Annual	15	–	0.15 [a]	–	–	–	–
EU directive 2008/50/EC	Daily (24 h)	–	50 [b]	–	–	–	–	–
	Annual	25	40	0.5	20[c]	6[c]	5[c]	1[c]

[a]The rolling three-month average.
[b]The limit 50 µg m^{-3} must not be exceeded 35 times a calendar year.
[c]Target value enters into force 31 December 2012.

Occupational exposure limits (OELs) specify guidelines that help protect people's health during exposure to natural or man-made substances, and several national and international organizations are currently investigating them. Some of those organizations clearly intend to approach health factors without considering feasibility or economic limitations. ACGIH is one of these pioneering organizations. Recently, Schenk et al. (2008) compared exposure limit values set by ACGIH with those of 17 well-known organizations in Europe, North America, Japan, and Australia. They reported that the highest substance coverage was offered by ACGIH, and that the OELs set by ACGIH were usually the lowest or nearly the lowest. The threshold limit value (TLV) is one of the indices used by ACGIH and refers to conditions under which nearly all

workers may be exposed day after day without adverse health effects. Table 5 shows some of these OELs for various materials and substances.

The threshold limit values (TLVs) is one of the indices used by ACGIH and refers to conditions under which nearly all workers may be exposed day after day without adverse health effects.

Table 5. Summary of selected occupational exposure limits (OELs) proposed by ACGIH.

Substance	**Chemical abstract number (CAS)**	**TLV (mg/ m³), time-weighted average for an 8-h day during a 40-h week**
Iron	7439-89-6	5
Nickel	7440-02-0	0.2, insoluble compound 10, metal/elemental
Chromium	7440-47-3 7440-47-3 13765-19-0 7789-06-2 7758-97-6	0.5, chromium (III) 0.05, soluble compounds of chromium (VI) 0.01, insoluble compounds of chromium (VI) unless listed below 0.001, calcium chromate 0.0005, strontium chromate 0.012, lead chromate
Molybdenum	7439-98-7	10, metal/insoluble/inhalable fraction 3, metal/insoluble/respirable fraction 0.5, metal/soluble/respirable fraction
Manganese	7439-96-5	0.2, inhalable fraction 0.02, respirable fraction
Silicon	7440-21-3	5, inhalable fraction 0.1, respirable fraction
Cobalt	7440-48-4	0.02
Cadmium	7440-43-9	0.01, inhalable fraction 0.002, respirable fraction
Aluminum	7429-90-5	10, inhalable fraction 1, respirable fraction
Titanium	7440-32-6	10
Zinc	7440-66-6	2
Tin	7440-31-5	2
Zirconium	10101-52-7	5
Calcium	7789-78-8	10, inhalable fraction 3, respirable fraction
Vanadium pentoxide	1314-62-1	0.05
Barium	7440-39-3 7727-43-7	0.5 10, barium sulfate
Copper	7440-50-8	1, dust 0.2, fumes (0.1 short-term exposure limit) 0.05, respirable fraction
Lead	7439-92-1	0.05
Antimony	1345-04-6	0.5
Arsenic	7440-38-2	0.01
Carbon	7440-44-0	10, inhalable fraction 3, respirable fraction
DPM (soot)	58-32-2	0.02, EC fraction[1], 0.16 TC fraction[2], 0.35 EC fraction[2]

[1] ACGIH withdrew the TLV of DPM from its lists in 2003.
[2] These TLVs were suggested by MSHA in 2005.

These OELs are set for time-weighted averages (TWA), usually for an eight-hour day during a 40-hour week. Short-term exposure limits (STEL) are used in rare cases and refer to 15-minute exposures. OELs are dependent on the chemical composition of the substances in question and a few particle characteristic factors, such as solubility, respirable fraction, and inhalable fraction.

It should be noted that when a mixture of various substances is being considered, cumulative effects are relevant. The summation ratios of OEL concentrations must be less than unity and can be represented as follows:

$$\frac{C_1}{OELs_1} + \frac{C_2}{OELs_2} + \ldots. + \frac{C_n}{OELs_n} < 1 \quad \text{Equation (I)}$$

3.2 ADVERSE HEALTH EFFECT

Hygienic or occupational problems concerning rail transport are not a new concern. Early studies by Winslow and Kligler (1912), Palmer et al. (1916), and Pincus and Stern (1937) exemplify the long history of such research.
However, only in recent years have these issues been considered in detail.
Exposure to diesel exhaust has been classified as likely carcinogenic to humans in EPA, WHO, IARC, and NIOSH cancer guidelines. Lung cancer is reported as the dominant disease by studies of various occupations exposed to diesel exhaust (Bhatia et al., 1998).
Diesel exhaust emissions were also reported to have non-cancer effects. The EPA reported ~~–t~~hat acute exposure to diesel exhaust has been associated with irritation of the eye, nose, and throat, respiratory symptoms (cough and phlegm), and neurophysiological symptoms such as headache, lightheadedness, nausea, vomiting, and numbness or tingling of the extremities" (EPA HAD, 2002). According to this study, neurobehavioral impairment (i.e., of blink relax latency, verbal recall, color vision confusion, and reaction time) was reported for railroad workers and electrical technicians exposed to diesel exhaust. Another study reported a higher incidence of chronic obstructive pulmonary disease (COPD) mortality among locomotive drivers and conductors exposed to diesel exhaust (Hart et al., 2006). Vinzents et al. (2005) also reported that ultrafine particle exposure resulted in DNA damage.
No evidence is reported concerning the allergic effects (e.g., asthma and immunologic effects) of diesel exhaust, but there are many reports that diesel exhaust can exacerbate those effects (Zhang et al., 2009; EPA report RIN 2060-AM06, 2008).
Another important factor when considering diesel exhaust emissions is soot, which is recognized as a carcinogen by IARC and DFG. Soot also affects both local and global climate (IARC, 2010; DFG, 2009).
Currently, no legislation regulates non-exhaust emissions, and most research into such emissions has compared measured levels with the limit values for outdoor air quality or OEL standards.
Pfeifer et al. (1999) reported that there was more manganese in London commuters' blood than in taxi drivers' blood. Crump reported that time spent in Toronto subways was the best predictor

of manganese in personal blood samples in his study (Crump, 2000). Chillrud et al. (2004, 2005) studied personal exposures to iron, manganese, and chromium dust among students and workers in New York City (NYC) and found that the NYC subway is the dominant source of these exposures.

The British Lung Foundation reported that using the London Underground (LU) may be hazardous because of the particle incidence (Britton, 2003). It was uncritically quoted that ~~–t~~ravelling for 20 minutes on the northern line through central London had the same effect on the lungs as smoking a cigarette."

The genotoxicity and oxidative stress effects of particles in the Stockholm subway have been compared with similar effects of aboveground particles by Karlsson et al. (2005). They reported that the subway particles were eight times more genotoxic and four times more effective at causing oxidative stress than were aboveground particles. The ability to form intracellular reactive oxygen was suggested as a possible explanation in their further studies (Karlsson et al., 2008). Midander et al. (2009) also reported that nanosized Cu and CuO particles are more genotoxic than those are microsized particles.

Another study examined the health impacts of rail traffic particulates on residents of London's King's Cross/St. Pancras area based on the observational health data (Haynes and Savage, 2007). This area of London is one of the most famous and oldest railway areas in the world, and rail traffic contributes substantially to the total pollution in the area. According to the study, in the area:
– low life expectancy at birth was reported for male and female residents
– the main causes of death for residents were cancer (25%), coronary heart disease (18%), and respiratory system disorders (12%) in 2001–2002
– cancer mortality, 1998–2002, among residents was higher than the national average
– circulatory and coronary heart disease mortality, 1998–2002, among residents was higher than the national average
– tuberculosis (TB) notification was higher among residents than in London or England as a whole

Nyström et al. (2010) conducted an experiment by investigating the effects of two-hour exposures on 20 healthy volunteers. According to their results, there was no cellular response in the volunteers' airways, but marked increases in fibrinogen and in regulatory T-cell expression of CD4/CD25/FOXP3 were observed in the volunteers' blood.

Another study of subway workers in NYC investigated several biomarkers, comparing them with the same biomarkers for bus drivers and subway office workers (Grass et al., 2010). DNA–protein cross-linkage and plasma chromium levels were markedly higher in subway workers than in bus drivers. However, no significant differences were observed between the biomarkers of subway workers and subway office workers.

It should be noted that no apparent health problems linked to these kinds of particles have been reported. In fact, some studies contradict the high risk of non-exhaust emissions from rail traffic.

Seaton et al. (2005) investigated the possible adverse health effects of particles in the LU. They reported a maximum iron oxide exposure of 200 μg m^{-3} in LU, and compared this with the OEL of 5000 μg m^{-3}. As the LU level was 25 times lower than the suggested OEL, they concluded that inhalation particles in LU should not be considered a serious problem, although efforts to reduce their emissions must continue as they are not nontoxic (Seaton et al., 2005).

Recently, some limited cohort studies have been conducted among subway drivers. In Stockholm, the frequency of heart attacks (Bigert, 2007) and lung cancer (Gustavsson, 2008) was investigated among male subway drivers and compared with other men with different occupations in the Stockholm subway. The frequency of lung cancer or heart attack was not increased among the male subway drivers in these studies.

3.3 PARTICLE CHARACTERISTIC

In this section, we review several particle characteristics, i.e., mass concentration, elemental composition, size, and morphology. The reviewed results for these characteristics are highly dependent on the original sources and test conditions. Exhaust emission particles are dependent on engine load, speed, and technology as well as on the type and elemental composition of the fuel, lubricant, engines, and after-treatment components. In non-exhaust emissions, operational factors (e.g., axle load and train speed), rail vehicle technical specifications (e.g., type of bogie, rail, and brake system), and infrastructure technical specifications (e.g., type of rail, overhead line, and masonry structures) all influence particle characteristics. Furthermore, meteorological conditions, instrument specifications, and measurement techniques are additional factors that influence results for both exhaust and non-exhaust emissions (Maricq, 2007; Nieuwenhuijsen et al., 2007; EPA RIN 2060-AM06, 2008; Salma, 2009; Abbasi et al., 2011a).

These selected results are useable to understand particle characteristics in rail transport, and generalising these data to other real cases must be done by concerning abovementioned limitations.

3.3.1 ELEMENT COMPOSITION

Kittelson investigated the composition of diesel exhaust particles from a heavy-duty diesel engine and reported a pie chart (Figure 1) for the element composition of his investigation (Kittelson, 2006; Kittelson, 1998). Carbon composed the main fraction in the diesel exhaust particles. SO_2, SO_3, and H_20 are other fractions. Fe, Mg, Ca, Cu, Zn, Pt, Pd, and Rh are the common detectable elements in the ash of diesel particles. According to Lombaret, wear of metal parts in the engine is the main source of Fe.

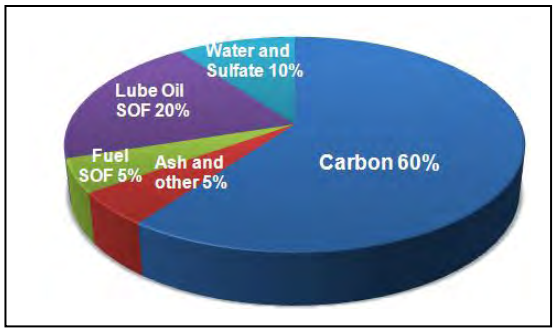

Figure 1. Typical PM composition of a heavy-duty diesel engine without after treatment; data from Kittelson (2006).

Lube oil additives are sources of Mg, Ca, Cu, and Zn (Lombaret et al., 2004). After treatment, components are suggested as the sources of particles contained Pt, Pd and Rh (Zereini et al., 2007).

The elemental composition of non-exhaust particles from rail transport was one of the initial issues considered by researchers. One of the oldest surveys, from 1909, considered particle characteristics in the NYC subway (Anonymous, 1909) and reported that subway dust comprised 60% iron and 20% organic material.

In recent years, a few more detailed investigations have been conducted to determine the elemental compositions of rail traffic particles. These results are summarized in Tables 6 and 7. Table 6 summarizes the findings regarding the composition of particles in underground stations; the reasons for the discrepancies between results are described in Section 3.3.

Table 6. Typical elemental compositions of particles in different size fractions in different subways; all values in µg m^{-3} unless otherwise specified.

Consistent	Gothenburg[1]		Budapest[2]		Tokyo[3]	Helsinki[4]	MexicoCity[5]	Rome[6]	NYC[7]	Stockholm[8]	London[9]
	$PM_{10-2.5}$	$PM_{2.5}$	PM_{10}	$PM_{2.5}$	PM_{10}	$PM_{2.5}$	$PM_{2.5}$	PM_{10}	$PM_{2.5}$	PM_{10}	$PM_{2.5}$
BC	0.52	0.59	3.1	3.1		6.3	3.7	–	–	–	–
Mg	–	–	0.43	0.13	0.4		–	–	–	–	–
Al	–	–	0.62	0.09	–	0.27	–	–	–	–	–
Si	–	–	2.5	0.4	4.9	0.4	2.4	–	–	–	2%
S	–	–	1.8	0.8	3.7	0.7	8.0	–	–	–	–
Cl	–	–	0.41	0.1	2.3	0.1	–	–	–	–	–
K	0.26	0.11	0.44	0.13	0.7	0.19	0.43	–	–	–	–
Ca	0.21	0.075	3	0.4	5.2	0.24	0.8	–	–	–	–
Ti	–	–	0.07	0.02	–	0.03	0.23	–	–	–	–
Cr	0.045	0.022	0.05	0.01	0.6	0.05	0.1	0.44	0.084	0.8%	0.1–0.2%
Mn	0.48	0.057	0.46	0.15	–	0.27	0.07	0.07	0.240	0.5%	0.5 – 1%
Fe	13	3.9	49	15	94	24.65	4.2	44	26	58.6%	64–71%
Ni	0.009	0.005	0.04	0.01	0.7	0.03	0.03	0.07	–	–	
Cu	0.26	0.17	0.69	0.19	1.0	0.15	1.6	2.5	–	–	0.1–0.9%
Zn	0.017	0.014	0.17	0.05	0.7	0.08	–	0.5	–	–	–
Pb	0.007	0.007	0.07	0.02		0.01	0.04	0.09	–	–	–
Ba	–	–	–	–	–	–	–	–	–	1%	–

1- Boman et al., 2009
2- Salma et al., 2007
3- Furuya et al., 2001
4- Aarnio et al., 2005
5- Nieuwenhuijsen et al., 2007
6- Ripanucci et al., 2006
7- Chillrud et al., 2004
8- Svartengren and Larsson, 2010
9- Seaton et al., 2005

Table 7 summarizes a recent investigation of the composition of particles from above ground rail traffic. The reasons for the discrepancies between results are described in Section 3.3.

Table 7. Typical element compositions of particles for different size fractions in different studies for above ground rail traffic.

	Stationary measurement (Lorenzo et al, 2006)		**Stationary measurement (Gehrig et al., 2007)**			**On-board measurement (Fridell et al., 2011)**	**On-board measurement (Abbasi, et al., 2011a)**	
	Sampling point 10 m far from railway site (µg m^{-3} of PM_{10})	Sampling point 120 m far from railway site (µg m^{-3} of PM_{10})	Röngenstrasse (µg m^{-3})	Gamperstrasse (µg m^{-3})	Zeughaus (µg m^{-3})	µg/filter	Sampling point near brake pad	Sampling point in the middle of axle
Fe	3.859	0.951	1.76	1.49	0.57	302	64.7%	59%
Si	*	*	–	–	–	53	**	**
Cu	–	–	0.081	0.053	0.021	18	9.9%	8.1%
Al	2.443	1.456	0.062	0.075	0.063	13	2.6%	6%
Zn	–	–	0.045	0.036	0.045	7.2	3.9%	3%
Na	–	–	0.12	0.12	0.12	5.9	1.6%	3.7%
Ni	–	–	0.003	0.003	0.002	1.7	0.7%	0.5%
S	*	*	0.99	1.03	1.05	–	–	–
P	–	–	0.017	0.018	0.014	–	–	–
Ca	0.648	0.209	0.30	0.40	0.32	10	4.9%	6%
K	–	–	0.29	0.29	0.31	8.4	**	**
Cr	–	–	0.006	0.006	0.002	1.5	0.7%	0.5%
Mn	–	–	0.018	0.017	0.008	3.2	0.7%	0.7%
Mg	–	–	0.067	0.077	0.064	8.6	4%	4.9%
Ba	–	–	–	–	–	0.33	0.4%	0.2%
B	–	–	–	–	–	0.32	–	–
V	–	–	–	–	–	0.51	<0.5%	<0.5%
Mo	–	–	–	–	–	0.66	<0.5%	<0.5%
Ti	–	–	–	–	–	1	<0.5%	<0.5%
Sb	–	–	–	–	–	4.6	2.9%	2.6%
Sn	–	–	–	–	–	–	<0.5%	<0.5%
Pb	–	–	0.013	0.012	0.011	0.46	<0.5%	<0.5%

* The number concentration of particles containing Si and S is also reported in that paper, but their mass concentration was not reported.

** The author reported that these elements occurred in greater amounts at the sampling point in the middle of the axle, while at the other sampling points they were under the detection limit.

3.3.2 RECORDED PM_{10} and $PM_{2.5}$

As reported in Tables 2–4, particle mass concentration is one of the main factors considered in current regulations. In this regard, several investigations have recorded the mass concentrations of PM_{10} and $PM_{2.5}$ in different railway locations, such as inside trains and on platforms. Tables 8-10 show summaries of these results. The differences in the presented results are attributable to reasons discussed in Section 3.3.

If we compare the results of Tables 8-9 with the limit values for PM_{10} and $PM_{2.5}$ in Table 4, we distinguish that these values are several times higher in the subway stations particularly in platforms.

Tables 8-10 show summaries of these results. The differences in the presented results are attributable to reasons discussed in Section 3.3.

If we compare the results of Tables 8-9 with the limit values for PM_{10} and $PM_{2.5}$ in Table 4, we distinguish that these values are several times higher in the subway stations particularly in platforms.

Table 8. Typical ranges and mean values of particle mass concentrations, µg m^{-3}, in different size fractions in various underground systems; measured inside train.

Location	PM_{10} size fraction(µg m^{-3})		$PM_{2.5}$ size fraction (µg m^{-3})		Measurement environment	Reference
	Range	Mean	Range	Mean		
Beijing	–	325	–	–	Inside train	Li et al., 2007
Berlin	–	147	–	–	Inside train	Fromme et al., 1998
Boston	–	–	–	47	Inside train	Hill and Gooch, 2010
Guangzhou	26–123	67	–	–	Inside train	Chan et al., 2002a
Helsinki	–	–	17–26	21	Inside train	Aarnio et al., 2005
Hong Kong	23–85	44	–	–	Inside train	Chan et al, 2002b
London	–	–	–	130–200	Inside train	Seaton et al., 2005
London	–	–	12–371	228	Inside train	Adams et al., 2001
Mexico city	–	–	6–68	–	Inside train	Gomez-Perales et al., 2007
New York City	–	–	–	62	Inside train	Chillrud et al., 2004
New York City	–	–	–	55	Inside train	Hill and Gooch, 2010
Prague	24–218	114	–	–	Inside train	Branis, 2006
Seoul	–	–	–	117	Inside train	Park and Ha, 2008
Seoul	–	–	115–136	126	Inside train	Kim et al., 2008
Taipe	–	–	8–68	32	Inside train	Cheng et al., 2008

Table 9. Typical ranges and mean values of particle mass concentrations, μg m^{-3}, in different size fractions in various underground systems.

Location	PM_{10} size fraction(μg m^{-3})		$PM_{2.5}$ size fraction (μg m^{-3})		Measurement environment	Reference
	Range	Mean	Range	Mean		
Budapest	25–232	155	–	51*	On platform	Salma et al., 2007
Buenos Aires	–	152–270**	–	–	On platform	Murruni et al., 2009
Cairo	974–1094**	938**	–	–	In tunnel station	Awad, 2002
Cairo	131–921**	447**	–	–	In surface station	Awad, 2002
Helsinki	–	–	23–103	60	On platform	Aarnio et al., 2005
London	–	1000–1500	–	270-480	On platform	Seaton et al., 2005
Prague	10–210	103	–	–	On platform	Braniš, 2006
Rome	71–877	407	–	–	On platform	Ripanucci et al., 2006
Seoul	–	–	82–176	129	On platform	Kim et al., 2008
Seoul	–	–	–	105	On platform	Park and Ha, 2008
Stockholm (Subway)	175–542	357	95–303	199	On platform (Weekdays)	Johansson and Johansson, 2003
Stockholm (Subway)	120–414	267	66–230	148	On platform (Weekends)	Johansson and Johansson, 2003
Stockholm (Arlanda S)	66–110	88	–	–	Tunnel	Gustafsson et al., 2006
Stockholm (Arlanda C)	162–312	237	–	–	Tunnel	Gustafsson et al., 2006
Taipei	–	–	7–100	35	On platform	Cheng et al., 2008
Taipei	10–104	40	4–60	16	Station concourse	Cheng and Lin, 2010
Tokyo	30–120	72	–	–	On platform	Furuya et al., 2001

* This measurement was done for $PM_{2.0}$.
** These measurements were done for TSP.

Table 10. Typical ranges and averages of particle mass concentrations, μg m^{-3}, for different size fractions in various aboveground rail traffic systems.

Type of rail vehicle	Location	PM_{10} Mean	$PM_{2.5}$ Mean	Measurement environment	Reference
Diesel powered train	Sydney	—	27	Inside train	Knibbs et al., 2010
	Boston—locomotive in front	—	70	Inside train	Hill and Gooch, 2010
	Boston—locomotive in rear	—	56	Inside train	Hill and Gooch, 2010
	NYC—locomotive in front	—	13	Inside train	Hill and Gooch, 2010
	NYC—locomotive in rear	—	5	Inside train	Hill and Gooch, 2010
Electric powered train	Beijing	108	37	Inside train	Li et al., 2007
	Hong Kong	48	38	Inside train	Chan et al., 2002b
	Gotenberg	41	—	On-board	Freidell et al., 2011

3.3.3 PARTICLE SIZE

According to Kittelson (1998, 2006), diesel exhaust particles may occur in a trimodal particle size distribution. The nuclei mode region, which refers to particles 5—50 nm in diameter, includes nearly 90% of the total number of particles. Diluted sulfur compounds, volatile organics, and metal ash are the main sources of such particles. An accumulation mode includes particles 100—300 nm in diameter; the main fraction of the total particle mass belongs to this mode and mainly comprises carbonaceous compounds. Finally, a coarse mode is defined, which includes particles over 1 μm in diameter. These particles are generated when the accumulation mode particles deposited on the cylinder or exhaust surfaces are retained. Coarse mode and nuclei mode particles account for 5—20% of the total particle mass (Kittelson, 1998, 2006).
Mohr reported that the primary soot particles from heavy duty diesel engines are 28.5–32.4 nm in diameter. He and his colleagues reported that the diameter of primary soot particles is reduced by increasing the fuel injection pressure, increasing the maximum flame temperature, or advancing the start of injection. However, operating exhaust gas recirculation (EGR) increases the diameter of those particles (Mohr et al., 2005).

It should be noted that the use of catalysts in diesel engines can also generate coarse particles containing Pt or Rh. According to Zereini et al. (2001), a combination of vibration and thermal effects causes catalyst wear, and these authors reported catalyst-derived particles >2 μm in diameter, with the distribution peak at a diameter of approximately 5 μm. Nevertheless, overall, catalysts significantly reduce particle emissions, and the emission of catalyst particles is negligible (Maricq, 2007).

Recently, a comprehensive field study of exhaust emissions was conducted by the Clean Air Task Force (Hill and Gooch, 2010). They measured the concentrations of UFPs and $PM_{2.5}$ in the train car air breathed by commuters riding diesel trains on the Boston–New York route. They investigated the effect of pull-train (diesel locomotive in front), push-train (diesel locomotive in rear), increasing speed, and decreasing speed on those factors. The Task Force reported that the average UFP concentration in the train air was 15–20 times higher than in outdoor ambient air for the pull-train configuration, but only 3–5 times higher than in outdoor ambient air for the push-train configuration.

Three particle size regions are also recognized for the non-exhaust emissions from rail vehicles according to field tests in subways or aboveground rail traffics.

The coarse region with the highest particle number frequency was the 2–7 μm diameter range (Gustafsson et al., 2006; Lorenzo et al., 2006; Salma, 2009; Abbasi et al., 2011a). The fine region with the highest particle number frequency was the 250–650 nm diameter range (Seaton et al., 2005; Gustafsson, 2009; Abbasi et al., 2010; Fridell et al., 2011). All these studies agreed that there was a peak at approximately 350 nm in diameter. Besides this peak, other peaks at 280 nm and 600 nm in diameter were found in laboratory tests by Sundh et al. (2009) and Abbasi et al. (2011a, b).

Finally, the fine region included particles <100 nm in diameter. A maximum frequency of fine particles 60—80 nm in diameter was reported by Norman and Johnsson (2005), while laboratory tests generating wear particles recorded a peak particle frequency at approximately 70—100 nm (Sundh et al., 2009; Abbasi et al., 2010). However, other researchers reported finer particle sizes. Salma et al. (2007) reported a dominant fraction of particles 10—50 nm in diameter for PM_2, while Gustafsson et al. (2006) reported a dominant fraction of particles 10—20 nm in diameter for Arlanda S and 20–50 nm for Arlanda C.

Cheng and Lin (2010) investigated the mass of particles from the Taipei Rapid Transit System according to various size fractions, reporting three peaks for the size fractions of 0.23—0.3 μm, 5—7.5 μm, and 10—15 μm.

3.3.4 PARTICLES MORPHOLOGY

Particle morphology is another important issue. Particle morphology not only influences the severity of adverse health effects (Madl and Pinkerton, 2009), but also conveys information about the factor/s contributing to particle formation (Lee et al., 2002; Stachowiak et al., 2008).

According to Kittelson (1998) and Maricq (2007), almost all particles from diesel exhaust are spherical before aggregation. Thermal processes such as dilution and condensation explain such spherical shapes (Hinds, 1999). However, these spherical particles can aggregate and form new shapes. Lee et al. (2002) reported that most diesel particles were amorphous in structure under low load conditions, whereas they displayed graphite structure under high loads. Lee et al. (2002) explained these phenomena by the differences in dominant aggregation mechanisms.

Particles from non-exhaust emissions come in many shapes. Nearly all coarse non-exhaust particles have flake shapes (Salma, 2009; Abbasi et al., 2011a, b; Sundh and Olofsson, 2011), whereas the fine and ultrafine particles are spherical, semi-spherical, or ellipsoidal in shape (Lorenzo et al., 2006; Abbasi et al., 2011a; Sundh and Olofsson, 2011). It is suggested that differences between the dominant wear mechanisms cause the differences in wear particle shape (Stachowiak et al., 2008). This suggestion was confirmed by Abbasi et al. (2011b) in an investigation of various railway components.

Figure 2 shows an image of particles from diesel exhaust. Several images of particles collected during on-board measurements from a running train are shown in Figures 3–4. Figures 5–9 show the morphology of particles from wheel–rail contact and braking materials, which were generated in a pin-on-disc machine.

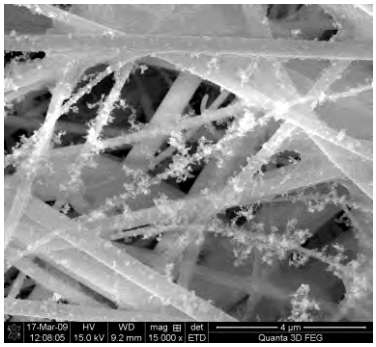

Figure 2. Typical particles from diesel exhaust (Tornehed, 2010).

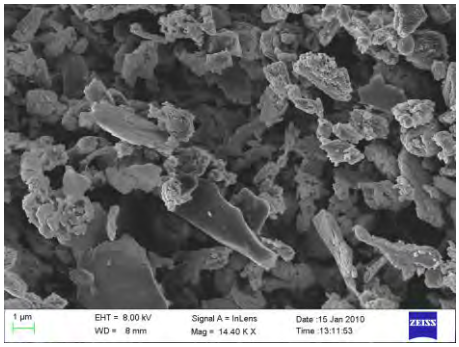

Figure 3. Typical particles from aboveground rail traffic (Abbasi, 2011a).

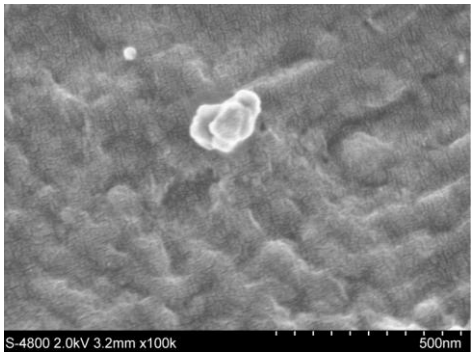

Figure 4. Typical particles from aboveground rail traffic in a field test (Abbasi, 2011a).

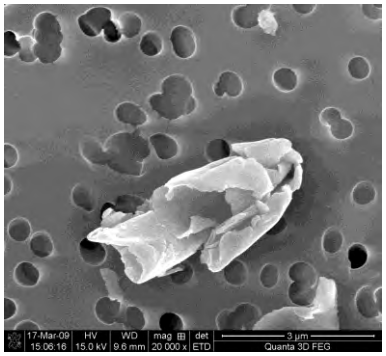

Figure 5. Typical particles from a wheel–rail contact in lab testing (Sundh and Olofsson, 2011).

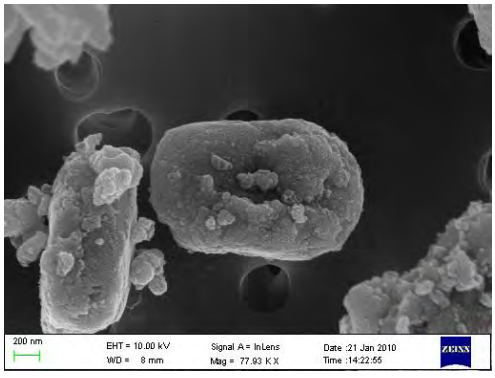

Figure 6. Typical particles from organic brake pad and steel brake disc materials in lab testing (Abbasi, 2010).

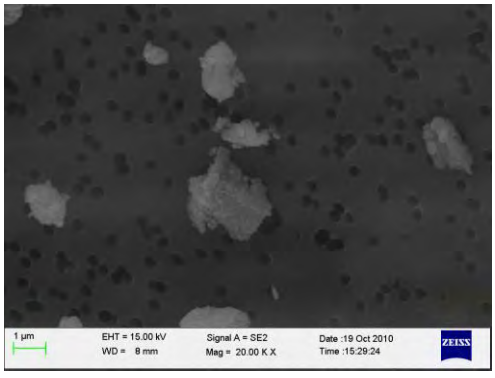

Figure 7. Typical particles from sintered brake pad and steel brake disc materials in lab testing (Abbasi, 2011b).

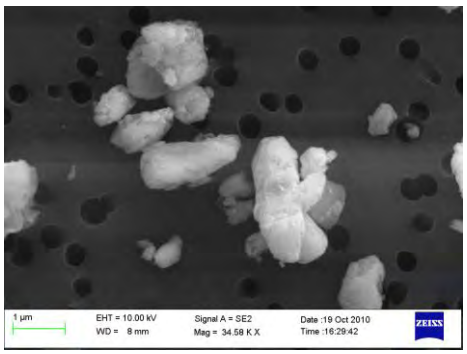

Figure 8. Typical particles from organic brake block and railway wheel materials in lab testing (Abbasi, 2011b).

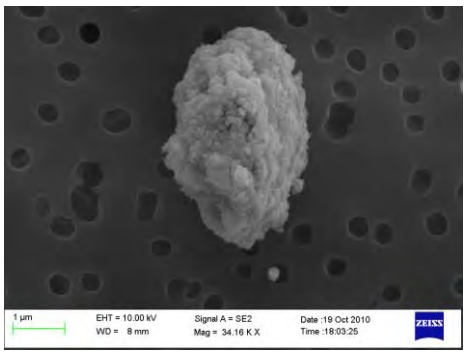

Figure 9. Typical particles from cast iron brake block and railway wheel materials in lab testing (Abbasi, 2011b).

3.4 ALTERNATIVES TO REDUCE PARTICLES

As more studies have examined diesel exhaust emissions, more solutions have been suggested. Recently, a number of these were reviewed by Silver (2007). He discussed the effects of oxygen enrichment, increased fuel injection pressure, injector design features, increased compression ratio, EGR systems, reduced injector sac volume, combustion chamber design, re-engining, variable valve timing, and single-bank idling as possible means to reduce the PM_{10} fraction from diesel exhaust emissions. Furthermore, he reviewed the implementation of exhaust after-treatment alternatives to reduce DPM. Options such as diesel oxidation catalysts (DOCs), diesel particle filters (DPFs), continuous regenerative traps (CRTs), selective catalytic reduction systems (SCRs), and combinations of these methods (SCR + CRT, SCR + DPF) were discussed in his work.

MECA suggested crank case emission control as another applicable method. According to MECA, this method could reduce DPM emissions to as low as 0.04 g bhp^{-1} (MECA, 2011). Mohammadi et al. (2003) suggested that high-frequency dielectric barrier discharge plasma may reduce DPM. The effects of fuel-born catalysts (FBCs) in terms of soot reduction were evaluated by Song et al. (2006). Other factors that affect particle emissions from diesel engines, such as the technology used in engine and fuel composition, have been reviewed by Maricq (2007). Recently, electrochemical reduction (ECR) systems were evaluated by Yoshinobu et al. (2010). In practice, when evaluating these solutions, their effects on emission factors must be weighed in light of technical and economic considerations. Nevertheless, a study conducted by UIC, UNIFE, Euromot, and AEA Technology found that SCRs, DPFs, SCR + DPF, and re-engining were the most promising alternatives in terms of benefit-to-cost ratio (Kollamthodi, 2006).

Various methods for reducing wear in the wheel–rail contact have been reviewed by Braghin et al. (2009). He noted that optimizing the wheel profile and applying friction modifiers on wheels or rails were successfully implemented and reported by various researchers. Optimizing the bogie design is also another suggested solution. These kinds of optimizations are intended to minimize creep forces and increase running performance. These objectives can be achieved by either reducing primary suspension stiffness (Andersson et al., 2007) or adding new systems, such as active primary suspension (Shen and Goodall, 1997), independent drive wheels (Gretzschel and Bose, 2002), active secondary suspension (Diana et al., 2002), and active wheel steering (Wickens, 1994). However, a series of technical and economic factors must be considered when optimizing or designing a new bogie to address wear problems. For example, using an articulated bogie is an attractive option in freight cars, whereas it is less attractive in passenger cars. On the other hand, the use of mechatronic bogies would be meaningless in freight transport.

Mosleh and Khemet (2006) reported the positive effects of radial grooves on brake discs in terms of reducing wear debris. According to their work, a cast iron disc machined with radial grooves running against a Jurid 539 brake pad produced less wear debris and less recorded friction variation. These interesting results were achieved by testing car braking materials; however, the approach can be considered potentially applicable to railway braking materials as well.

Applying a proper filtering system was also suggested and discussed as a method for reducing exposure to particles. Tokarek and Bernis investigated the effect of using an electrostatic precipitator in the existing ventilation system in a Paris subway station (2006). They reported that the particle concentration declined to half the initial value after this retrofit.

As presented in Tables 7 and 8, particle concentrations measured inside (Table 8) and outside trains (Table 9) differ significantly, based on results from Helsinki and Taipei. These differences were explained by the filtration systems installed in the rail vehicles.

4. DISCUSSION AND CONCLUSION

Various alternatives for reducing particle emissions from rail transport have been discussed. National and international regulations usually prompt manufacturers to pay attention to the particle emissions of their products. This is made clear by comparing the particle emission rates of light passenger cars produced by European, American, and Japanese manufacturers, where a huge reduction in the exhaust emission rates has occurred over the past 20 years.

Nevertheless, existing regulations apply only to the *exhaust* emissions from engines. In all of these regulations, emission amounts are evaluated based on particle mass (i.e., mg) per distance (km) or particle mass (i.e., mg) per engine power (kwh). In rail transport, EU Directive

2004/26/EC (TIER 03 and Tier 04) mandates limiting and reducing the exhaust emissions from locomotives and other diesel rail traction vehicles.

In the field of non-exhaust emissions, few studies have been conducted so only a few relevant regulations can be discussed. However, the phenomenon of non-exhaust emissions is well-known in road transport, where it involves airborne particles from tire, braking materials, and roads. One existing regulation prohibits or limits the use of studded tires, the adverse effects of which on health and PM_{10} are documented by Dahl et al. (2006), Ljungman et al. (2007) and Gustafsson et al. (2009). Such results justify banning or limiting the use of studded tires. For example, the use of studded tires is prohibited in Japan, the UK, Germany, Bulgaria, Croatia, the Czech Republic, Hungary, Netherlands, Poland, Slovania, Slovakia, Romania, Portugal, and 10 states in the USA (Götzfried, 2008). There are also seasonal restrictions in Austria, Switzerland, Sweden, Norway, and most US states. Recently, various findings regarding emissions from tires, braking material, and road surfaces were reviewed in the EMEP/CORINAIR Guidebook (Ntziachristos and Boulter, 2009). The total particle fractions are expressed in mg km^{-1} according to testing conditions defined for specific vehicles.

There is lack of a similar methodology for non-exhaust emissions from rail transport. Abbasi et al. (2011b) suggested a method for measuring the airborne wear particle emission rate (AWPER) from wheel–rail contacts and braking materials. This method can be used by manufacturers to demonstrate the competitive advantage of their products. It was suggested that this method be used by governmental organizations to force manufacturers to consider the wear particle emission rates of their products and to optimize their products in accordance with the proposed regulations so as to minimize related emissions.

Another strategy for reducing non-exhaust emissions would be to impose a non-exhaust emission tax. This would encourage train operators or railcars owners to retrofit or replace bogies with poor steering performance or materials with high AWPER values. Consequently, the particle emission rate from non-exhaust sources would be lowered.

According to Tables 7 and 8, iron is the dominant element identified in almost all reviewed studies. Some of the studies considered the characteristics of iron to be the main source of its adverse health effects (Seaton et al., 2005). However, if we compare the Mn/Fe, Cu/Fe, and Cr/Fe from Tables 7 and 8 with the predetermined OELs for these materials in Table 5, we understand that the risks caused by those non-ferrous materials are markedly higher than that of iron, particularly on subway platforms.

Furthermore, the concentrations of these elements can be increased by road traffic or other pollutant sources. For example, Boudia et al. (2006) reported how the MMT content of road vehicle fuel can affect manganese concentrations in subways. He measured the respirable fraction (<5 μm) and total concentration of Mn in three stations in Montreal, Canada, over two weeks. He found that the Mn concentrations were lower in stations located near lower road traffic. No correlation between subway traffic and Mn concentrations was found in his study.

Meanwhile, the amounts of Ca, Si, Al, and Na reported in Tables 7 and 8 are also considerable. So instead of focusing on the concentrations of single elements, the combined, cumulative concentrations of elements such as Fe, Cu, Cr, Mn, Na, Al, Si, and Ca as well as soot must be considered by using equation (I).

Furthermore, the adverse health effects of particles from rail vehicles on more sensitive people, such as children and people with pre-existing respiratory problems (Tager, 2005; Knibbs et al., 2011) or diabetes (Golhd, 2008), must be studied in depth.

Exposure to UFPs is another important issue in rail traffic. Actually, most studies of the adverse health effects of UPFs focus on diesel exhaust. However, laboratory results presented by Sundh et al. (2009), Abbasi et al. (2010, 2011b), and Olofsson (2010) indicate that UFPs are also generated by wear processes involving rail, wheel, and braking materials. Jansson et al. (2010) also commented on the traditional view that associates only particles >1 μm with wear processes, ignoring the role of wear process in generating submicron particles (2010).

Knibbs reported that diesel-powered trains generate a weighted mean number concentration of UFPs of 9.0×10^4 particles cm^{-3}, while electric-powered trains generate 3.0×10^4 particles cm^{-3} (2011). As predicted, the amount was lower for electric-powered trains, though still high. Madl and Pinkerton (2009) identified more than 30 different particle characteristics and exposure factors to be used in evaluating the health effects of particles. Particle mass, which was one of these particle factors, has been widely used in research and regulations. These factors are obvious in the summarized data presented in Tables 2–5 and 8–10. In contrast, other particle characteristic factors, such as size, shape, number, and composition, have been poorly investigated and considered in current regulations. The development of efficient and proactive countermeasures calls for further studies of particle characteristics, generation mechanisms, and exposure factors, particularly by focusing on non-exhaust emissions from rail transport.

References

Abbasi, S., Olander, S., Olofsson, U., Wahlström, K., Larsson, C., Sellgren, U., 2010. A study of airborne wear particles generated from organic railway brake pads and brake discs. Wear, special issue Nordtrib 2010, In press.

Abbasi, S., Olander, L., Olofsson, U., Larsson, C., Jansson, A., Sellgren, U., 2011a. A field test study of airborne wear particles from a running regional train. Journal of Rail and Rapid Transit, in press.

Abbasi, S., Jansson, A.,Olander, L., Olofsson, U., Sellgren, U., 2011b. A pin-on-disc study of the rate of airborne wear particle emissions from railway braking materials. Submitted to Wear.

Aarnio, P., Yli-Tuomi, T., Kousa, A., Mäkelä T., Hirsikko, A., Hämeri, K., Päisänen, M., Hillamo, R., Koskentalo, T., Jantunen, M., 2005. The concentrations and composition of and exposure to fine particles (PM2.5) in the Helsinki subway system. Atmospheric Environment 39, 5059–5066.

Adams, H.S., Nieuwenhuijsen, M.J., Colvile, R.N., McMullen, M.A.S., Khandelwal, P., 2001. Fine Particle (PM2.5) Personal exposure levels in transport microenvironments, London, UK. Science of the Total Environment 279, 29–44.

Andersson, E., Berg, M., Stichel, S., 2007. Rail Vehicle Dynamics. Division of Rail Vehicles, Department of Aeronautical and Vehicle Engineering, KTH, Stockholm.

Anonymous, 1909. Hygienische Forderungen für Untergrundbahnen. Internationale Wochenschrift für Wissenschaft, Kunst und Technik 38, 1205–1208 (in German).

Awad, A.H.A., 2002. Environmental study in subway metro stations in Cairo, Egypt. Journal of Occupational Health 44, 112–118.

Braghin, F., Bruni, S., and Lewis, R., (2009). Railway wheel wear, in: R. Lewis, U. Olofsson (Eds.), Wheel–Rail Interface Handbook, CRC Press, USA, 2009, pp. 172-210.

Bhatia, R., Lopipero, P., Smith, A., 1998. Diesel exposure and lung cancer. Epidemiology 9(1), 84–91.

Bigert, C., Klerdal, K., Hammar, N., Gustavsson, P., 2007. Myocardial infarction in Swedish subway drivers. Scandinavian Journal of Work, Environment & Health, 33(44), 267–271.

Boman, J., Carvalho, M.L., Alizadeh, M.B., Rezaievara, P., Wagnera, A., 2009. Elemental content of aerosol particles in an underground tram station. X-Ray Spectrometry 38, 322–326.

Bönnen, N., 2009. NRMM Directive: Introduction of flexibility for rail applications, UNIFE. Available at http://www.unife.org/uploads/090708_UNIFE_on_NRMM_flexibility_-_final%281%29.pdf (accessed 3 March 2011).

Braniš, M., 2006. The contribution of ambient sources to particulate pollution in spaces and trains of the Prague underground transport system. Atmospheric Environment 40, 348–356.

Britton, M., 2003. Lifestyle and Your Lungs. Lung Report III. British Lung Foundation, London.

Chan, L.Y., Lau, W.L., Lee, S.C., Chan, C.Y., 2002a. Commuter exposure to particulate matter in public transportation modes in Hong Kong. Atmospheric Environment 36, 3363–3373.

Boudia, N., Halley, R., Kennedy, G., Lambert, J., Gareau, L., Zayed, J., 2006. Manganese concentrations in the air of the Montreal (Canada) subway in relation to surface automobile traffic density. Science of the Total Environment, 366, 143–147.

Chan, L.Y., Lau, W.L., Zou, S.C., Cao, Z.X., Lai, S.C., 2002b. Exposure level of carbon monoxide and respirable suspended particulate in public transportation modes while commuting in urban area of Guangzhou, China. Atmospheric Environment 36, 5831–5840.

Cheng, Y.H., Lin, Y.L., Liu, C.C., 2008. Levels of PM10 and PM2.5 in Taipei Rapid Transit System. Atmospheric Environment 42, 7242–7249.

Cheng, Y.H, Lin, Y.L., 2010. Measurement of particle mass concentrations and size distributions in an underground station. Aerosol and Air Quality Research, 10, 22–29.

Cooper, H.M., 1989. Integrating research: a guide for literature reviews. Applied Social Research Methods Series, vol. 2. SAGE Publications, Newbury Park/London/New Delhi.

Chillrud, S.N., Epstein, D., Ross, J.M., Sax, S.N., Pederson, D., Spengler, J.D., Kinney, P.L., 2004. Elevated airborne exposures of teenagers to manganese, chromium, and steel dust and New York City's subway system. Environmental Science & Technology 38, 732–737.

Chillrud, S.N., Grass, D., Ross, J.M., Coulibaly, D., Slavkovich, V., Epstein, D., Sax, S.N., Pederson, D., Johnson, D., Spengler, J.D., Kinney, P.L., Simpson, H.J., Brandt-Rauf, P., 2005. Steel dust in the New York City subway system as a source of manganese, chromium, and iron exposures for transit workers. Journal of Urban Health—Bulletin of the New York Academy of Medicine 82, 33–42.

Crump, K.S., 2000. Manganese exposures in Toronto during use of the gasoline additive, methyl cyclo penta dienyl manganese tricarbonyl. Journal of Exposure Analysis and Environmental Epidemiology 10, 227–239.

Dahl, A., Gudmundsson, A., Swietlicki, E., Bohgard, M., Blomqvist G., and Gustafsson, M., (2006). Size-Resolved Emission Factor for Particle Generation Caused by Studded Tires – Experimental Results. 7th International Aerosol Conference, American Association for Aerosol Research (AAAR), St. Paul, Minnesota, USA (2006).

DFG, 2009. List of MAK and BAT Values 2009: Maximum Concentrations and Biological Tolerance Values at the Workplace. Report 45 (MAK & BAT Values), Wiley-VCH Verlag GmbH, Weinheim, Germany

Diana, G., Bruni, S., Cheli, F., Resta, F., 2002. Active control of the running behaviour of a railway vehicle: stability and curving performances. Vehicle System Dynamics Supplement 37, 157–170.

EPA HAD, 2002. Health Assessment Document for Diesel Engine Exhaust. U.S. EPA, 600/8-90/057F. Available at http://www.epa.gov/ttn/atw/dieselfinal.pdf (accessed 3 March 2011).

EPA NAAQS, 2011. National Ambient Air Quality Standards (40 CFR, part 50). Available at http://www.epa.gov/air/criteria.html (accessed 18 April 2011).

EPA Locomotives, 2011. Locomotives: Exhaust Emission Standards (40 CFR, part 1033). Available at http://www.epa.gov/oms/standards/nonroad/locomotives.htm (accessed 3 March 2011).

EPA RIN 2060-AM06, 2008. Control of Emissions of Air Pollution from Locomotive Engines and Marine Compression-Ignition Engines Less than 30 Liters per Cylinder (40 CFR, parts 9, 85, 86, 89, 92, 94, 1033, 1039, 1042, 1065, and 1068). Available at http://emerginglitigation.shb.com/Portals/f81bfc4f-cc59-46fe-9ed5-7795e6eea5b5/lm-preamble.pdf (accessed 3 March 2011).

EU Directive 2008/50/EC, 2008. On ambient air quality and cleaner air for Europe. Available at http://eur-lex.europa.eu/LexUriServ/LexUriServ.do?uri=OJ:L:2008:152:0001:0044:EN:PDF (accessed 3 March 2011).

EU Directive 2004/26/EC, 2004. On the approximation of the laws of the Member States relating to measures against the emission of gaseous and particulate pollutants from internal combustion engines to be installed in non-road mobile machinery. Available at

‹http://eur-lex.europa.eu/LexUriServ/site/en/oj/2004/l_225/l_22520040625en00030107.pdf (accessed 3 March 2011).

Fridell, E., Ferm, M., Björk, A., Ekberg, A., 2011. On-board measurement of particulate matter emissions from a passenger train. Journal of Rail and Rapid Transit, 225, 99–106.

Fromme, H., Oddoy, A., Piloty, M., Krause, M., Lahrz, T., 1998. Polycyclic aromatic hydrocarbons (PHA) and diesel engine emission (elemental carbon) inside a car and a subway train. Science of the Total Environment 217, 165–173.

Furuya, K., Kudo, Y., Okinaga, K., Yamuki, M., Takahashi, S., Araki, T., Hisamatsu, Y., 2001. Seasonal variation and characterization of suspended particulate matter in the air of subway stations. Journal of Trace and Microprobe Techniques, 19(4), 469–485.

Gehrig, R., Hill, M., Lienemann, P., Zwicky, C.N., Bukowiecki, N., Weingartner, E., Baltensperger, U., Buchmann, B., 2007. Contribution of railway traffic to local PM10 concentrations in Switzerland. Atmospheric Environment 41, 923–933.

Grass, D.S., Ross, J.M., Family, F., Barbour, J., James, S.H., Coulibaly, D., Hernandez, J., Chen, Y., Slavkovich, V., Li, Y., Graziano, J., Santella, R.M., Brandt-Rauf, P., Chillrud, S.N., 2010. Airborne particulate metals in the New York City subway: a pilot study to assess the potential for health impacts. Environmental Research 110(1), 1–11.

Golhd, D.R., 2008, Vulnerability to Cardiovascular Effects of Air Pollution in People with Diabetes, Current Diabetes Reports, 8(5), 333–335.

Gómez-Perales, J.E., Colvile, R.N., Fernández-Bremauntz, A.A., Gutiérrez-Avedoy, V., Páramo-Figueroa, V.H., Blanco-Jiménez, S., Bueno-López, E., Bernabé-Cabanillas, R., Mandujano, F., Hidalgo-Navarro, M. and Nieuwenhuijsen, M.J., 2007. Bus, minibus, metro inter-comparison of commuters' exposure to air pollution in Mexico City. Atmospheric Environment 41, 890–901.

Gretzschel, M., Bose, L., 2002. A new concept for integrated guidance and drive of railway running gears. Control Engineering Practice, 10(9), 1013–1021.

Gustafsson, M., Blomqvist, G., Gudmundsson, A., Dahl, A., Jonsson, P., Swietlicki, E., 2009. Factors influencing PM10 emissions from road pavement wear. Atmospheric Environment, 43, 4699–4702.

Gustafsson, M., 2009. Airborne particles from the wheel–rail contact. In: Lewis, R., Olofsson, U. (Eds.), Wheel–Rail Interface Handbook. CRC Press, Boca Raton, FL, pp. 550–575.

Gustafsson, M., Blomqvist, G., Dahl, A., Gudmunsson, A., Swietlicki, E., 2006. Inandningsbara partiklar I järnvägsmiljöer. VTI Rapport 538. VTI, Linköping, Sweden (in Swedish).

Gustavsson, P., Bigert, C., Polla, M., 2008. Incidence of lung cancer among subway drivers in Stockholm. American Journal of Industrial Medicine, 51, 545–547.

Götzfried, F., 2008. Policies and strategies for increased safety and traffic flow on European road networks in winter. In: Proceedings of the Final Conference of the COST Action 353: Winter Service Strategies for Increased European Road Safety, Dresden, Germany, 26–28 May 2008.

Hart, J.E., Laden, F., Schenker, M.B., Garshick, E., 2006. Chronic obstructive pulmonary disease mortality in diesel-exposed railroad workers. Environmental Health Perspectives 114(7), 1013–1016.

Haynes, R., Savage, A., 2007. Assessment of the health impacts of particulates from the redevelopment of Kings Cross. Environmental Monitoring and Assessment 130, 47–56.

Hill, L.B, Gooch, J., 2010. A Multi-City Investigation of Exposure to Diesel Exhaust in Multiple Commuting Modes. Clean Air Task Force Special Report 2007-1. Available at

http://www.catf.us/resources/publications/files/Multi_City_Commuter_Exposure_Report.pdf (accessed 3 March 2011).

Hinds, WC., 1999. Aerosol Technology. Wiley-Interscience, Chichester, UK.

IARC, 2010. Agents Classified by the *IARC Monographs*, Volumes 1–100. Available at http://monographs.iarc.fr/ENG/Classification/ClassificationsAlphaOrder.pdf (accessed 18 April 2011).

Jansson, A., Olander, L., Olofsson, L., Sundh, J., Söderberg, A., Wahlström, J., 2010. Ultrafine particle formation from wear. International Journal of Ventilation 9(1), 83–88.

Johansson, C., Johansson, P.Å., 2003. Particulate matter in the underground of Stockholm. Atmospheric Environment 37, 3–9.

Song, J., Wang, J., and Boehmana, A. L.,(2006). The role of fuel-borne catalyst in diesel particulate oxidation behavior, Combustion and Flame, 146(1-2), pp. 73-84.

Karlsson, H.L., Holgersson, A., Möller, L., (2008), Mechanisms related to the genotoxicity of particles in the subway and from other sources. Chemical Research in Toxicology, 21, pp. 726–731.

Karlsson, H.L., Nilsson, L. and Möller, L., 2005. Subway particles are more genotoxic than street particles and induce oxidative stress in cultured human lung cells. Chemical Research in Toxicology 18, 19–23.

Kim, K.Y., Kim, Y.S., Roh, Y.M, Lee, C.M. Kim, C.N., 2008. Spatial distribution of particulate matter (PM10 and PM2.5) in Seoul Metropolitan Subway stations. Journal of Hazardous Materials 154, 440–443.

Knibbs, L.D., Cole-Hunter, T., Morawska, L., 2011. A review of commuter exposure to ultrafine particles and its health effects. Atmospheric Environment 45, 2611–2622.

Knibbs, L.D., de Dear, R.J., Morawsk, L., 2010. Effect of cabin ventilation rate on ultrafine particle exposure inside automobiles. Environmental Science & Technology 44, 3546–3551.

Kittelson, D.B., 1998. Engines and nanoparticles: a review. Journal of Aerosol Science 29, 575–588.

Kittelson, D.B., 2006. Diesel aerosol measurement and control. In: Particle Society of Minnesota Meeting, University of Minnesota, 1 November 2006.

Kollamthodi, S., 2006. Rail Diesel Study: Management Summary (ED05010/MS/R01). AEA Technology Environment, Harwell International Business Centre, Oxfordshire, UK.

Lee, K.O., Cole, R., Sekar, R., Choi, M.Y., Kang, J.S., Bae, C.S., Shin, H.D., 2002. Morphological investigation of the microstructure, dimensions, and fractal geometry of diesel particulates. Proceedings of the Combustion Institute 29(1), 647–653.

Li, T.T., Bai, Y.H., Liu, Z.R., Li, J.L., 2007. In-train air quality assessment of the railway transit system in Beijing: a note. Transportation Research Part D 12, 64–67.

Lombaert, K., Morel, S., Le Moyne, L., Adam, P., Tardieu de Maleissye, J., and Amouroux, J., (2004). Nondestructive analysis of metallic elements in diesel soot collected on filter: Benefits of laser induced breakdown spectroscopy. Chemistry of Material Science, 24, pp. 41–56.

Lorenzo, R., Kaegi, R., Gehrig, R., Grobéty, B., 2006. Particle emissions of a railway line determined by detailed single particle analysis. Atmospheric Environment 40, 7831–7841.

Ljungman, A.G., Lindbom, J., Gustafsson, M., Blomqvist, G., Dahl, A., Gudmundsson, A., Swietlicki, E., 2007. Wear particles generated from studded tires and pavement induces inflammatory reactions in mouse macrophage cells. Chemical Research in Toxicology 20, 937–946.

Madl, K.A., Pinkerton, E.K., 2009. Health effects of inhaled engineered and incidental nanoparticles. Critical Reviews in Toxicology 39, 629–658.

Maricq, M.M., 2007. Chemical characterization of particulate emissions from diesel engines: a review. Aerosol Science 38, 1079–1118.

MECA, 2011. Manufacturers of Emission Controls Association, Off-road Diesel Equipment. Available at http://www.meca.org (accessed 3 March 2011).

Midander, K., Leygraf, C., Wallinder, I.O, Elihn, K, Cronholm, P., Karlsson, H.L., Möller, L., 2009. Surface characteristics, copper release, and toxicity of nano- and micrometer-sized copper and copper(ii) oxide particles: a cross-disciplinary study. Small 5 (3), 389–399.

Mohammadi, A., Kaneda, Y., Sogo, T., Kidoguchi, Y., Miwa, K., 2003. A study on diesel emission reduction using a high-frequency dielectric barrier discharge plasma. SAE Transactions 112(4), 1524–1531.

Mohr, M., Mattis, U., Kaegi, R., Bertola, A., Boulouchos, K., 2005. Influence of diesel engine combustion parameters on primary soot particle diameter. Environmental Science & Technology 39, 1887–1892.

Mosleh, M., Khemet, B.A., 2006. A surface texturing approach for cleaner disc brakes. Tribology Transactions 49(2), 279–283.

Murruni, L.G., Solanes, V., Debray, M., Kreiner, A.J., Davidson, M., Davidson, J., Ozafrán, M., Vázquez, M.E., 2009. Concentrations and elemental composition of particulate matter in the Buenos Aires underground system. Atmospheric Environment 43, 4577–4583

Nieuwenhuijsen, M.J., Gómez-Perales, J.E., Colvile, R.N., 2007. Levels of particulate air pollution, its elemental composition, determinants and health effects in metro systems. Atmospheric Environment 41, 7995–8006.

Nyström, A.K., Svartengren, M., Grunewald, J., Pousette, C., Rodin, I., Lundin, A., Skold, C.M., Eklund, A., Larsson, B.M., 2010. Health effects of a subway environment in healthy volunteers. European Respiratory Journal 36, 240–248.

Norman, M. and Johansson, C., 2005. Karaktärsering av partikelförekomsten vid Mariatorgets tunnelbanestation. ISLB Rapport 1:2005. SLB analys, Environment and Health Protection Adminstration, Stockholm, Sweden (in Swedish).

Ntziachristos and Boulter, 2009, EMEP/EEA emission inventory guidebook 2009, Available at http://www.eea.europa.eu/publications/emep-eea-emission-inventory-guidebook-2009/part-b-sectoral-guidance-chapters/1-energy/1-a-combustion/1-a-3-b-vi-road-tyre-and-brake-wear.pdf (accessed 18 April 2011).

Olofsson, U., 2010, A study of airborne wear particles generated from the train traffic—Block braking simulation in a pin-on-disc machine, Wear 271(1–2), 86–91.

Park, D.U. and Ha, K.C., 2008. Characteristics of PM10, PM2.5, CO_2 and CO monitored in interiors and platforms of subway train in Seoul, Korea. Environment International 34, 629–634.

Pincus, S., Stern, A.C., 1937. A study of air pollution in New York City. American Journal of Public Health 27, 321–333.

Palmer, G.T., Coleman, L.V., Ward, H.C., 1916. A study of methods for determining air dustiness. American Journal Public of Health 6, 1049–1075.

Pfeifer, G.D., Harrison, R.M., Lynam, D.R., 1999. Personal exposures to airborne metals in London taxi drivers and office workers in 1995 and 1996. Science of the Total Environment 235, 253–260.

Ripanucci, G., Grana, M., Vicentini, L., Magrini, A. and Bergamaschi, A., 2006. Dust in the underground railway tunnels of an Italian town. Journal of Occupational and Environmental Hygiene 3, 16–25.

Salma, I., 2009. Air pollution in underground railway systems. In: Hester, R.E., Harisson, R.M. (Eds.), Air Quality in Urban Environments. Royal Society of Chemistry, Cambridge, UK, pp. 65–85.

Salma, I., Weidinger, T. and Maenhaut, W., 2007. Time-resolved mass concentration, composition and sources of aerosol particles in a metropolitan underground railway station. Atmospheric Environment 41, 8391–8405.

Seaton, A., Cherrie, J., Dennekamp, M., Donaldson, K., Hurley, J.F. and Tran, C.L., 2005. The London Underground: dust and hazards to health. Occupational and Environmental Medicine 62, 355–362.

Schenk, L., Hansson, S.V., Rudén, C., Gilek, M., 2008. Occupational exposure limits: a comparative study. Regulatory Toxicology and Pharmacology 50(2), 261–270.

Shen, G., Goodall, R., 1997. Active yaw relaxation for improved bogie performance. Vehicle System Dynamics 28, 273–289.

Silver, I., 2007. The Future of the Diesel Engine. RSSB, London. Available at http://www.rssb.co.uk/SiteCollectionDocuments/pdf/reports/research/T536_rpt_final.pdf (accessed 3 March 2011).

Stachowiak, G.W., Stachowiak, G.P., Posidalo, P., 2008. Automated classification of wear particles based on their surface texture and shape features. Tribology International 41, 34–43.

Sundh, J., Olofsson, U., Olander, L., Jansson, A., 2009. Wear rate testing in relation to airborne particles generated in wheel–rail contact. Journal of Lubrication Science 21, 135–150.

Sundh, J., and Olofsson, U., (2011). Relating contact temperature and wear transitions in a wheel–rail contact, Wear, 271 (1-2), pp. 78-85.

Svartengren, M., Larsson, B.M., 2010. Hälsoeffekter, luftvägar, partiklar i Stockholms tunnelbana. Institutionen för folkhälsovetenskap, Karolinska Institutet, Stockholm.

Tager I. B., 2005, Ch. 24 Health effects of aerosols*:* mechanisms and epidemiology, Eds Ruzer L. S., Aerosols Handbook: Measurement, Dosimetry and Health Effects, CRC, FL, USA.

Tokarek, S. and Bernis, A., 2006. An example of particle concentration reduction in Parisian subway stations by electrostatic precipitation. Environmental Technology 27(11), 1279–1287.

Tornehed, P., 2010, Particulate emissions associated with diesel engine oil consumption, Doctoral thesis, Stockholm, Sweden, 2010.

Vinzents, P.S., Møller, P., Sørensen, M., Knudsen, L.E., Hertel, O., Jensen, F.P., Schibye, B., Loft, S., 2005. Personal exposure to ultrafine particles and oxidative DNA damage. Environmental Health Perspectives, 113, 1485–1490.

Wickens, A.H., 1994. Dynamic stability of articulated and steered railway vehicles guided by lateral displacement feedback. Vehicle System Dynamics 23, 541–553.

Williams, T.I., Schaaf Jr., W.E., Burnette, E., 2000. A History of Invention: From Stone Axes to Silicon Chips. Checkmark Books, New York.

Winslow, C.E.A., Kligler, I.J., 1912. A quantitative study of the bacteria in city dust with special reference to intestinal and buccal forms. American Journal of Public Health 2, 663–701.

Yoshinobu, Y., Tsuda, Y., Ueda, H., Nkanishi, Y., Gong, J., 2010. Simultaneous reduction of NOx and PM in diesel exhaust based on electrochemical reaction. SAE International Journal of Fuels and Lubricants 3(1), 50–60.

Zereini, F., Wiseman, C., Alt, F., Messerschmidt, J., Müller, J., & Urban, H., 2001. Platinum and rhodium concentrations in airborne particulate matter in Germany from 1988 to 1998. Environmental Science & Technology, 35, 1996–2000.

Zhang, J.J., McCreanor, J.E., Cullinan, P., Chung, K.F., Ohman-Strickland, P., Han, I.K., Järup, L., Nieuwenhuijsen, M.J., 2009. Health effects of real-world exposure to diesel exhaust in persons with asthma. Research Report 138. Health Effects Institute, Boston, MA.